

CLASSIFICATION CHANGED

UNCLASSIFIED

~~CONFIDENTIAL~~
NACA

Copyright

7707

F-12/3

Authority of *H. d. Dryden* Date *9-16-52*
per NACA Release form #770-1947 By *HAR, 10-6-52*

RESEARCH MEMORANDUM

for the

Air Materiel Command, Army Air Forces

LATERAL STABILITY CHARACTERISTICS OF A 1/8.33-SCALE

POWERED MODEL OF THE REPUBLIC XF-12 AIRPLANE

By

Edward Pepper and Gerald V. Foster

Langley Memorial Aeronautical Laboratory
Langley Field, Va.

CLASSIFIED DOCUMENT

This document contains classified information affecting the National Defense of the United States within the meaning of the Espionage Act, USC 50:31 and 32. Its transmission or the revelation of its contents in any manner to an unauthorized person is prohibited by law. Information so classified may be imparted only to persons in the military and naval services of the United States, appropriate civilian officers and employees of the Federal Government who have a legitimate interest therein, and to United States citizens of known loyalty and discretion who, if necessary must be informed thereof.

~~CONTAINS PROPRIETARY INFORMATION~~

NATIONAL ADVISORY COMMITTEE FOR AERONAUTICS

WASHINGTON

FEB. 27 1947

NACA LIBRARY
LANGLEY MEMORIAL AERONAUTICAL
LABORATORY
Langley Field, Va.

~~CONFIDENTIAL~~

UNCLASSIFIED



NATIONAL ADVISORY COMMITTEE FOR AERONAUTICS

RESEARCH MEMORANDUM

for the
Air Materiel Command, Army Air Forces

LATERAL STABILITY CHARACTERISTICS OF A 1/8.33-SCALE
POWERED MODEL OF THE REPUBLIC XF-12 AIRPLANE

By Edward Pepper and Gerald V. Foster

SUMMARY

The XF-12 airplane is a high-performance photo-reconnaissance aircraft designed for the Army Air Forces by the Republic Aviation Corporation. An investigation of a 1/8.33-scale powered model was made in the Langley 19-foot pressure tunnel to obtain information relative to the aerodynamic design of the airplane. The model was tested with and without the original vertical tail and with two revised tails. For the revised tail no. 1, the span of the original vertical tail was increased about 15 percent and the portion of the vertical tail between the stabilizer and fuselage behind the rudder hinge line was allowed to deflect simultaneously with the main rudder. Revision no. 2 incorporated the increased span, but the lower rudder was locked in the neutral position.

For all the tail arrangements investigated it was indicated that the airplane will possess positive effective dihedral and will be directionally stable regardless of flap or power condition. The rudder effectiveness is greater for the revised tails than for the original tail, but this is offset by the increase in directional stability caused by the revised tails.

All the rudder arrangements appear inadequate in trimming out the resultant yawing moments at zero yaw in a take-off condition with the left-hand outboard propeller windmilling and the remaining engines developing take-off power.

It is indicated that the lower rudder of tail no. 1 is ineffective.

UNCLASSIFIED

~~CONFIDENTIAL~~

INTRODUCTION

In order to provide the Army Air Forces with a long-range, high-altitude, high-speed, photo-reconnaissance aircraft, the Republic Aviation Corporation has undertaken the design of the XF-12 airplane. This design is based on a normal gross weight of 103,000 pounds, a wing span of 129.17 feet and a wing area of 1640 square feet. Each of the four supercharged Pratt & Whitney R-4360 engines is capable of delivering 3000 horsepower.

At the request of the Air Materiel Command, Army Air Forces, an investigation has been conducted in the Langley 19-foot pressure tunnel to determine the stability characteristics of a 1/8.33-scale powered model of the XF-12 airplane. The results of that part of the investigation made to determine the static longitudinal stability and stalling characteristics are reported in reference 1. The results of that phase of the investigation made to determine some of the static lateral stability characteristics of the model with the original tail and two revised tails for several flight and power conditions are presented herein and include rudder effectiveness tests. Results of tests with asymmetrical power are also included.

COEFFICIENTS AND SYMBOLS

The positive directions of the forces and moments and of the angular displacements of the airplane and control surfaces are shown in figure 1. The coefficients and symbols used are defined as follows:

C_L	lift coefficient	(L/qS)
C_X	longitudinal-force coefficient	(X/qS)
C_Y	lateral-force coefficient	(Y/qS)
C_m	pitching-moment coefficient	$(M/qS\bar{c})$
C_l	rolling-moment coefficient	(L'/qSb)
C_n	yawing-moment coefficient	(N/qSb)
T_c	thrust coefficient per propeller	$(T/2qD^2)$

Q_c	torque coefficient per propeller ($Q/2\rho D^3$)
V/nD	propeller advance ratio
$\partial C_L/\partial \psi$	variation of rolling-moment coefficient with angle of yaw
$\partial C_N/\partial \psi$	variation of yawing-moment coefficient with angle of yaw
$\partial C_Y/\partial \psi$	variation of lateral-force coefficient with angle of yaw
$\partial \psi/\partial \delta_r$	variation of angle of yaw with rudder deflection
$\partial C_N/\partial \delta_r$	variation of yawing-moment coefficient with rudder deflection
q	dynamic pressure of free stream ($\rho V^2/2$)
ρ	mass density of air
V	airspeed
L	lift (-Z)
X	force along longitudinal axis
Y	force along lateral axis
M	pitching moment
N	yawing moment
L^r	rolling moment
T	effective thrust
Q	torque
D	propeller diameter
n	propeller rotational speed
S	wing area
b	wing span

\bar{c}	mean aerodynamic chord (M.A.C.)
α	angle of attack of root chord
ψ	angle of yaw
δ_f	flap deflection
δ_r	rudder deflection, positive with trailing edge to left
V_i	indicated airspeed
R	Reynolds number ($\rho V \bar{c} / \mu$)
μ	coefficient of viscosity
Γ_{eff}	effective dihedral angle, degrees
β	propeller blade angle at 0.75 tip radius

The subscripts used herein are defined as follows:

trim.	condition when C_N equals zero
($\psi = 0^\circ$)	condition when angle of yaw is zero degrees

MODEL AND TESTS

Model.— The 1/8.33-scale complete model of the XF-12 airplane is shown in figure 2 mounted on a single support strut for yaw tests in the Langley 19-foot pressure tunnel. Principal model dimensions are given in figure 3 and general design details are presented in table I. The model is constructed of wood and reinforced with steel. A description of the model details is contained in reference 1. The surfaces were sprayed with lacquer and kept aerodynamically smooth by filling surface irregularities with glazing putty and rubbing with fine abrasive paper.

The model is equipped with partial-span double-slotted flaps which extend from the fuselage to 61.5 percent of the semispan. The flaps were fixed at the appropriate settings by suitable brackets. The tricycle landing gear and wheel-well doors were installed when the flaps were deflected.

The vertical tail consists of a fin and rudder and is of NACA 65₁-011 airfoil sections. The vertical tail incorporated a dorsal and ventral fin. The dorsal fin faired into the fuselage at 38.6 percent of the fuselage length from the nose (maximum fuselage diameter). Three arrangements of the vertical tail were investigated and are designated as the original tail, revision no. 1, and revision no. 2. Principal dimensions and details of the tail arrangements are shown in figure 4. For revision no. 1, the span of the original fin was increased 15 percent, the span of the original rudder was increased 20 percent, and the portion of the vertical tail between the stabilizer and fuselage behind the rudder hinge line was allowed to deflect simultaneously with the main rudder. Revision no. 2 incorporated the increased span but the lower rudder was locked in the neutral position with all gaps sealed. The rudders were not internally balanced but had felt wiper seals to prevent air leakage through the rudder-fin gap. The rudder surfaces were remotely actuated and the amount of deflection was determined by an electric control position indicator. The rudders deflect through a range from -20° to 20° .

The horizontal tail is attached to the vertical tail above the fuselage as shown in figure 4. For these tests the elevator was locked in the neutral position and the stabilizer incidence was -2° to the wing root chord.

All of the tests were made with the NACA wing duct inlet lip no. 5 located at the wing leading edge. Details of the internal-flow arrangement are furnished in reference 1. The four-blade, right-hand, adjustable pitch, tractor propellers are geometrically similar to the airplane propellers. Each of the four propellers was driven by a water-cooled induction motor, housed in each nacelle. A variable-frequency alternator supplied the current with speed adjustment attained by regulation of the frequency. For asymmetrical power conditions, the motors of the windmilling propellers were disconnected from the power source.

Tests.— The yaw tests were made at a dynamic pressure of 26 pounds per square foot with the density of the air in the tunnel maintained at approximately 0.00515 slugs per cubic foot. Under these conditions the Reynolds number and Mach number were approximately 2,170,000 and 0.09, respectively.

The directional stability characteristics and the rudder effectiveness of the model were investigated through a range of ψ equal to -25° to 25° at angles of attack of approximately 2.0° and 11.0° for each flap and power configuration. A few conditions were investigated with the angle of attack at 6.8° . Values of

rudder deflection were selected to satisfactorily cover the complete range of control surface deflections. An investigation was made for similar conditions with the complete impennage (horizontal and vertical tail) removed and replaced by a fuselage tail cone. (See fig. 5.)

The model propellers were operated at constant values of V/nD throughout the yaw range for each angle of attack. The values of propeller rotational speed were selected to duplicate full-scale torque conditions at corresponding lift coefficients only when $\psi = 0^\circ$ for the power conditions listed in table II. It is believed that the variations of Q_c for other values of ψ were small and consequently the blade angle was set at 21.5° for (M.P.)₂ and 28° for 0.50 (R.P.) so that full-scale values of T_c could be approximately simulated as shown in table IV. The variation of the calculated T_c with C_L for these power conditions is shown in figure 6. A comparison of the variation of Q_c with T_c is given in figure 7 for the full-scale variable-pitch propeller and the model adjustable fixed-pitch propeller. For the asymmetrical power conditions the blade setting of the windmilling propeller was kept at 21.5° and these propellers were allowed to rotate freely by the action of the air stream. Several asymmetrical power tests were made at $\psi = 0^\circ$ to determine the rudder deflection required for trim through a suitable speed range. This was accomplished by setting the angle of attack at selected values and varying the rudder setting by remote operation to obtain trim conditions.

The internal air-flow conditions for the nacelles and ducts were the same as for the tests reported in reference 1.

DATA COMPUTATIONS AND CORRECTIONS

The data have been referred to the stability axes, which are a system of axes having their origin at the center of gravity and in which the Z-axis is in the plane of symmetry and perpendicular to the relative wind, the X-axis in the plane of symmetry and perpendicular to the Z-axis, and the Y-axis is perpendicular to the plane of symmetry as shown in figure 1. All the moments are computed about the normal center of gravity located on the fuselage center line at 27.43 percent of the mean aerodynamic chord.

The equations used to transfer from the wind axes to the stability axes are as follows:

$$C_l = C_l' \cos \psi + \frac{b}{c} C_m' \sin \psi$$

$$C_m = C_m' \cos \psi - \frac{b}{c} C_l' \sin \psi$$

$$C_n = C_n'$$

$$C_x = C_x' \cos \psi + C_y' \sin \psi$$

$$C_L = C_L'$$

$$C_Y = C_Y' \cos \psi - C_X' \sin \psi$$

Primed coefficients denote values referred to the wind axes ($\psi = 00$).

Corrections to the data were determined for the model at $\psi = 00$ and applied to the results of the tests made with the model yawed. These corrections were applied to compensate for the following: (1) model support-strut interference effects on the lift, drag; and pitching-moment coefficients; (2) jet-boundary interference effects on the drag and pitching-moment coefficients and angle of attack; and (3) the effects of air-flow misalignment on the drag coefficient and angle of attack. The lateral-force, rolling-, and yawing-moment coefficients were corrected to account only for asymmetrical model and air-flow conditions.

An inspection and calibration of the scale system at the conclusion of the investigation indicated the possibility of inaccurate rolling-moment measurements for some of the conditions tested. Consequently, those test results that are deemed unreliable have been omitted. It is believed, however, that the more important conditions were satisfactorily measured and hence test results for those conditions are presented in this paper.

RESULTS AND DISCUSSION

The aerodynamic forces and moments measured during the investigation together with analytical results are presented in figures 8 to 28.

Rudder-Fixed Lateral Stability Characteristics

Original vertical tail.— Aerodynamic characteristics of the model in yaw are presented in figures 8 to 12 for the symmetrical power conditions tested. (See table II.) The angle of attack and power conditions investigated were selected so that a large range of flight conditions would be covered and so that effects of angle of attack, power condition, and flap deflection on the lateral-stability characteristics could be readily interpreted. The high angle-of-attack values of about 11.0° closely represent the attitude of the airplane shortly after take-off. The low value of angle of attack of approximately 2° is in the region of high-speed flight at sea level.

The results of figures 8 to 12 are summarized in table III. No consistent trends are noted for the effects of power, angle-of-attack change, and flap deflection on the values presented. Computations to determine the effective dihedral were based on a theoretical value of $\partial C_L / \partial \psi = 0.000262$ for each degree of dihedral. (See reference 2.) The values of $\partial C_L / \partial \psi$ or effective dihedral are somewhat reduced with increasing angle of attack when the flaps are deflected. The smallest amount of directional and lateral stability exists for the condition with flaps deflected 55° and 0.50(R.P.). Values of $\partial C_Y / \partial \psi$ remain about the same for changes of power and angle of attack, but increase with flap deflection.

Asymmetrical power.— The results of the asymmetrical power tests of the model with the original tail are presented in figure 13 for the flaps retracted condition. For these tests the left-hand outboard propeller was allowed to windmill to simulate the most severe single-engine-out condition and the remaining propellers were operated to simulate the (M.P.)₂ power condition. Also included for comparative purposes is the condition with $\delta_r = 0^\circ$ and $T_0 = 0$. A cross plot of these figures is presented in figure 14 for the two speeds corresponding to the high and low angles of attack tested and summarizes variation of rudder deflection required for trim with yaw angles. Data were also obtained for the estimation of the rudder deflection required for trim at 125 miles per hour by remotely controlling the rudder deflection while yawing the model. It should be noted from table IV that full-scale thrust coefficients were not exactly duplicated during the tests and this would affect the results to a small extent. The adverse yaw due to aileron deflection makes it necessary to employ additional rudder during flight as does the rudder spring tab at full deflection. The effect of the rudder spring tab on the rudder effectiveness varies with rudder deflection, and sufficient information is unavailable to

estimate the rudder-tab deflection for the conditions tested. An analysis of the results in reference 3, however, indicated that when the rudder is at -20° with the rudder-tab deflected 25° the rudder effectiveness is reduced to that of the rudder at 12° with the rudder-tab undeflected. From the foregoing it may be seen that the results presented in figure 14 are optimistic in the prediction of the rudder behavior for the airplane in flight. At the low speed of 125 miles per hour it is indicated that the airplane cannot be trimmed at $\psi = 0^\circ$ with the left-hand outboard propeller windmilling and the remaining propellers operating at take-off power, (M.P.)₂.

The results of the foregoing analysis were qualitatively confirmed during flight tests of the full-scale airplane, conducted at the same time as the model tests in the Langley 19-foot pressure tunnel. It was learned from the results of the flight tests that unsatisfactory directional control occurred with one propeller windmilling. Consequently, the two revisions of the vertical tail were tested (revision no. 1 and revision no. 2) on the model in an effort to find a remedy for the rudder deficiencies.

Tail revisions.— Aerodynamic characteristics of the model with tail revision no. 1 and with flaps retracted are presented in figures 15 and 16. These results are for the angle of attack and power conditions similar to those obtained for the original tail. The results obtained for tail revision no. 2 are for similar conditions and are shown in figures 17 and 18. In addition, some test results are presented in figure 19 for the model with tail revision no. 2 and for a take-off condition ($\alpha = 10.7^\circ$, (M.P.)₂, $\delta_F = 20^\circ$). The results are summarized in table V. Effect of power and flap deflection on the stability characteristics of the model are similar to those experienced for the model with the original tail. Indications are that if the airplane is equipped with either of the revised tails, the effective dihedral will decrease with increase of power and flap deflection. The values of $\partial C_Y / \partial \psi$ remain essentially constant. Even though increases of thrust coefficient tend to decrease the values of $\partial C_n / \partial \psi$ at large angles of attack, it is indicated that the airplane will possess a high degree of directional stability with either revised tail.

Analysis.— The rudder deflection required for trim and the rudder effectiveness for the test conditions listed in tables III and V are presented in figures 20 to 23. The derivation of these curves did not take into account the effects of banking or rudder trim-tab deflection on the amount of rudder deflection required for trim. Because the data were meager for flaps deflected 55° at the low angle of attack, curves for this condition are not presented. The data are summarized in table VI.

In general, increases of power cause negative increases in $\partial\psi/\partial\delta_r$, with the most marked changes occurring when the flaps are deflected 55° . Changes of tail configuration have small effect on the values of $\partial\psi/\partial\delta_r$ obtained.

Power effects are negligible on $\partial C_n/\partial\delta_r$ for the original tail where flaps are retracted. The effects become more pronounced when flaps are deflected. However, values of $\partial C_n/\partial\delta_r$ increase negatively with power for the revised tails when the flaps are retracted. Although little difference exists in the values of $\partial C_n/\partial\delta_r$ between the revised tails, there is a marked increase in the negative values over those for the original tail. The increases in $\partial C_n/\partial\delta_r$ due to the revised tails are offset by the increase in directional stability caused by these tails (compare tables III and V) and hence little change is experienced over the original tail in the range of yaw angles through which the rudder can trim. For the original and revised tail configurations the difference in yaw angle at which maximum rudder deflection for trim occurs ($\delta_{rtrim} = 20^\circ$) is no case greater than 2° . As expected, the revised tails generally increased the effective dihedral by a small amount.

The original tail rather than the revised tails may be preferred for normal four-engine flight operation because it does not cause an excessive amount of directional stability and the problems associated with rudder pedal forces, therefore, should be less severe than for the larger revised tails. For asymmetrical power operation, however, the revised tails proved more effective in trimming the model to lower speeds at $\psi = 0^\circ$ as shown in figure 24. These data were obtained for several tail flap and power conditions by remotely controlling the rudder deflection during the tests of the model to obtain trimmed conditions. The results show that little difference exists between either of the two revisions and hence indicate that the lower rudder of revision no. 1 is ineffective. It is of interest to note that the variation of rudder deflection required to trim with indicated velocity at $\psi = 0^\circ$ is about the same for revision no. 2 with two engines inoperative on one side and the original tail with the left-hand outboard propeller windmilling.

Although the data are limited in scope, it seems possible that flap deflections for take-off ($\delta_f = 20^\circ$) will not greatly affect the trends shown. From the results, it appears that difficulty at the low take-off speeds will be experienced for any of the tail configurations in the event of single-engine failure and two-engine failure on one side may prove catastrophic during take-off. The curves presented in figure 24 are somewhat optimistic for the reasons previously stated in the explanation of figure 14.

Tail Removed

The results of the yaw tests with the vertical tail removed and flaps retracted are presented in figures 25 and 26 for several power conditions and with propellers removed. Similar results are shown in figures 27 and 28 with the flaps deflected 55° . These results are summarized in table VII for $\psi = 0^\circ$.

Changes in the stability derivatives due to removal of the tail were normal in that values of $\partial C_n / \partial \psi$ increased positively to give directional instability, values of $\partial C_y / \partial \psi$ decreased to a reasonable extent, and the effective dihedral decreased a moderate amount.

CONCLUSIONS

On the basis of tests of a 1/8.33-scale powered model of the Republic XF-12 airplane in the Langley 19-foot pressure tunnel the following conclusions are indicated:

1. With either the original tail or the revised tails the airplane will possess positive effective dihedral and will be directionally stable for all the flap and power conditions tested.
2. The variation of yawing-moment coefficient with rudder deflection at zero yaw, is greater for the revised tails than for the original tail. However, this is offset by the increase in directional stability caused by the revised tails.
3. At take-off with the left-hand outboard propeller windmilling and the remaining engines developing take-off power, all the rudder arrangements appear to be inadequate in trimming out the resultant yawing moments at zero yaw.

4. The lower rudder of tail revision no. 1 is ineffective.

Langley Memorial Aeronautical Laboratory
National Advisory Committee for Aeronautics
Langley Field, Va.

Edward Pepper
Aeronautical Engineer

Gerald V. Foster
Gerald V. Foster
Aeronautical Engineer

Approved:

Clinton H. Dearborn
Clinton H. Dearborn
Chief of Full-Scale Research Division

CJB

REFERENCES

1. Pepper, Edward, and Foster, Gerald V.: Longitudinal Stability and Stalling Characteristics of a 1/8.33-Scale Model of the Republic XF-12 Airplane. NACA RM No. L6L12, Army Air Forces, 1946.
2. Pearson, Henry A., and Jones, Robert T.: Theoretical Stability and Control Characteristics of Wings with Various Amounts of Taper and Twist. NACA Rep. No. 635, 1938.
3. MacIachlan, Robert: Wind-Tunnel Tests of a 1/6-Scale Model of Republic XF-12 Vertical Tail with Stub Fuselage and Stub Horizontal Tail. NACA MR No. 65E21, Army Air Forces, 1945.

TABLE I
DESIGN CHARACTERISTICS OF THE REPUBLIC XF-12
AIRPLANE AND A 1/8.33-SCALE XF-12 MODEL

Item	Full scale	1/8.33 scale
Wing:		
Root chord (theoretical)		
Section (Republic)	R-4,40-318-1	R-4,40-318-1
Chord	17.79 ft	25.63 in.
Angle of incidence	2°	2°
Tip chord (theoretical)		
Section (Republic)	R-4,40-413-.6	R-4,40-413-.6
Chord	7.70 ft	11.09 in.
Angle of incidence	-2°	-2°
Area (projected)	1639.62 sq ft	23.62 sq ft
Span (projected)	129.17 ft	15.51 ft
Aspect ratio	10.18	10.18
Mean aerodynamic chord	13.43 ft	19.34 in.
Sweepback (at 50 percent chord)	0°	0°
Taper ratio	2.31	2.31
Dihedral (from wing-root chord plane)	6°	6°
Aileron (one surface):		
Area (projected)	42.38 sq ft	87.88 sq in.
Span (projected)	23.08 ft	33.24 in.
Root chord	2.08 ft	3.00 in.
Tip chord	1.59 ft	2.29 in.
Distance from centroid to center of gravity	52.9 ft	76.22 in.
Deflection	-22.5° to 17.5°	-22.5° to 17.5°
Flaps:		
Area (total)	185.14 sq ft	2.68 sq ft
Span (one side)	34.53 ft	49.72 in.
Deflection	65° maximum	65° maximum

TABLE I.- Continued

DESIGN CHARACTERISTICS OF THE REPUBLIC XF-12 AIRPLANE.- Continued

Item	Full scale	1/8,33 scale
Horizontal tail:		
Root chord		
Section (NACA)	651-012	651-012
Chord	11.88 ft	17.11 in.
Tip chord (theoretical)		
Section	651-012	651-012
Chord	5.95 ft	8.55 in.
Area (total projected)	388.88 sq ft	5.63 sq ft
Span	44.00 ft	63.36 in.
Aspect ratio	5.14	5.14
Taper ratio	2	2
Mean aerodynamic chord	9.27 ft	13.35 in.
Dihedral (to chord plane)	6°	6°
Sweepback (at 68 percent horizontal tail chord)	0°	0°
Tail length (27.43 percent wing mean aerodynamic chord to 25 percent tail mean aerodynamic chord)	52.1 ft	75.02 in.
Elevator (one surface)		
Area (projected behind hinge line)	52.59 sq ft	7.58 sq in.
Span (projected)	18.65 ft	26.86 in.
Root chord	3.62 ft	5.21 in.
Tip chord	2.01 ft	2.89 in.
Deflection	-25° to 15°	-25° to 15°
Vertical tail (original):		
Area (fuselage not included)		
Vertical	213.56 sq ft	3.08 sq ft
Dorsal fin	49.82 sq ft	0.72 sq ft
Ventral fin	10.23 sq ft	0.15 sq ft
Root chord (theoretical)	13.33 ft	19.20 in.
Section (NACA)	651-011	651-011
Aspect ratio	2.06	2.06
Sweepback (at 65 percent vertical tail chord)	0°	0°
Mean aerodynamic chord	11.91 ft	17.14 in.
Span	21.67 ft	31.21 in.
Tail length (27.43 percent wing mean aerodynamic chord to 25 percent tail mean aerodynamic chord)	51.09 ft	74.67 in.

TABLE I.- Continued

DESIGN CHARACTERISTICS OF THE REPUBLIC XF-12 AIRPLANE.- Continued

Item	Full-scale	1/8.33 scale
Vertical tail (original).-- Concluded		
Rudder		
Area (behind hinge line)	54.87 sq ft	0.79 sq ft
Root chord	4.54 ft	6.54 in.
Tip chord	1.94 ft	2.79 in.
Span	15.00 ft	21.60 in.
Deflection	-20° to 20°	-20° to 20°
Vertical tail (revised):		
Area (fuselage not included)		
Vertical	213.56 sq ft	3.08 sq ft
Dorsal fin	49.82 sq ft	0.72 sq ft
Ventral fin	10.23 sq ft	0.15 sq ft
Root chord (theoretical)	13.33 ft	19.20 in.
Section (NACA)	651-011	651-011
Sweepback (at 68 percent vertical tail chord)	0°	0°
Mean aerodynamic chord	11.25 ft	16.2 in.
Span	24.9 ft	35.88 in.
Tail length (27.43 percent wing mean aerodynamic chord to 25 percent tail mean aerodynamic chord)	51.5 ft	74.22 in.
Rudder:		
Area (behind hinge line-- top rudder)	66.6 sq ft	0.96 sq ft
Root chord	4.54 ft	6.54 in.
Tip chord	1.94 ft	2.79 in.
Span (top rudder only)	18.03 ft	25.95 in.
Deflection	20° to 20°	-20° to 20°
Fuselage:		
Length	92.54 ft	133.26 in.
Maximum diameter	10.25 ft	14.76 in.
Frontal area	82.52 sq ft	1.20 sq ft

TABLE I - Concluded

DESIGN CHARACTERISTICS OF THE REPUBLIC XF-12 AIRPLANE.- Concluded

Item	Full scale	1/8.33 scale
Nacelles:		
Length		
Inboard	29.38 ft	42.31 in.
Outboard	27.82 ft	40.06 in.
Maximum width	5.21 ft	7.50 in.
Maximum height	5.22 ft	7.52 in.
Frontal area	21.33 sq ft	0.31 sq ft
Direction of thrust line	Parallel to fuselage center line	
Propellers:		
Number	4	4
Number of blades per propeller	4	4
Diameter	16 ft 2 in.	23.29 in.
Activity factor per blade	118.5	118.5
Type	Aeroproducts C-40-198-4	
For Full-Scale Airplane		
Weight-normal	103,000 lb	
Wing loading	62.8 lb/sq ft	
Engines		
Number	4	
Type	P. & W R-4360-31	
Rating per engine		
Military	3000 hp at 2700 rpm	
Rated power	2500 hp at 2550 rpm	
Gear ratio	0.425	
Superchargers		
Number	2 per engine	
Type	G.E. BM-4 and BM-5 (one each per engine)	
Power loading	7.33 hp/sq ft	
Ground angle (from root chord)		
Static position	4°45'	
Maximum tail-down position	9°30'	

TABLE II

FULL-SCALE POWER CONDITIONS

(Simulated in tests of the 1/8.33-scale model
of the XF-12 airplane)

Power condition	Symbol	Brake horsepower (per engine)	Cooling-fan horsepower (per fan)	Airplane Gross Weight (lb)	Altitude (ft)	Engine speed (rpm)	Gear ratio	Propeller speed (rpm)
Military power	(M.P.) ₂	3000	54	103,000	0 (Sea level)	2700	0.425	1148
50-percent rated power	0.50 (R.P.)	1250	14	103,000	0 (Sea level)	1500	0.425	638
Thrust coefficient equal zero	$T_c = 0$	Low	Low	All weights	0 (Sea level)	Low	0.425	Low

NACA RM No. 17B21

NATIONAL ADVISORY
COMMITTEE FOR AERONAUTICS

TABLE III

18

LATERAL STABILITY CHARACTERISTICS

ORIGINAL VERTICAL TAIL - SYMMETRICAL POWER

$$[\delta_r = 0^\circ; \alpha \psi = 0^\circ]$$

Power condition	δ_r (deg)	α (deg)	ψ trim (deg)	$\frac{\partial C_{Df}}{\partial \psi}$	$\frac{\partial C_L}{\partial \psi}$	$\frac{\partial C_Y}{\partial \psi}$	Γ_{eff} (deg)	Figure
(M.P.) ₂	0	2.0	2.0	-0.00177	0.00180	0.0120	6.9	8 (a)
		6.8	.2	-.00162	.00158	.0120	6.0	8 (b)
		11.0	.1	-.00138	.00151	.0122	5.8	8 (c)
0.50 (R.P.)	0	6.8	0	-.00171	.00166	.0121	6.3	9 (a)
		11.0	.1	-.00162	.00174	.0115	6.6	9 (b)
$T_c = 0$	0	2.0	.3	-.00176	.00200	.0121	7.6	10 (a)
		6.8	.9	-.00184	.00164	.0120	6.3	10 (b)
		11.0	7	-.00186	.00176	.0120	6.7	10 (c)
0.50 (R.P.)	55	2.0	-.3	-.00180	.00218	.0142	8.3	11 (a)
		11.8	3.3	-.00130	.00097	.0139	3.7	11 (b)
$T_c = 0$	55	1.9	.6	-.00186	.00202	.0142	7.7	12 (a)
		11.5	-.1	-.00198	.00087	.0139	3.3	12 (b)

NATIONAL ADVISORY
COMMITTEE FOR AERONAUTICS

NACA RM No. 17B21

TABLE IV
 THRUST AND TORQUE COEFFICIENTS OBTAINED DURING TESTS
 OF A 1/8.33-SCALE MODEL OF THE XF-12 AIRPLANE
 [$\psi = 0^\circ$]

δ_P (deg)	Power condition	α (deg)	β (deg)	T_c		Q_c	ΔT_c^a (a)
				Obtained	Required		
0	(M.P.) ₂	2.0	21.5	0.036	0.028	0.0066	0.008
		6.8		.139	.136	.0205	.003
		11.0		.270	.278	.0305	-.008
	0.50 (R.P.)	6.8	28.0	.064	.050	.0138	.014
		11.0		.111	.098	.0218	.013
	$T_c = 0$	2.0	21.5	0	0	-----	-----
6.8		-----		-----			
11.0		-----		-----			
20	(M.P.) ₂	10.7	21.5	.405	.430	.0500	-.025
55	0.50 (R.P.) 	2.0	28.0	.168	.130	.0304	.038
		11.8		.301	.304	.0500	-.003
	$T_c = 0$	1.9	28.0	0	0	-----	-----
11.8		-----		-----			

^a ΔT_c is the increment difference between T_c obtained and T_c required.

TABLE V

LATERAL STABILITY CHARACTERISTICS

Tail revision no. 1 and no. 2 - Symmetrical power

$$\left[\delta_r = 0^\circ; \text{ or } \psi = 0^\circ \right]$$

Power condition	δ_r (deg)	α (deg)	ψ trim (deg)	$\frac{\partial C_n}{\partial \psi}$	$\frac{\partial C_l}{\partial \psi}$	$\frac{\partial C_Y}{\partial \psi}$	Γ_{eff} (deg)	Figure
(M.P.) ₂	0	2.0	0.1	-0.00242	0.00208	0.0133	7.9	15 (a); 17 (a)
		11.0	.5	-.00194	.00163	.0134	6.2	15 (b); 17 (b)
$T_c = 0$	0	2.0	.3	-.00242	.00183	.0132	7.0	16 (a); 18 (a)
		10.8	1.3	-.00242	.00202	.0130	7.7	16 (b); 18 (b)
(M.P.) ₂	20	10.7	-1.3	-.00178	.00138	.0165	5.3	19

NATIONAL ADVISORY
COMMITTEE FOR AERONAUTICS

TABLE VI
 RUDDER POWER AND RUDDER EFFECTIVENESS

$$\left[\psi = 0^\circ; \text{ or } C_n = 0 \right]$$

δ_r (deg)	Power condition	α (deg)	$\partial\psi/\partial\delta_r(\text{trim})$			$\partial C_n/\partial\delta_r$		
			Original	Revision no. 1	Revision no. 2	Original	Revision no. 1	Revision no. 2
0	(M.P.) ₂	2.0	-0.70	-0.76	-0.72	-0.00132	-0.00209	-0.00202
		6.8	-.73	-----	-----	-.00135	-----	-----
		11.0	-.86	-.94	-.85	-.00132	-.00200	-.00206
	0.50 (R.P.)	6.8	-.74	-----	-----	-.00136	-----	-----
		11.0	-.82	-----	-----	-----	-----	-----
	T _c = 0	2.0	-.67	-.75	-.69	-.00129	-.00188	-.00188
		6.8	-.67	-----	-----	-.00132	-----	-----
		11.0	-.63	-.74	-.67	-.00132	-.00198	-.00187
	20	(M.P.) ₂	10.7	-.83	-----	-----	-.00193	-----
55	0.50 (R.P.)	11.8	-.99	-----	-----	-.00142	-----	-----
	T _c = 0	11.8	-.60	-----	-----	-.00128	-----	-----

NATIONAL ADVISORY
 COMMITTEE FOR AERONAUTICS

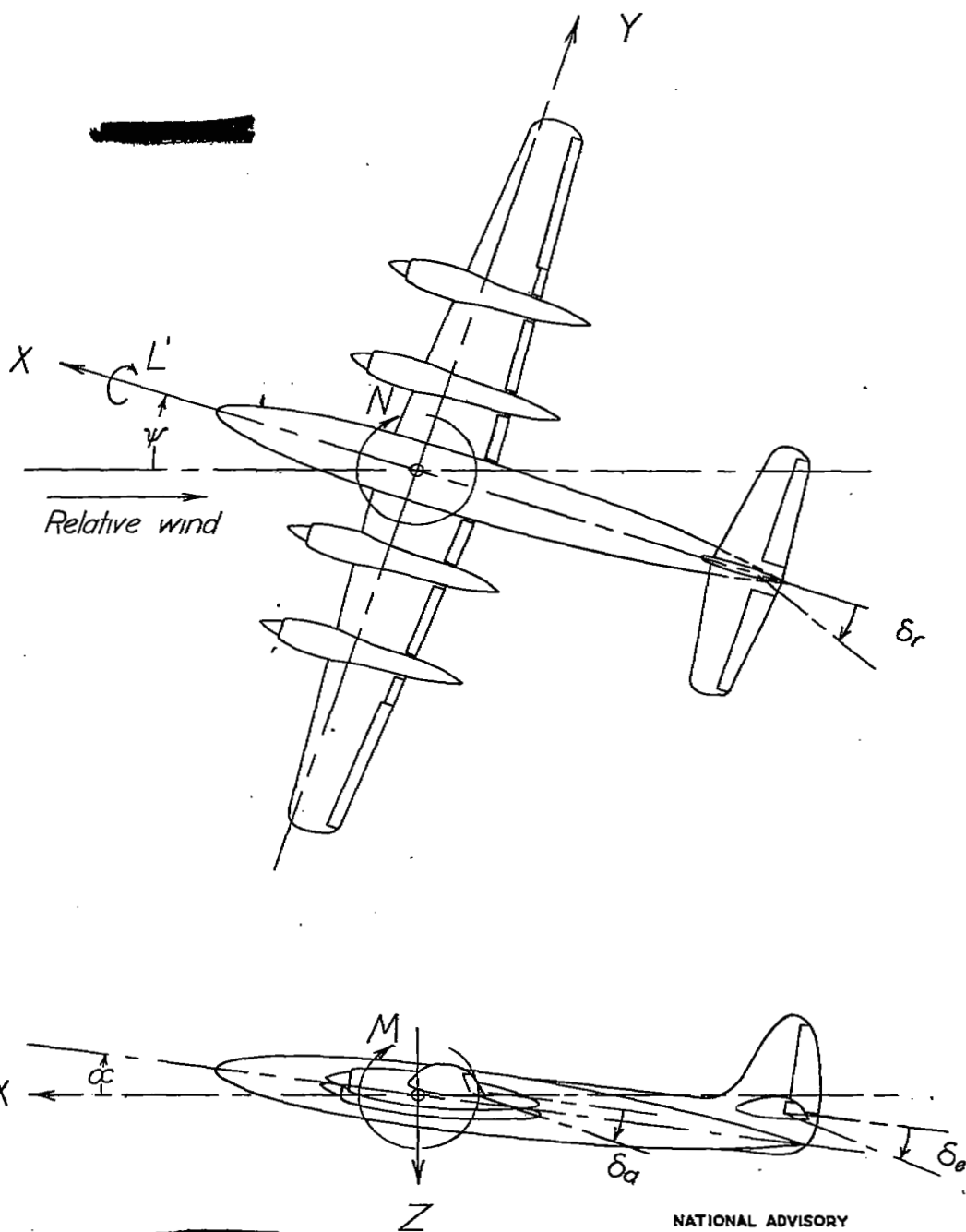
TABLE VII
LATERAL STABILITY CHARACTERISTICS

TAIL REVOLVED

[$\psi = 0^\circ$]

Power condition	δ_F (deg)	α (deg)	$\frac{\partial C_n}{\partial \psi}$	$\frac{\partial C_l}{\partial \psi}$	$\frac{\partial C_y}{\partial \psi}$	Γ_{eff} (deg)	Figure
(M.P.) ₂	0	2.1	0.00060	0.00126	0.0051	4.8	25
		11.1	.00082	.00124	.0068	4.7	25
$T_0 = 0$	0	2.1	.00060	.00133	.0051	5.1	25
		10.9	.00060	.00155	.0051	5.9	25
Propellers removed	0	2.1	.00044	.00162	.0035	6.2	26
		10.9	.00050	.00097	.0035	3.7	26
0.50 (R.P.)	55	2.2	.00051	.00137	.0077	5.2	27
		11.8	.00067	-----	.0082	---	27
$T_0 = 0$	55	2.0	.00041	.00137	.0080	5.2	27
		11.4	.00056	.00104	.0074	4.0	27
Propellers removed	55	2.0	.00036	.00117	.0062	4.5	28
		11.3	.00010	-----	.0062	---	28

NATIONAL ADVISORY
COMMITTEE FOR AERONAUTICS



NATIONAL ADVISORY
COMMITTEE FOR AERONAUTICS

Figure 1. - System of axes and deflections.
Positive values of forces and angles are as
indicated by arrows.

204

NACA RM No. L7E21

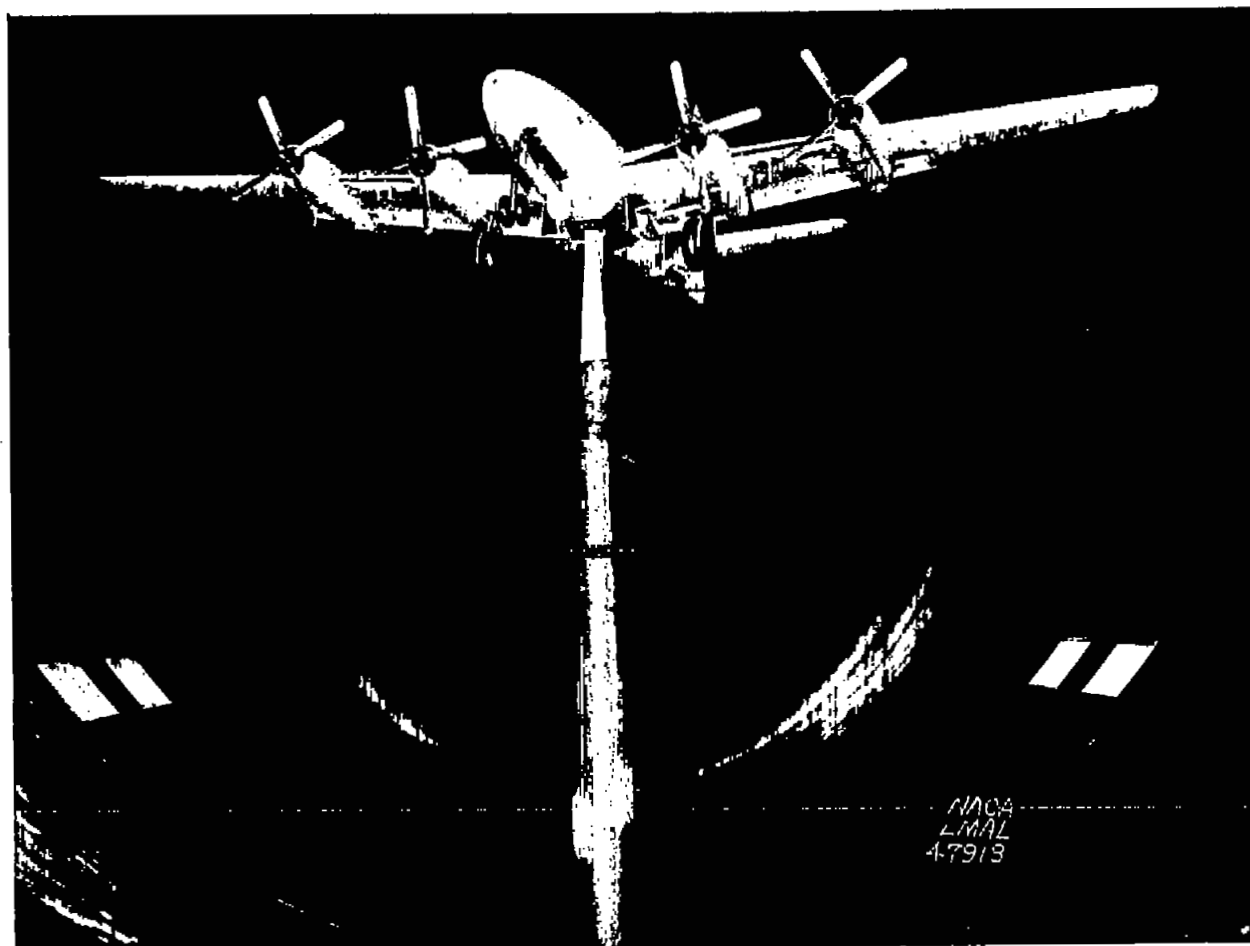
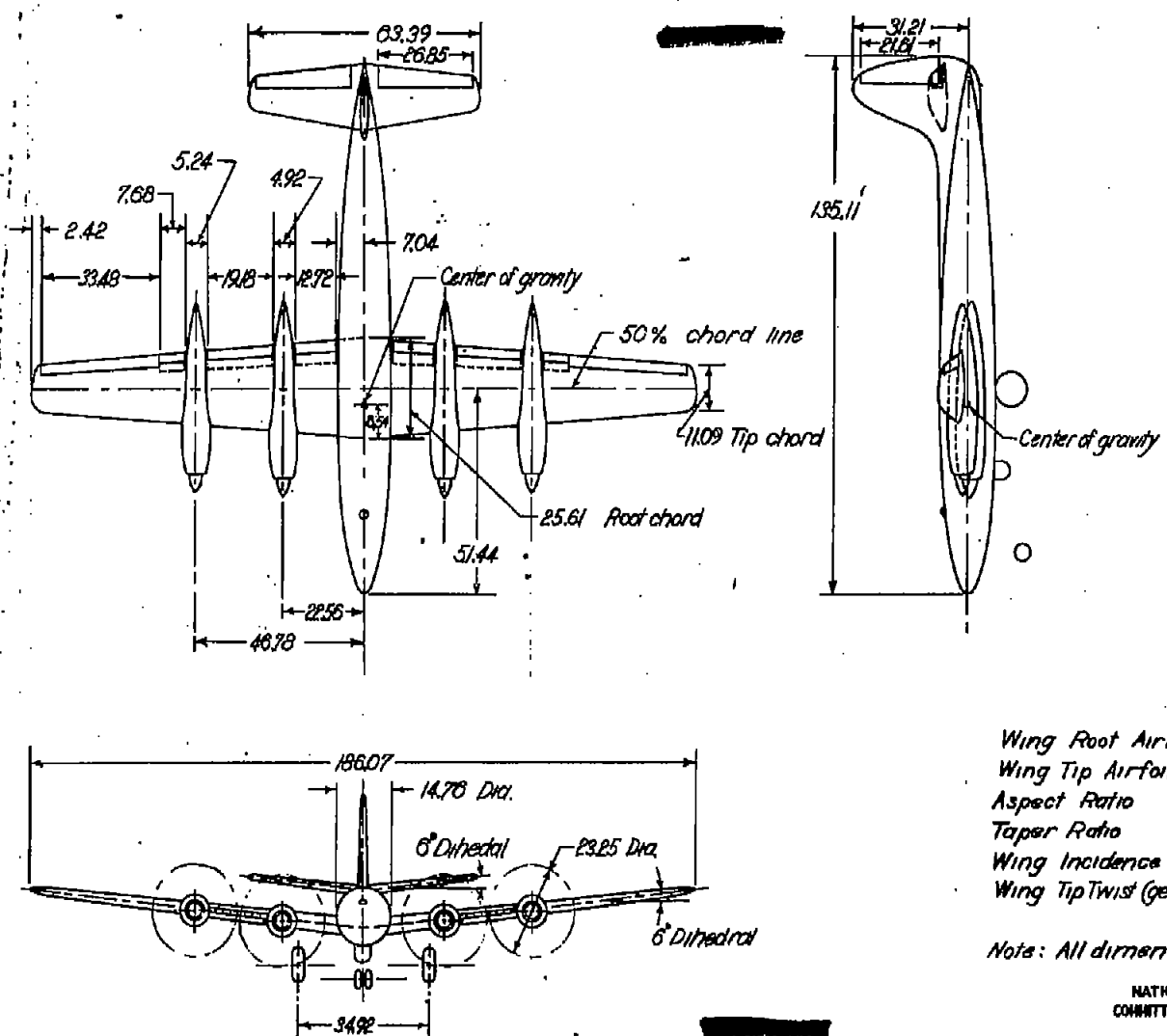


Figure 2.- The $\frac{1}{8.33}$ -scale model of the XF-12 airplane mounted on a single support strut in the Langley 19-foot pressure tunnel.

FIG. 2



Wing Root Airfoil	R-4,40-318-1
Wing Tip Airfoil	R-4,40-413-6
Aspect Ratio	10.18
Taper Ratio	2.31 : 1
Wing Incidence	+2° to ϕ of fuselage
Wing Tip Twist (geometric)	-4°

Notes: All dimensions are given in inches

NATIONAL ADVISORY
COMMITTEE FOR AERONAUTICS

Figure 3 .- Three view drawing of a 1/33 - scale model of the Republic XF-12 airplane.

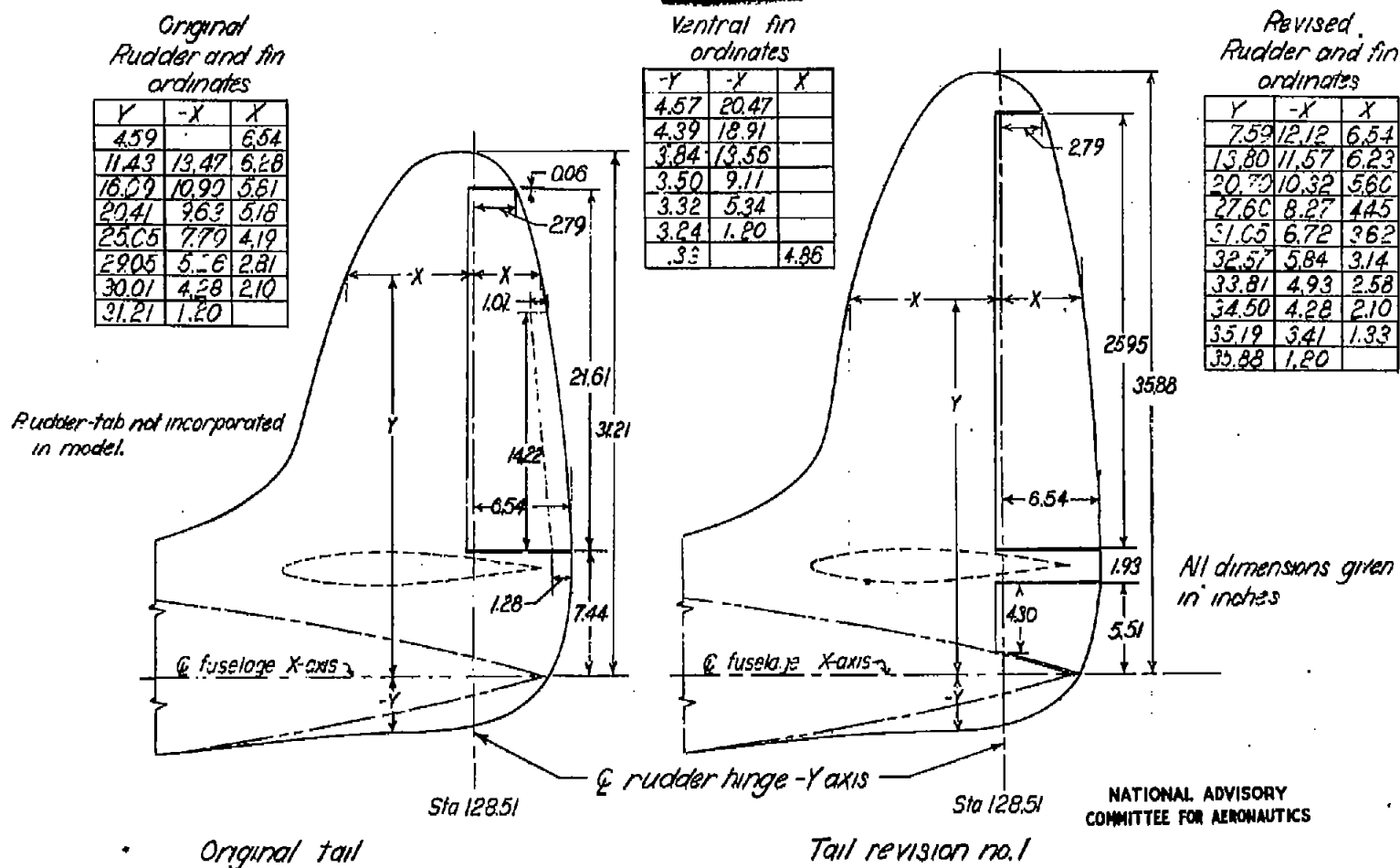


Figure 4. - Details of the vertical tails of the 1/8.33-scale model of the Republic XF-12 airplane.

204

NACA RM No. L7E21

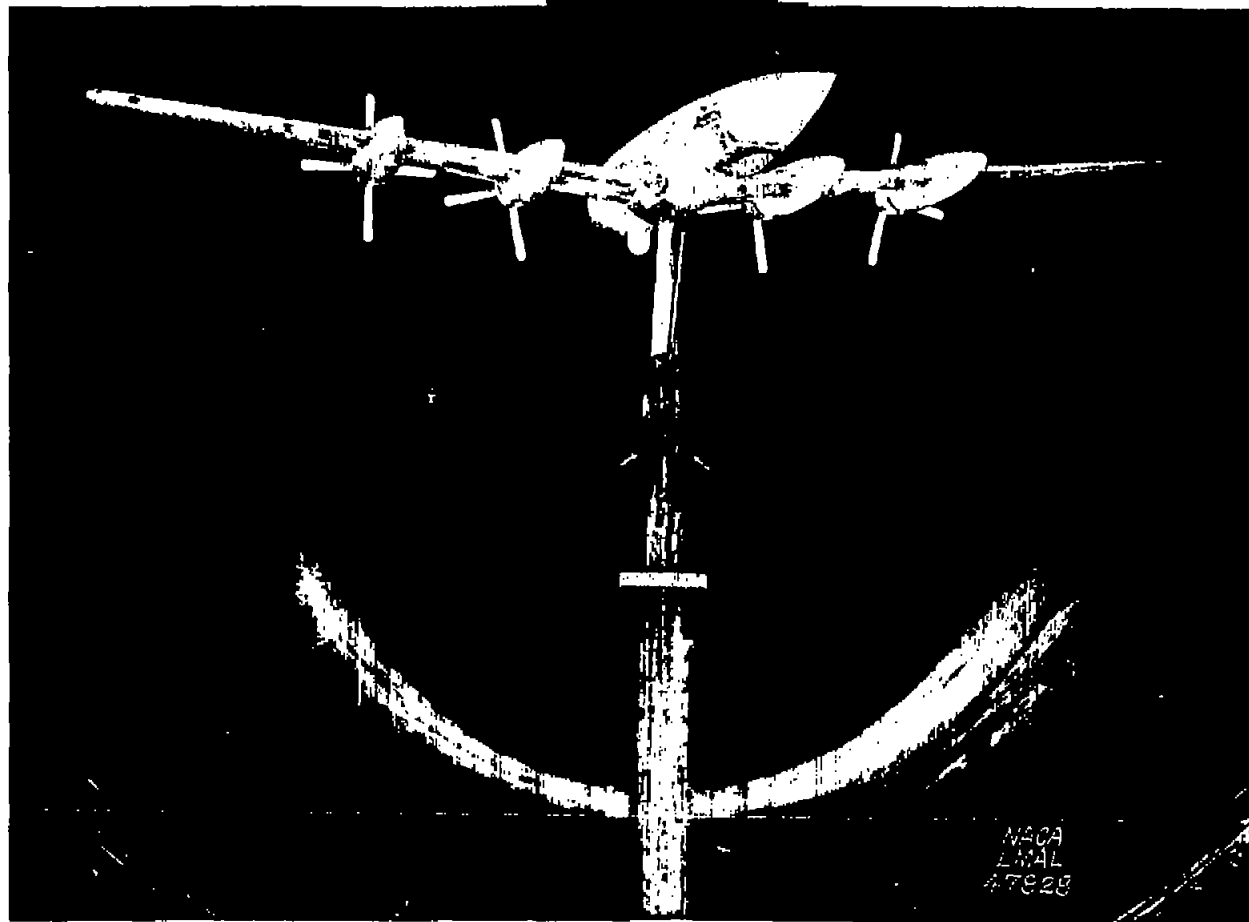


Figure 5.- The $\frac{1}{8.33}$ -scale model of the XF-12 airplane with the tail removed.

NATIONAL ADVISORY COMMITTEE FOR AERONAUTICS
LANGLEY MEMORIAL AERONAUTICAL LABORATORY - LANGLEY FIELD VA

FIG. 5

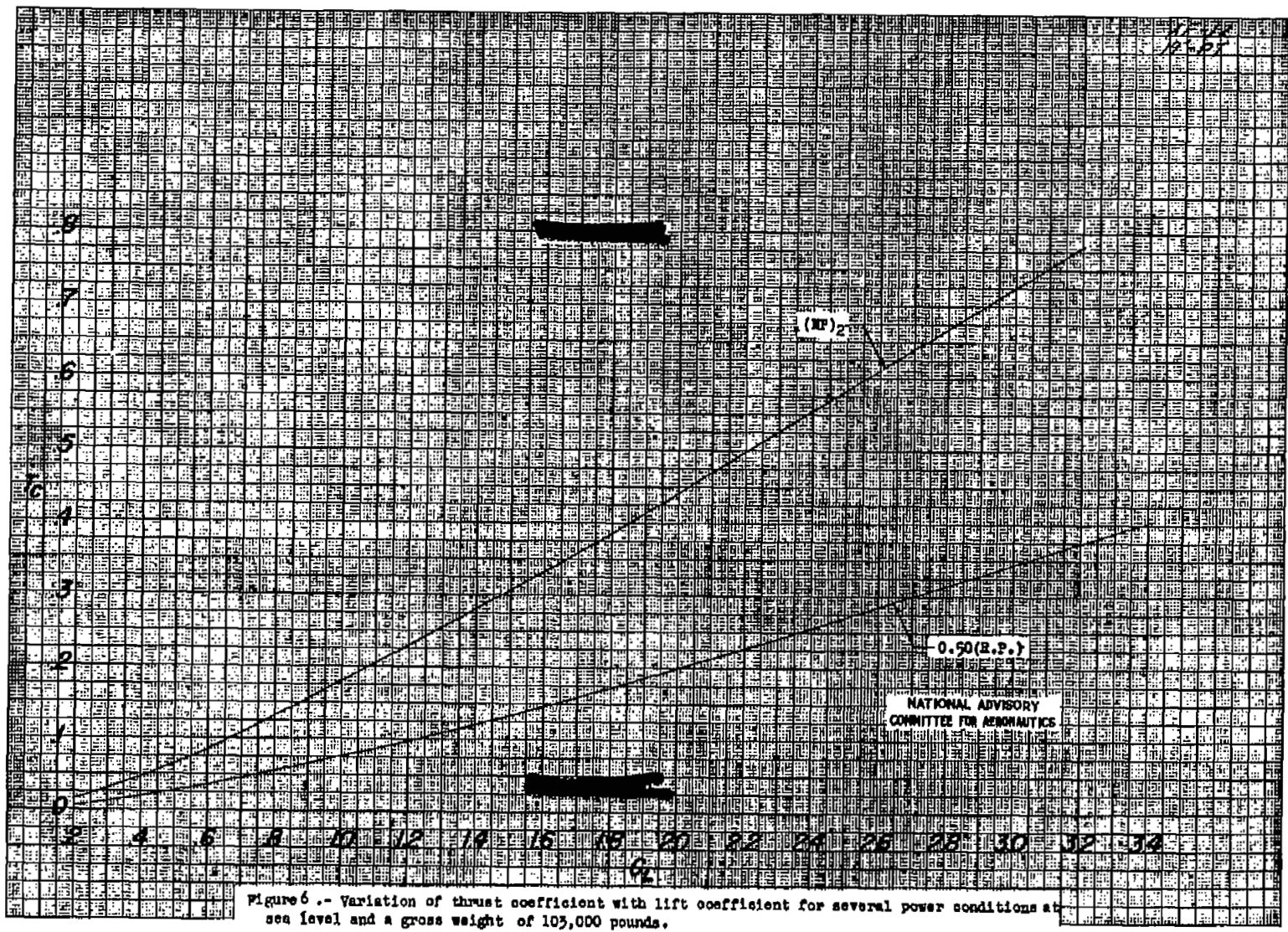
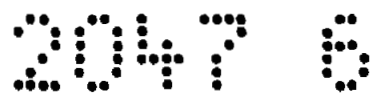
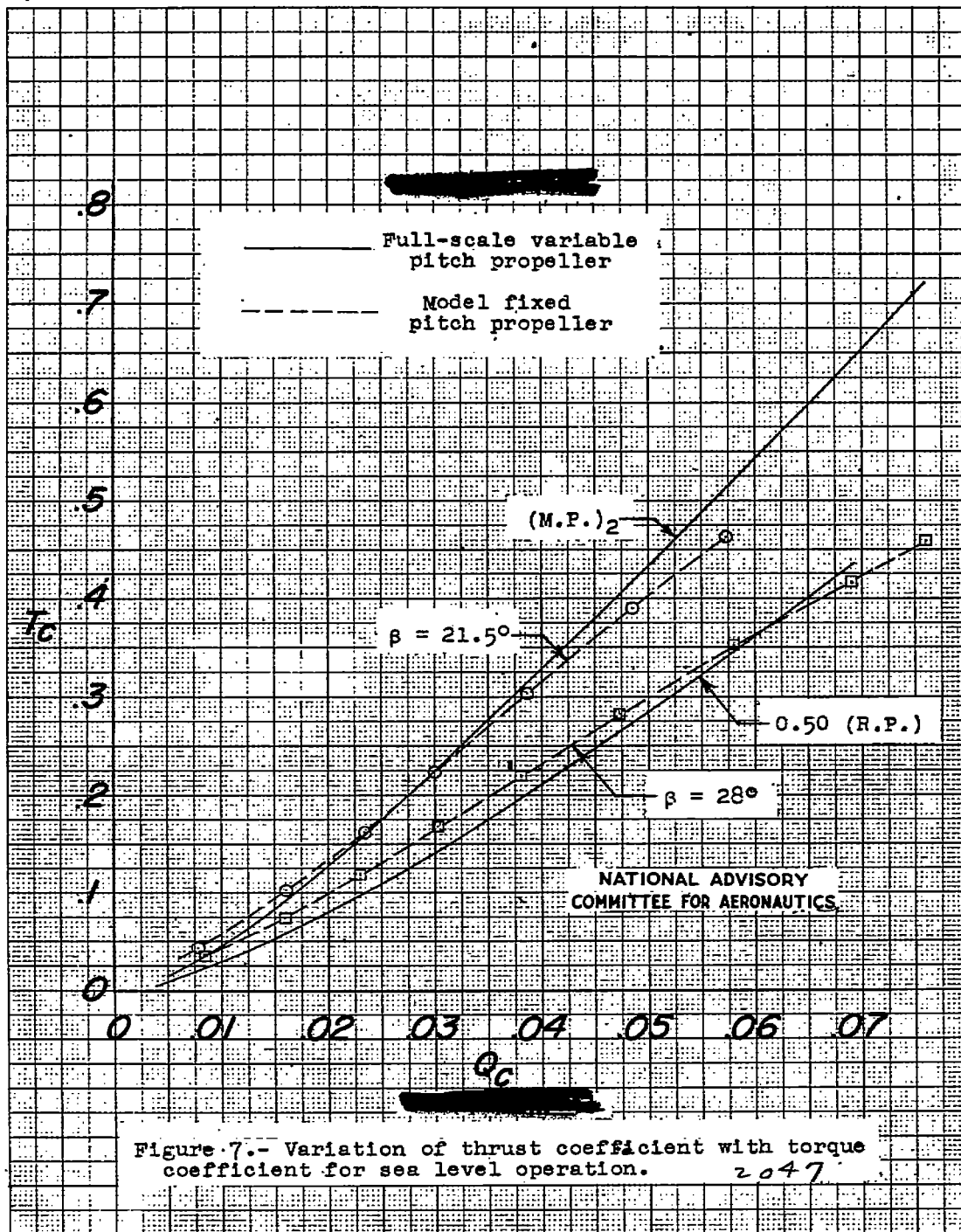


Figure 6.- Variation of thrust coefficient with lift coefficient for several power conditions at sea level and a gross weight of 105,000 pounds.



2047

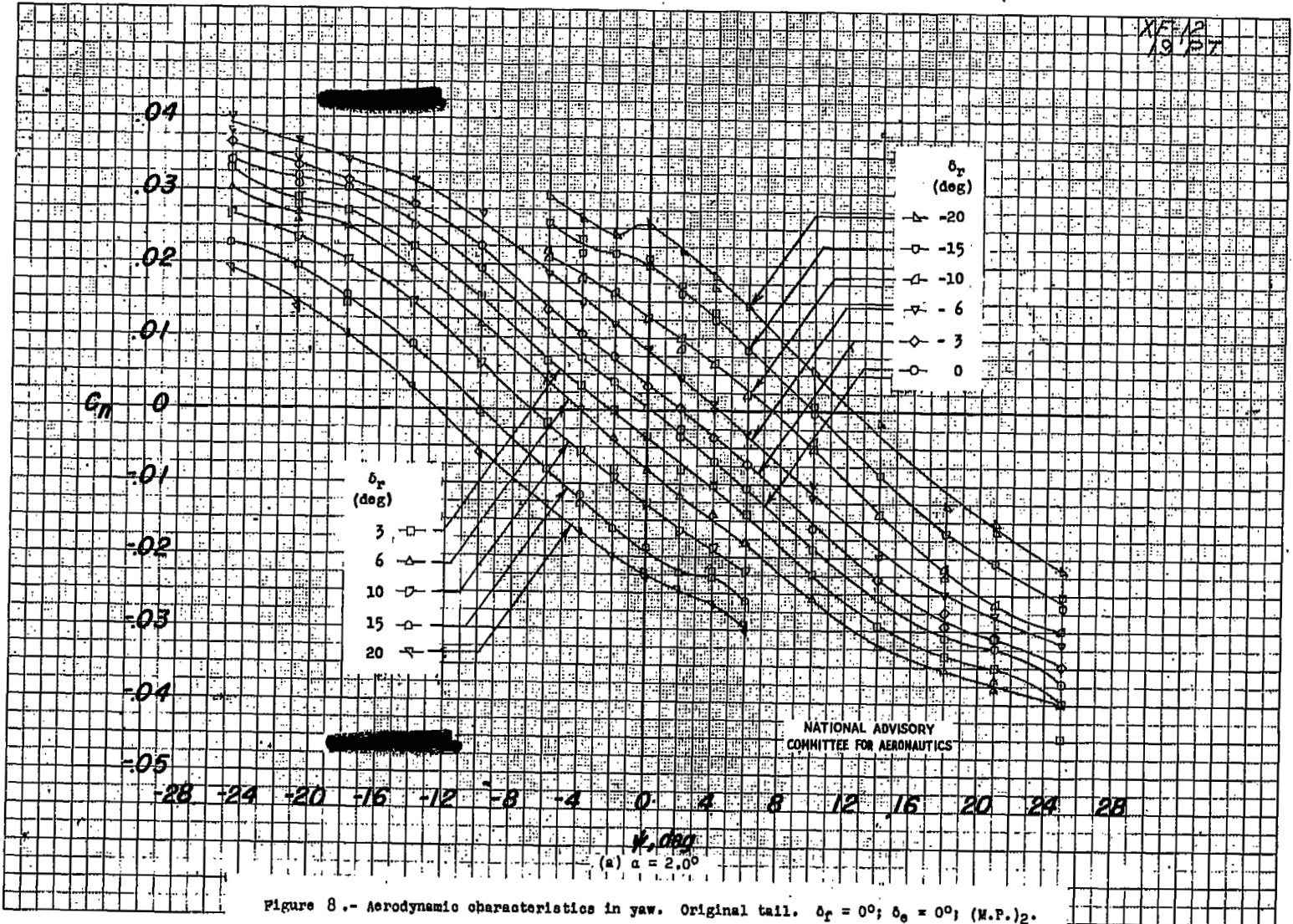


Figure 8.- Aerodynamic characteristics in yaw. Original tail. $\delta_r = 0^\circ$; $\delta_\theta = 0^\circ$; (M.P.)₂.

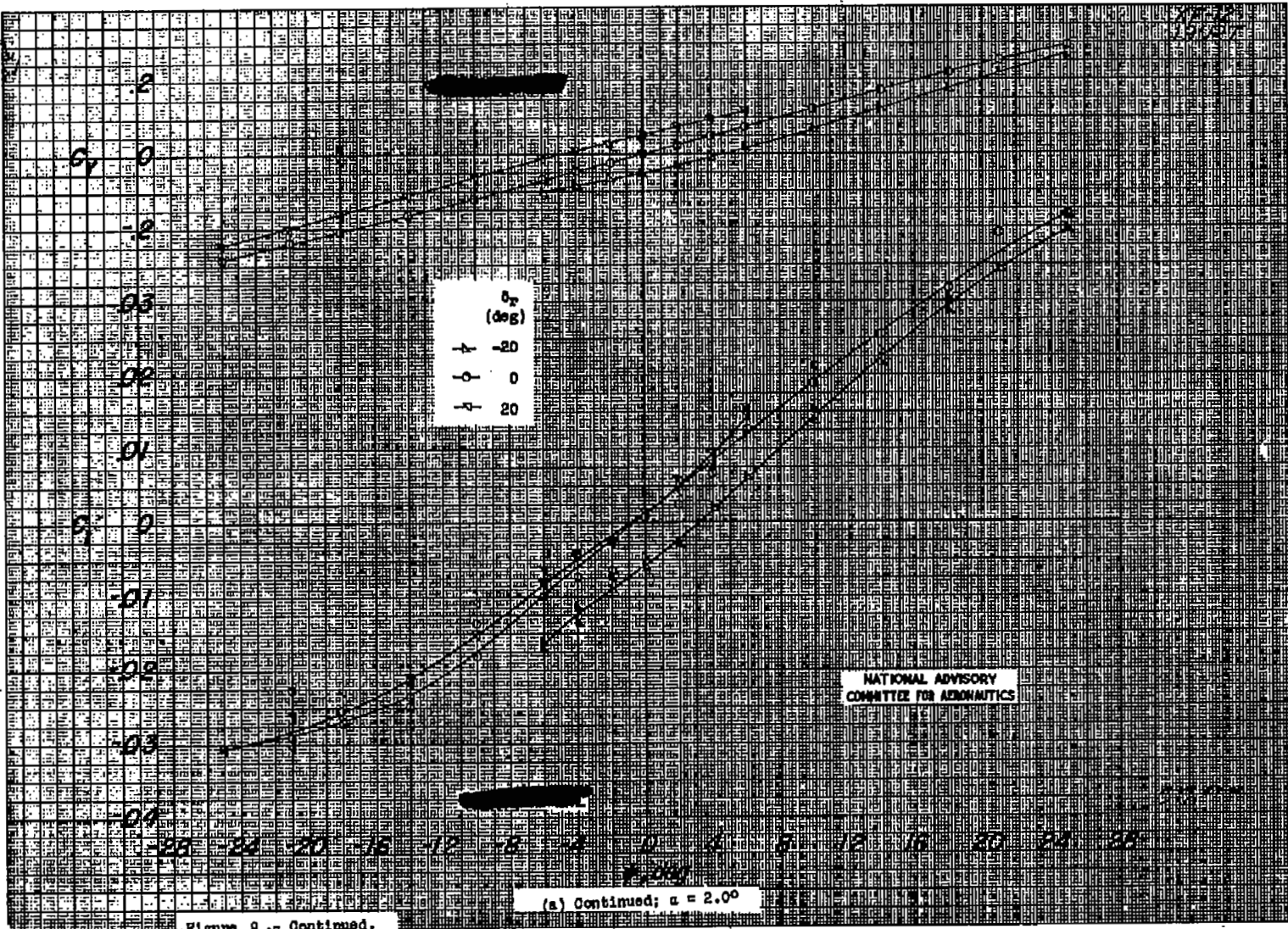


Figure 8.- Continued.

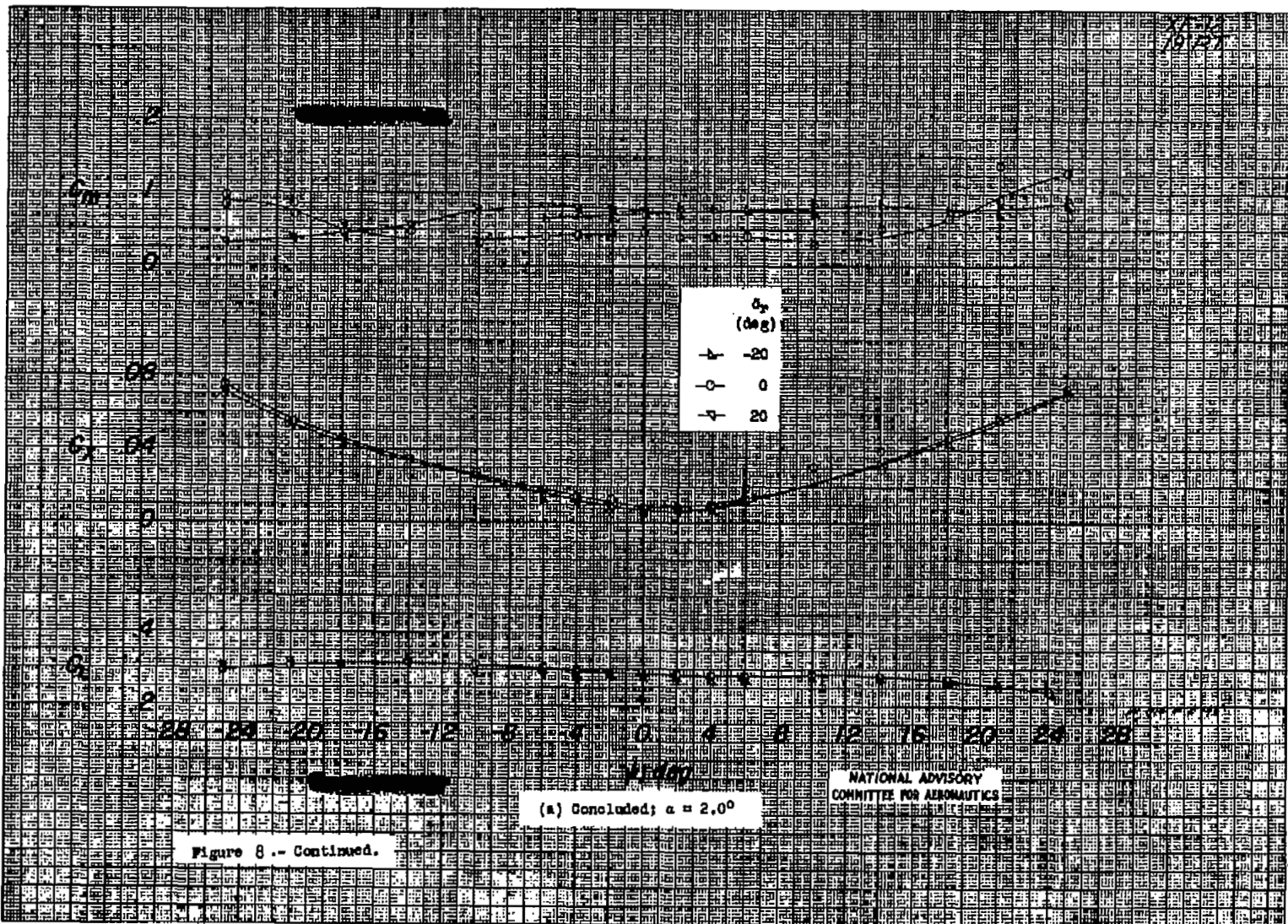


Figure 8.- Continued.

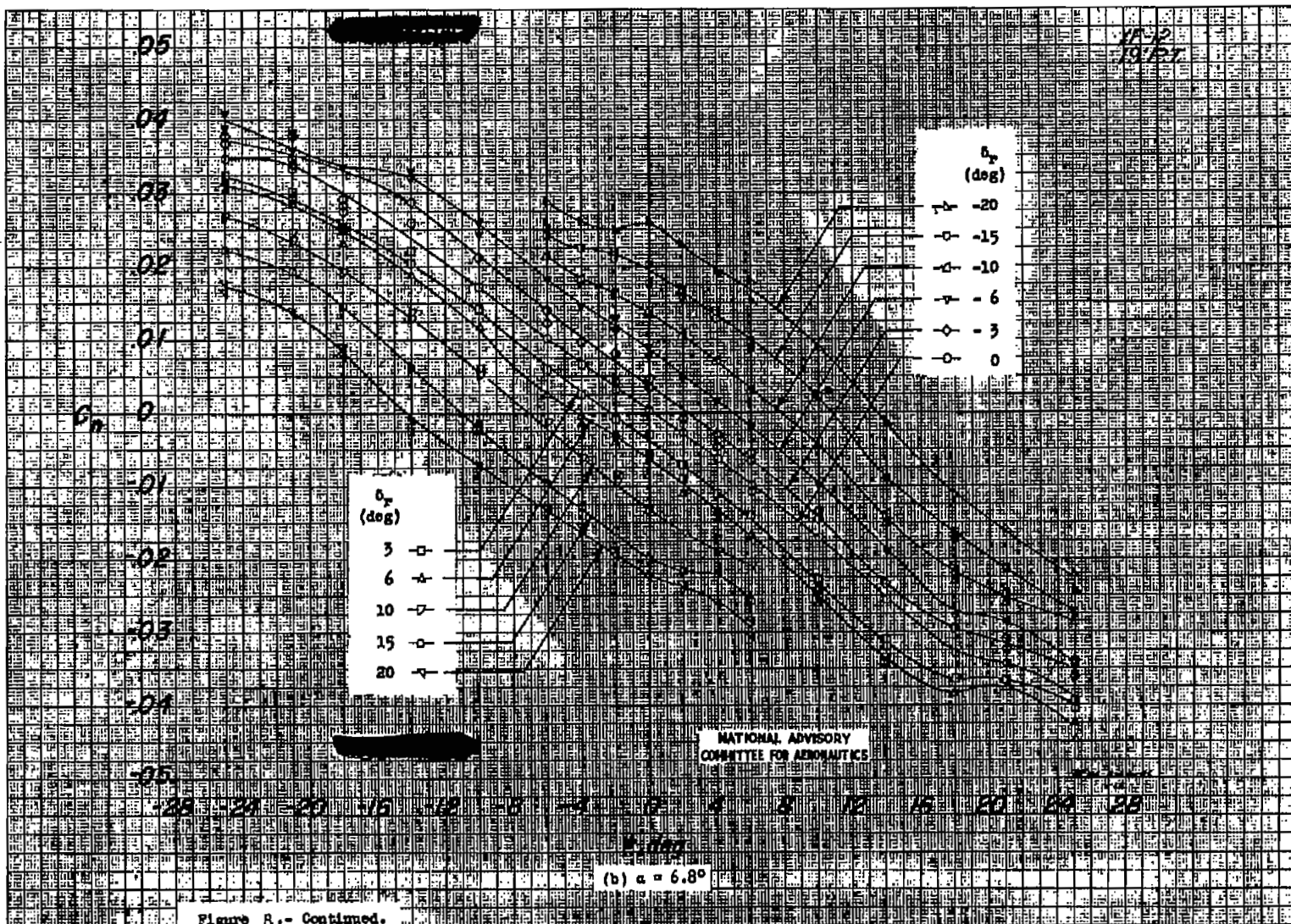


Figure 8.- Continued.

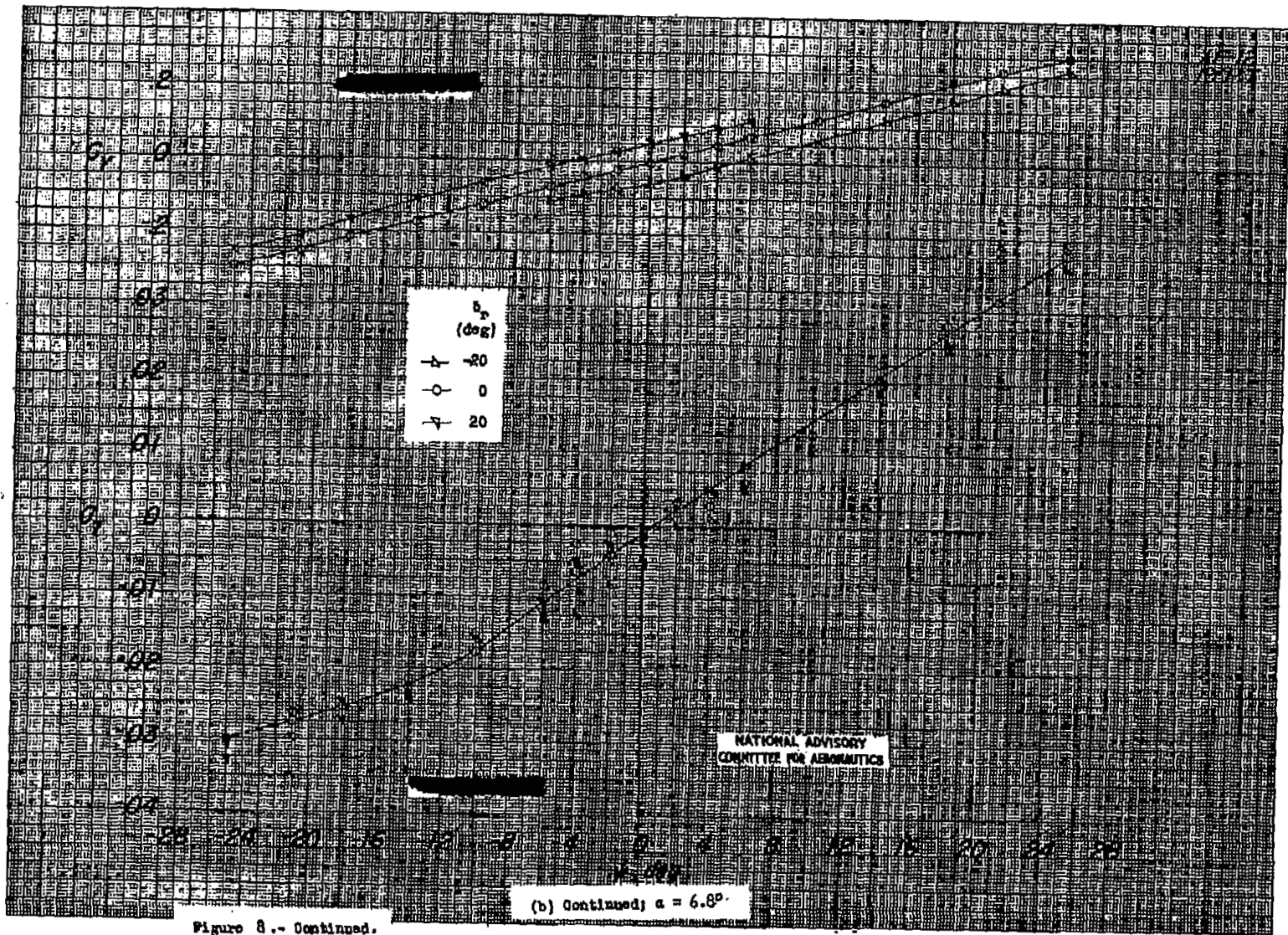


Figure 8.- Continued.



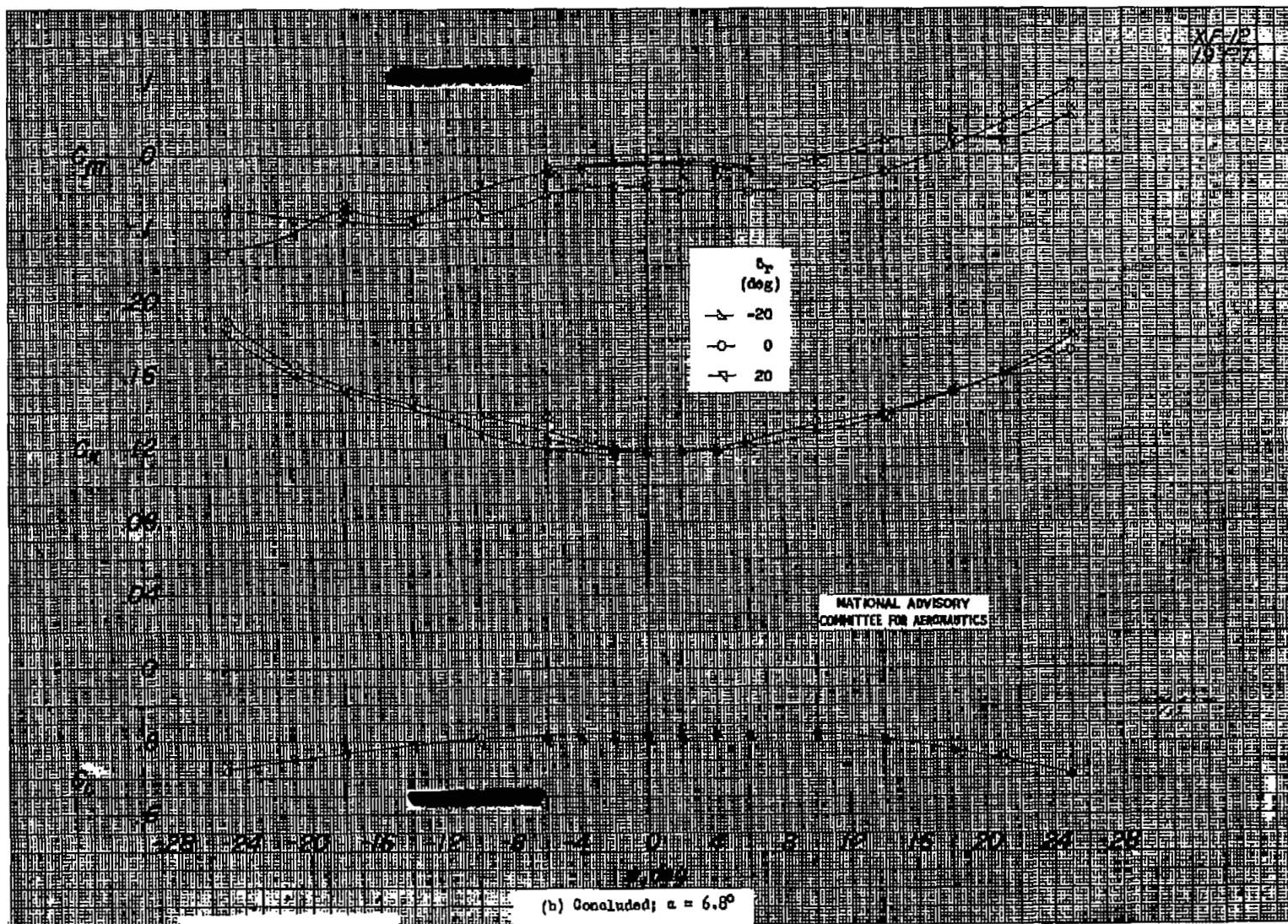


Figure 8.- Continued.

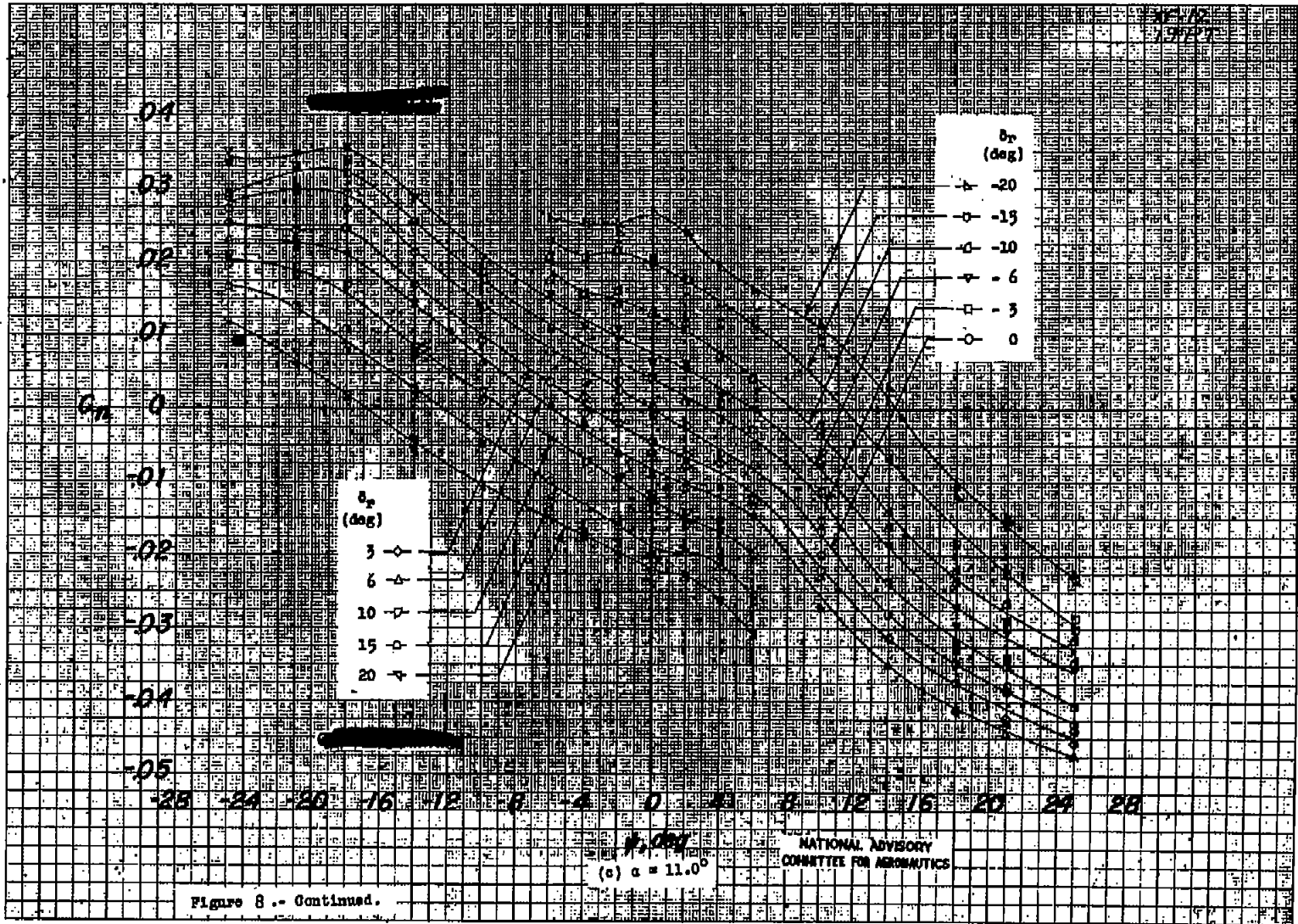


Figure 8.- Continued.

(c) $\alpha = 11.0^\circ$

NATIONAL ADVISORY
COMMITTEE FOR AERONAUTICS

2047

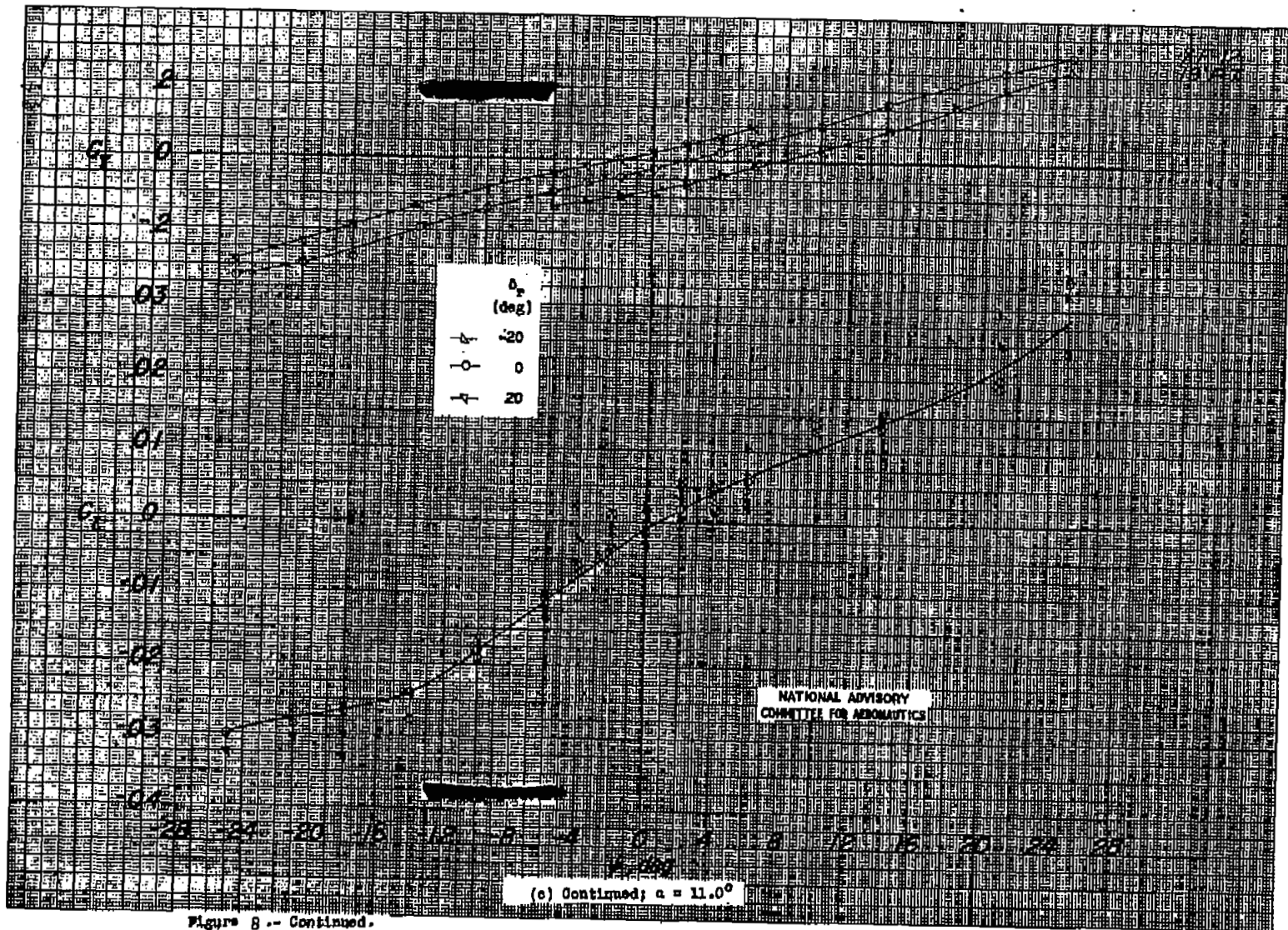
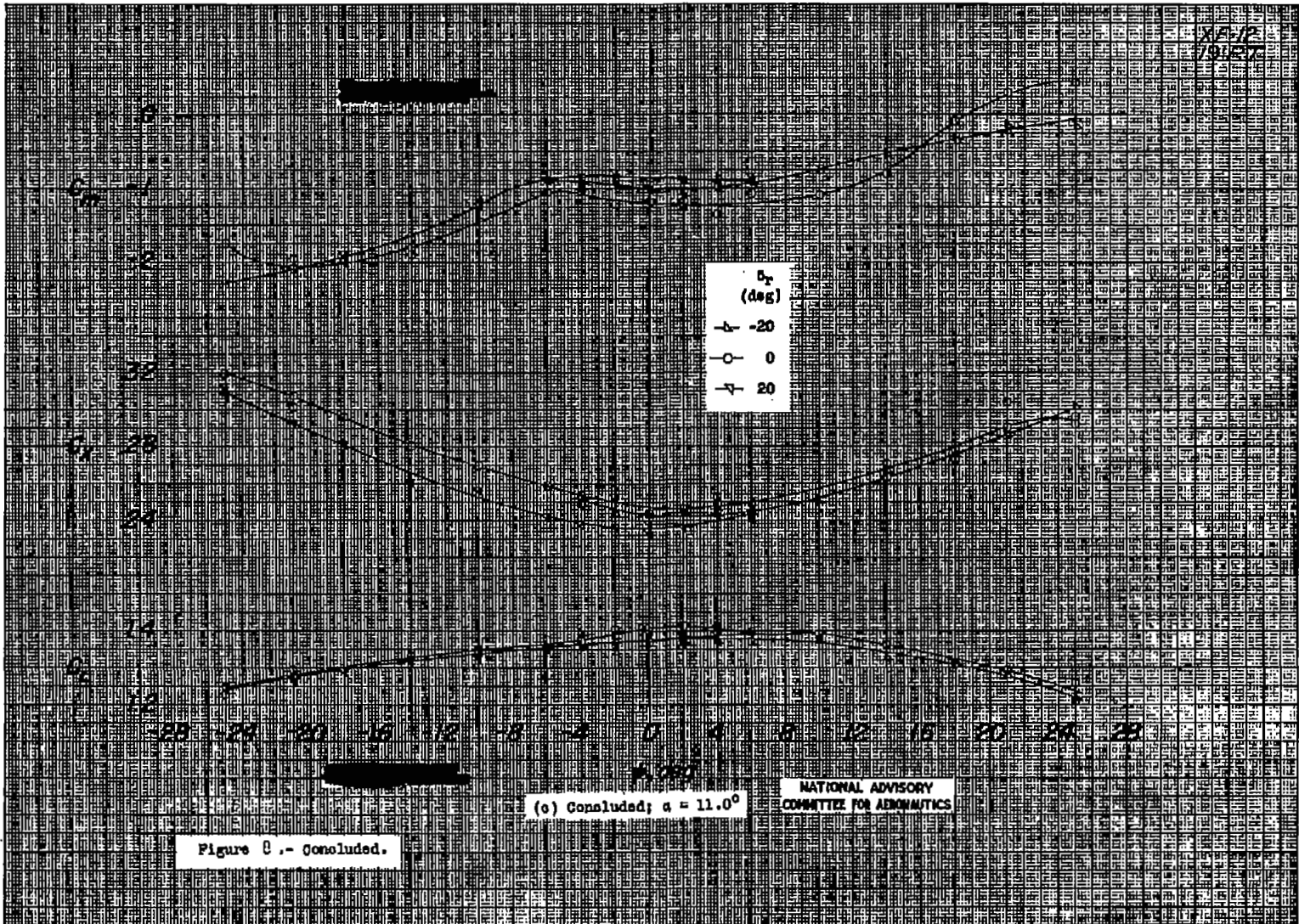
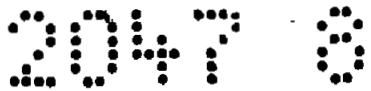


Figure 8 -- Continued.



2047

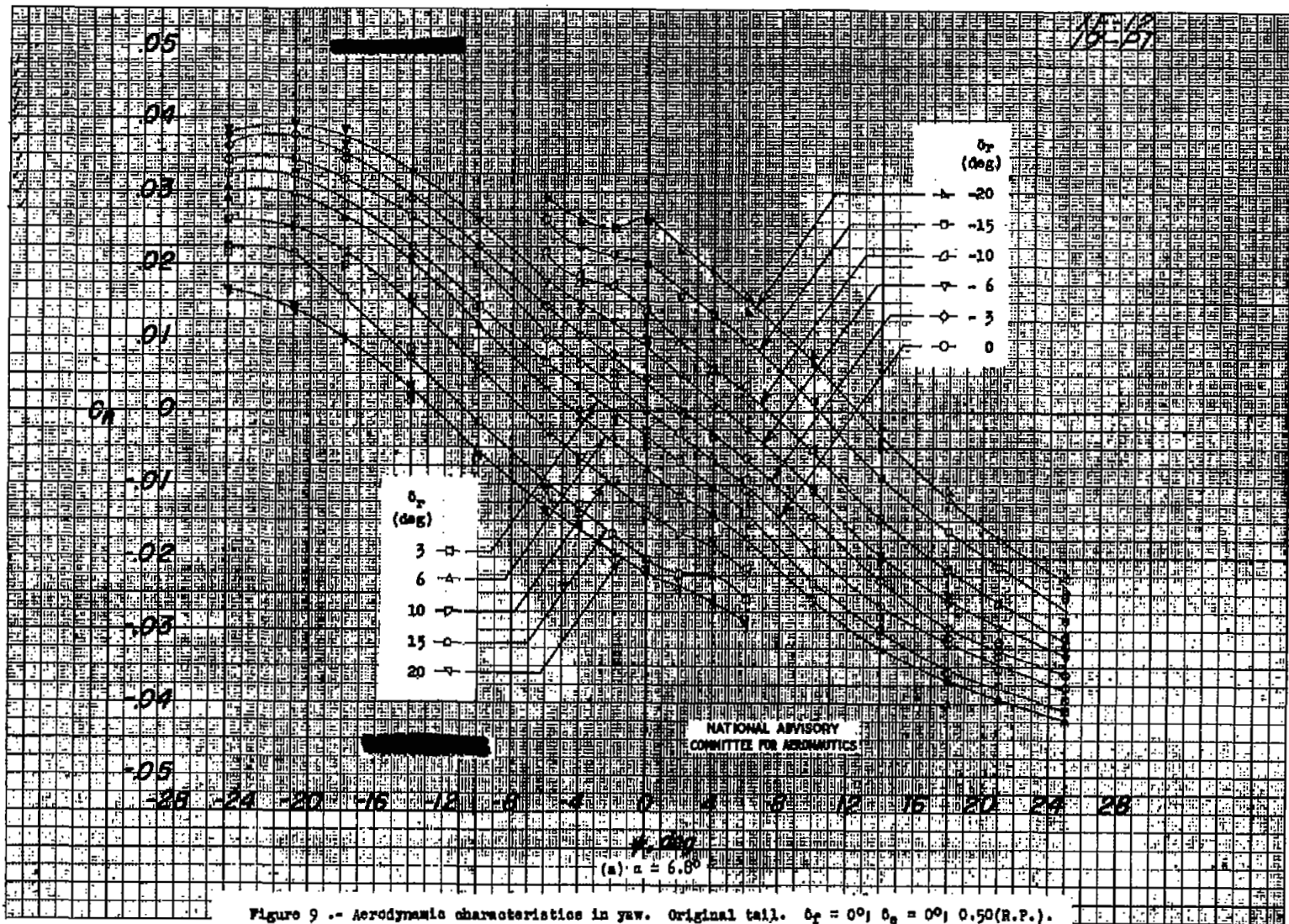


Figure 9 -- Aerodynamic characteristics in yaw. Original tail. $\delta_p = 0^\circ$; $\delta_e = 0^\circ$; 0.50(R.P.).

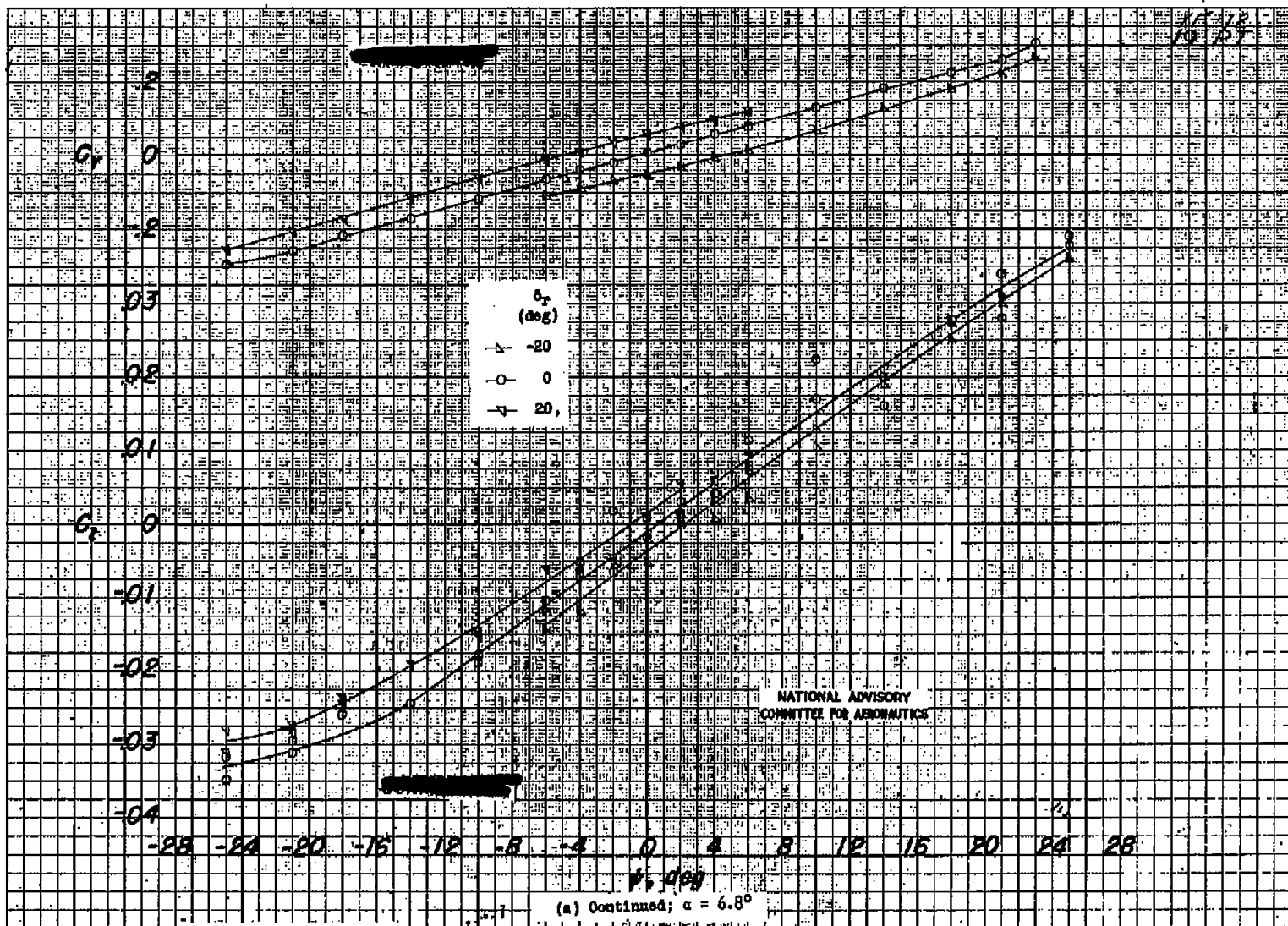


Figure 9.- Continued.

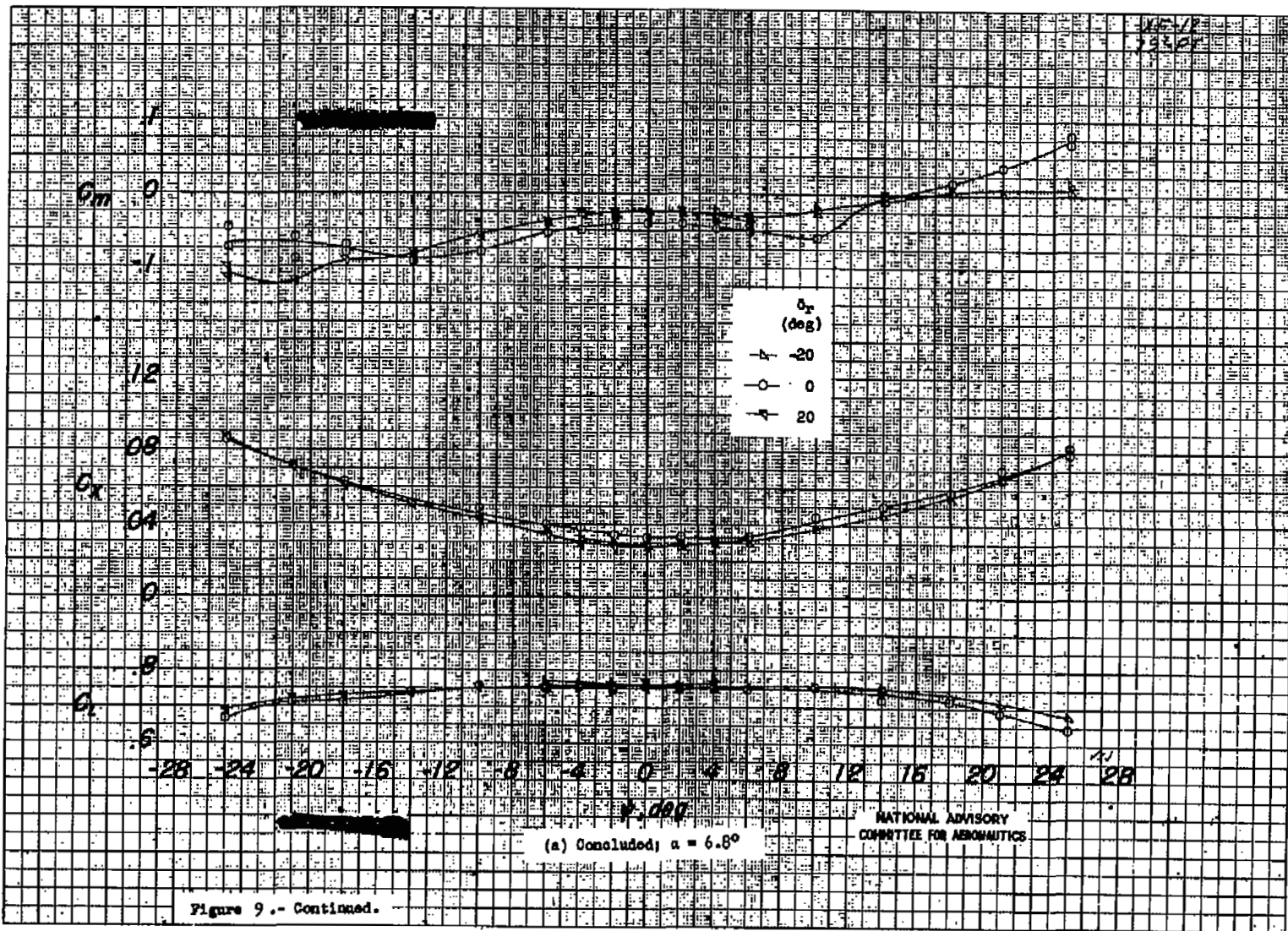
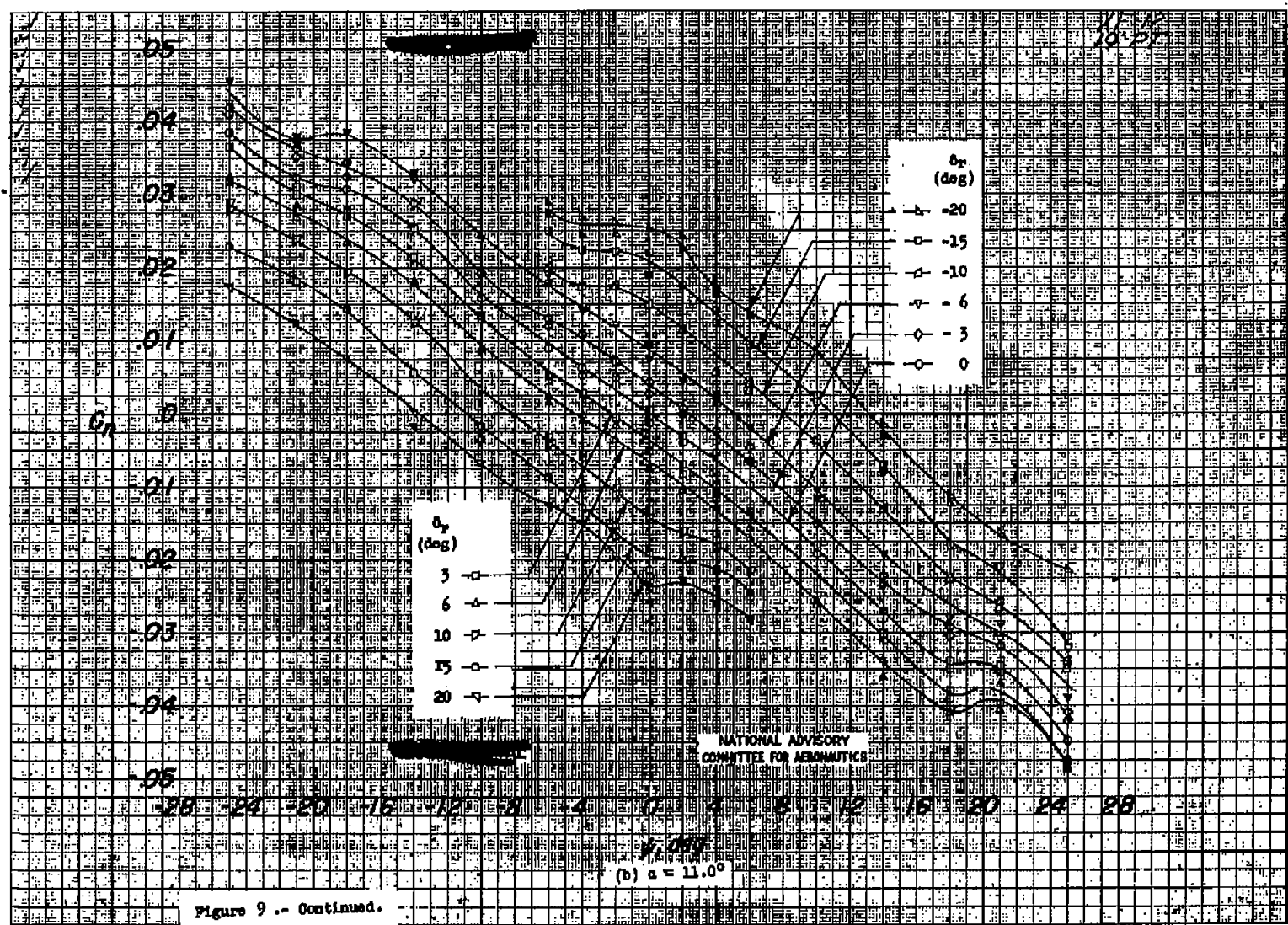


Figure 9.- Continued.

Fig. 9a conc.



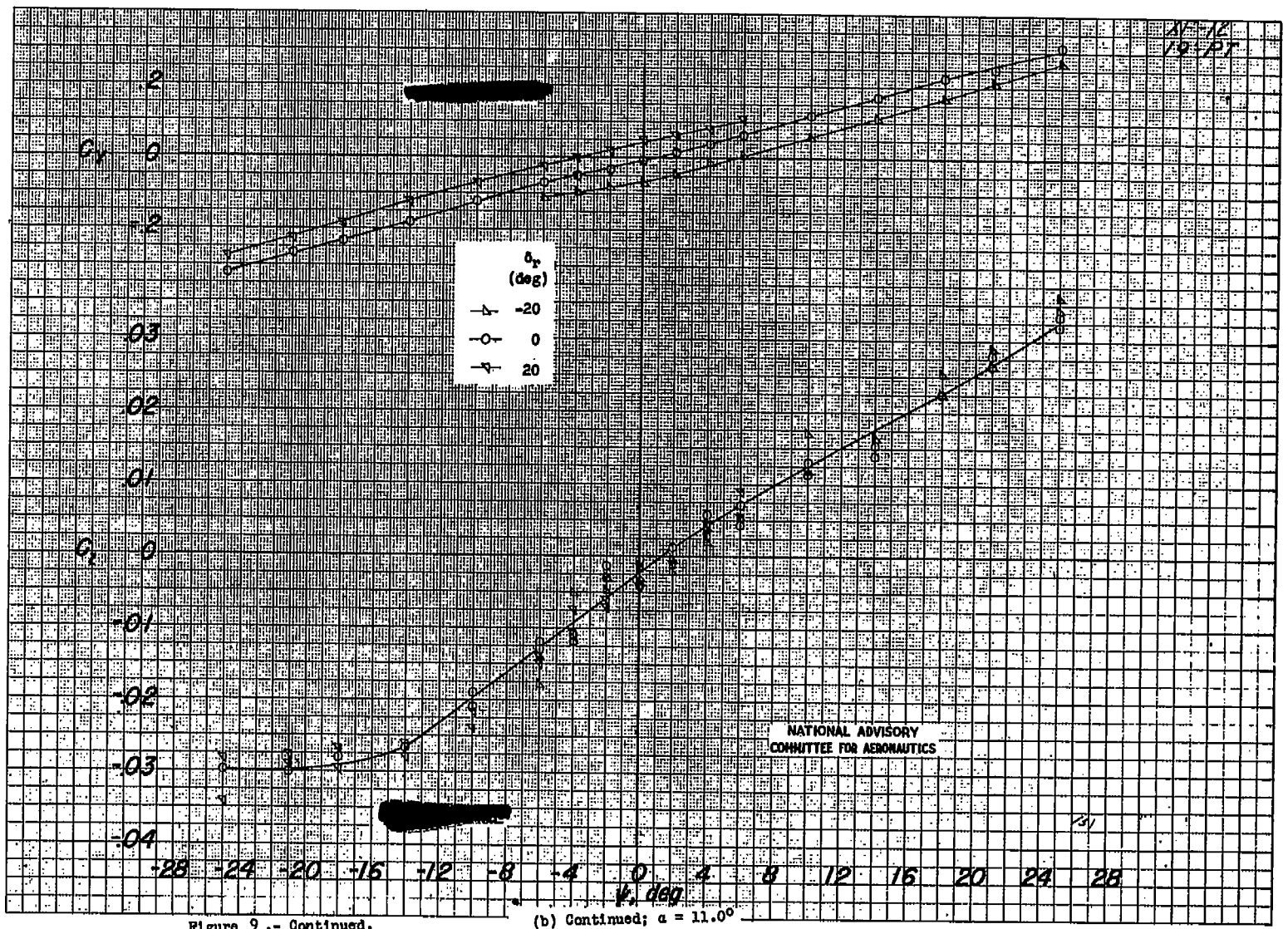


Figure 9.- Continued.

(b) Continued; $\alpha = 11.0^\circ$

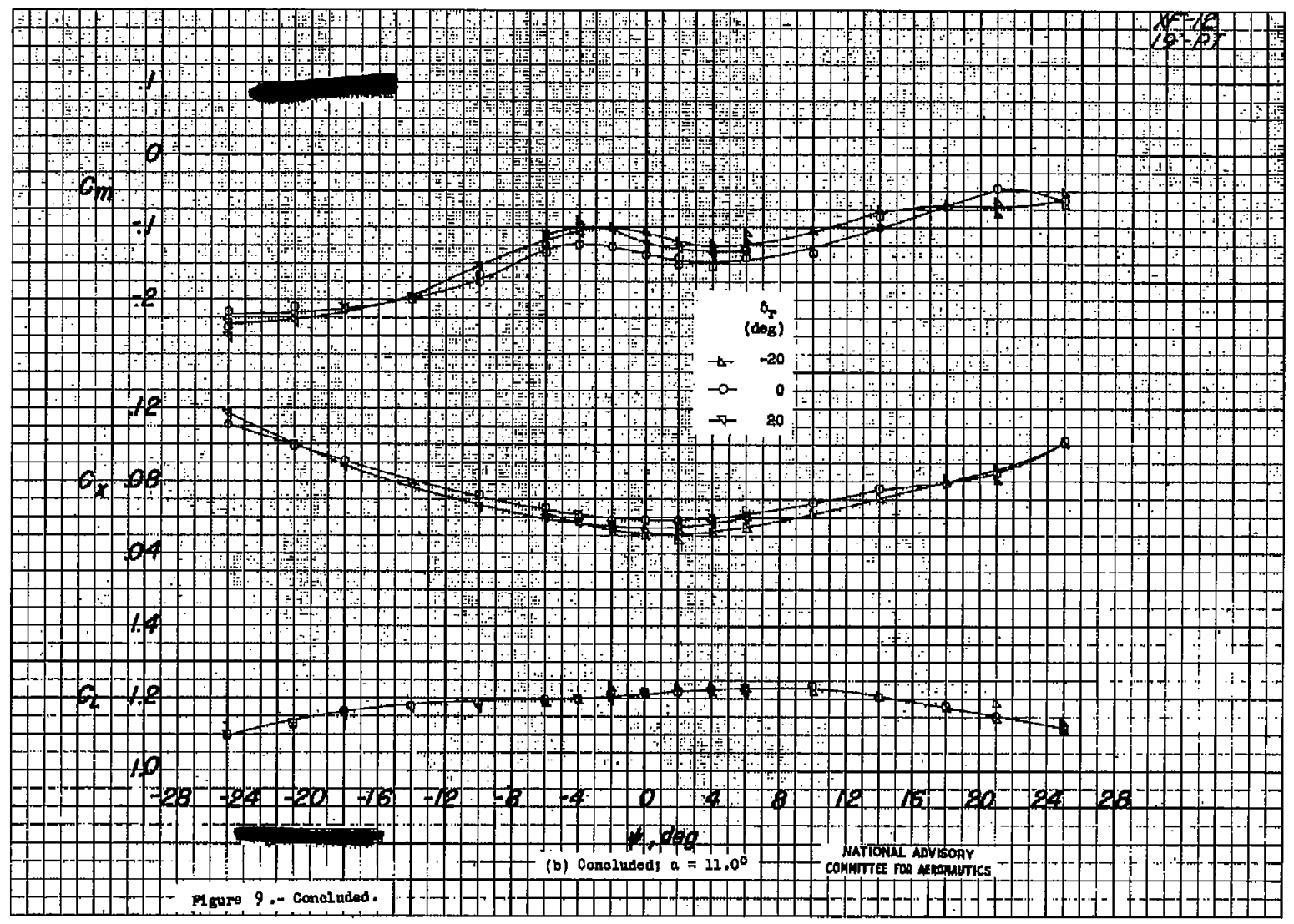


Figure 9.- Concluded.

Fig. 9b conc.

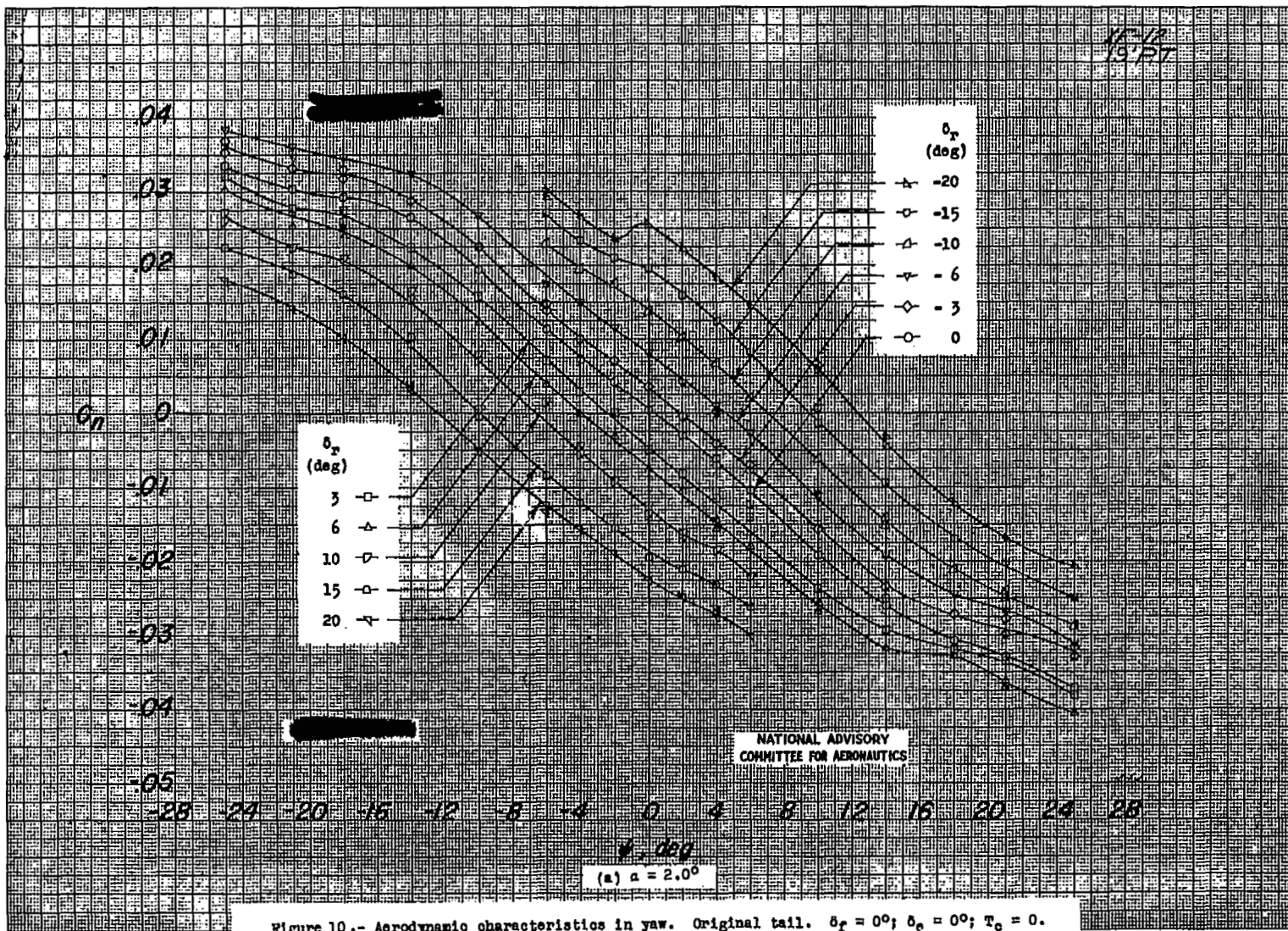


Figure 10.- Aerodynamic characteristics in yaw. Original tail. $\delta_f = 0^\circ$; $\delta_e = 0^\circ$; $T_c = 0$.

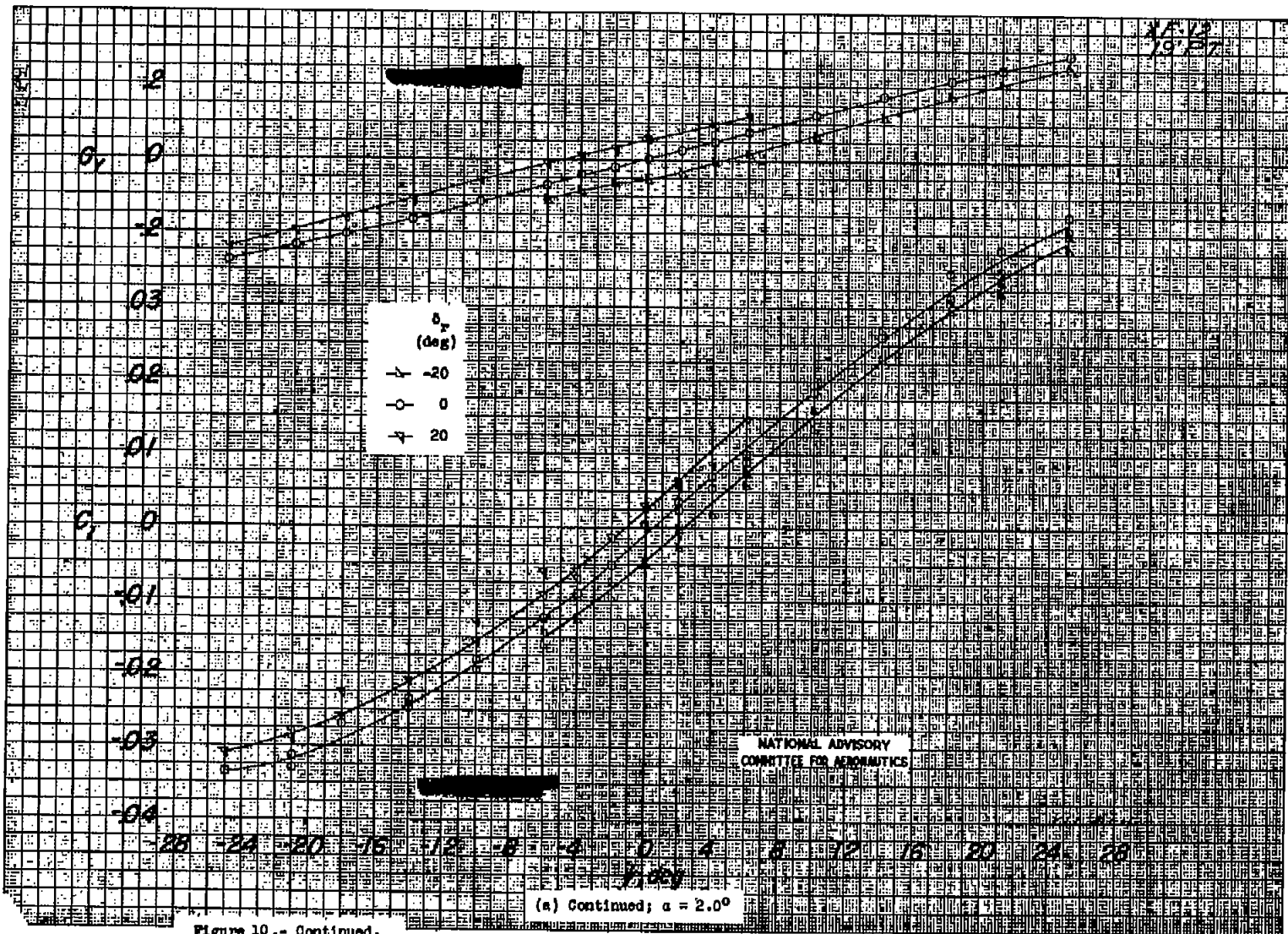
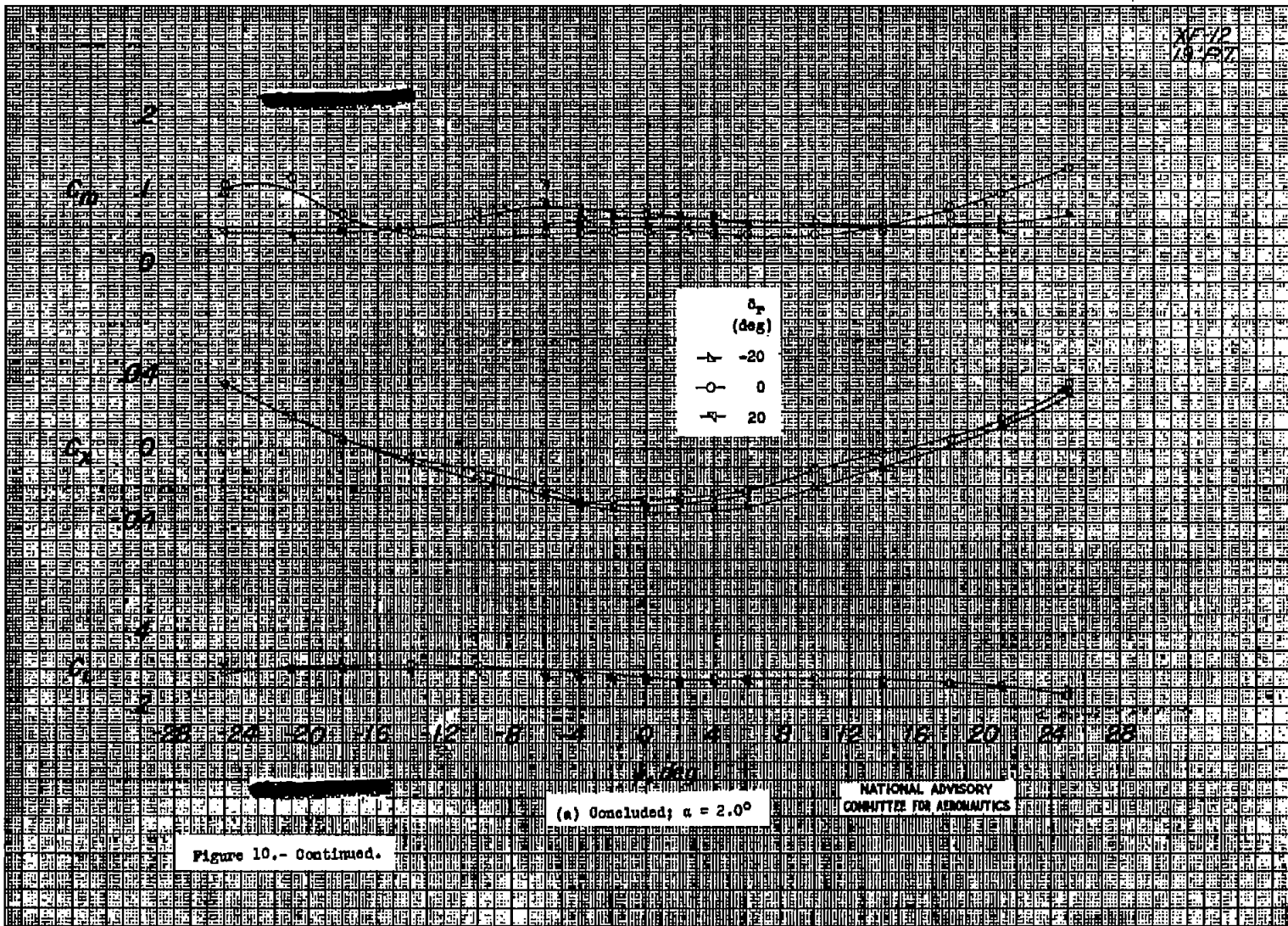
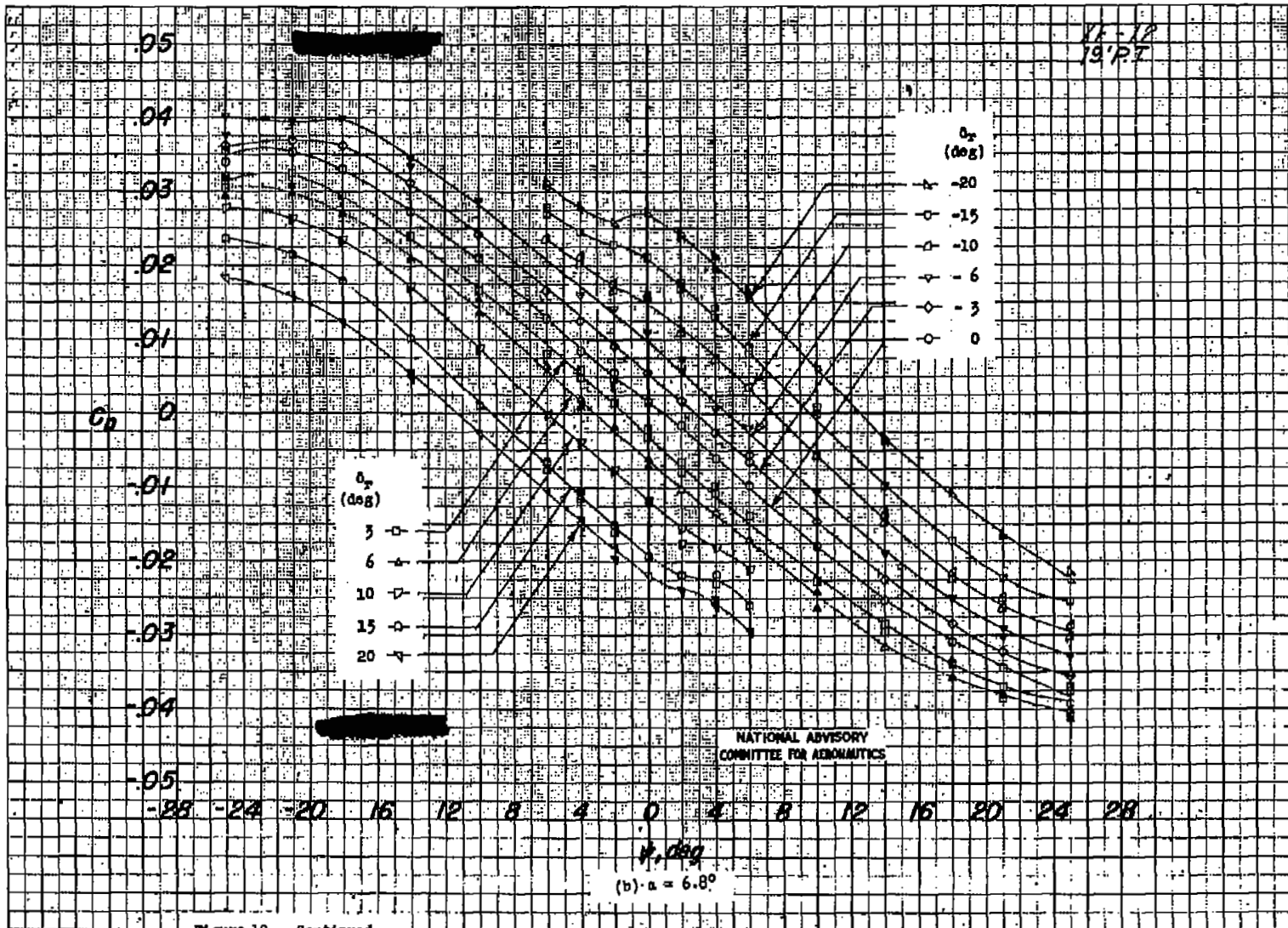


Figure 10.- Continued.





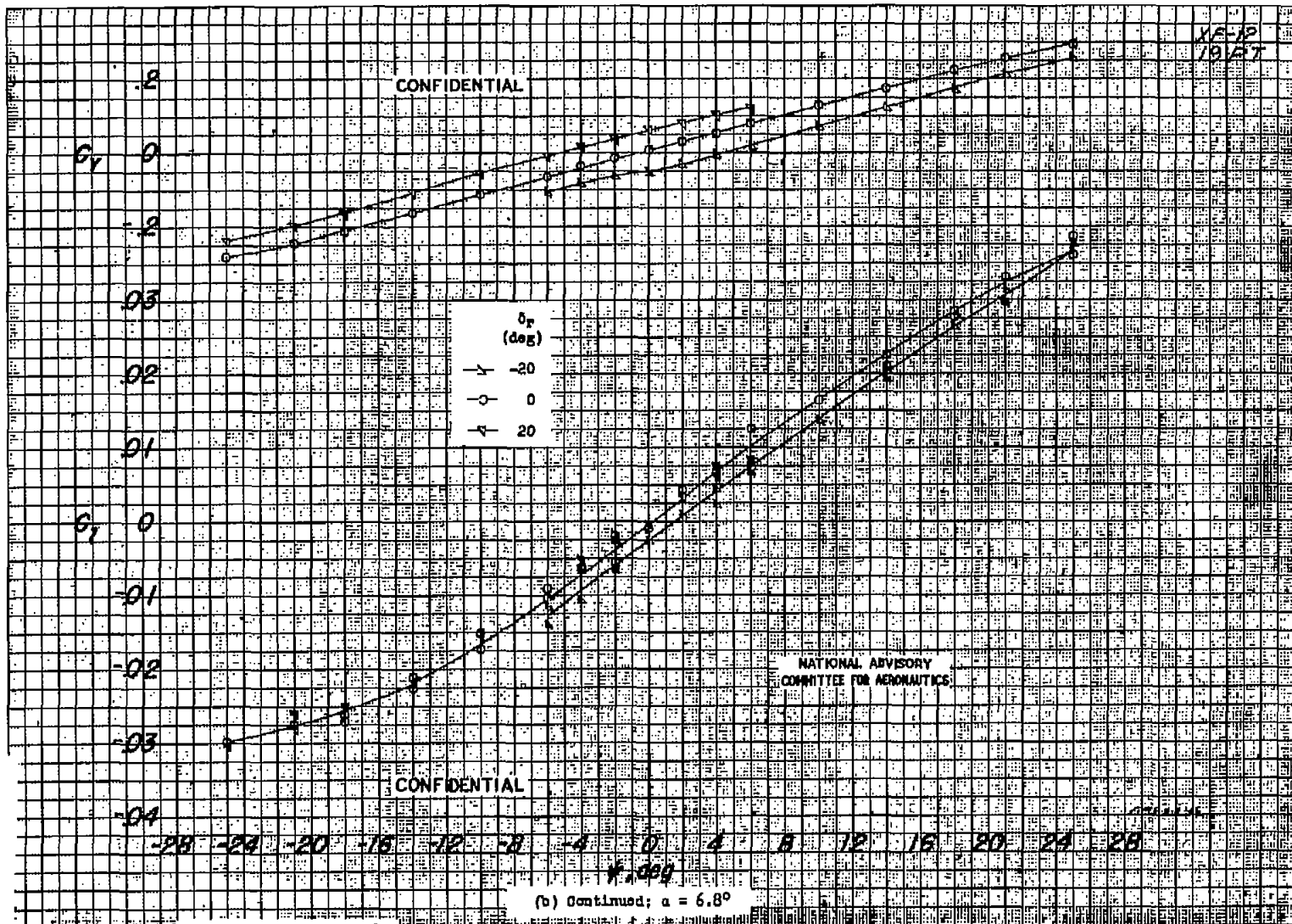


Figure 10 -- Continued.

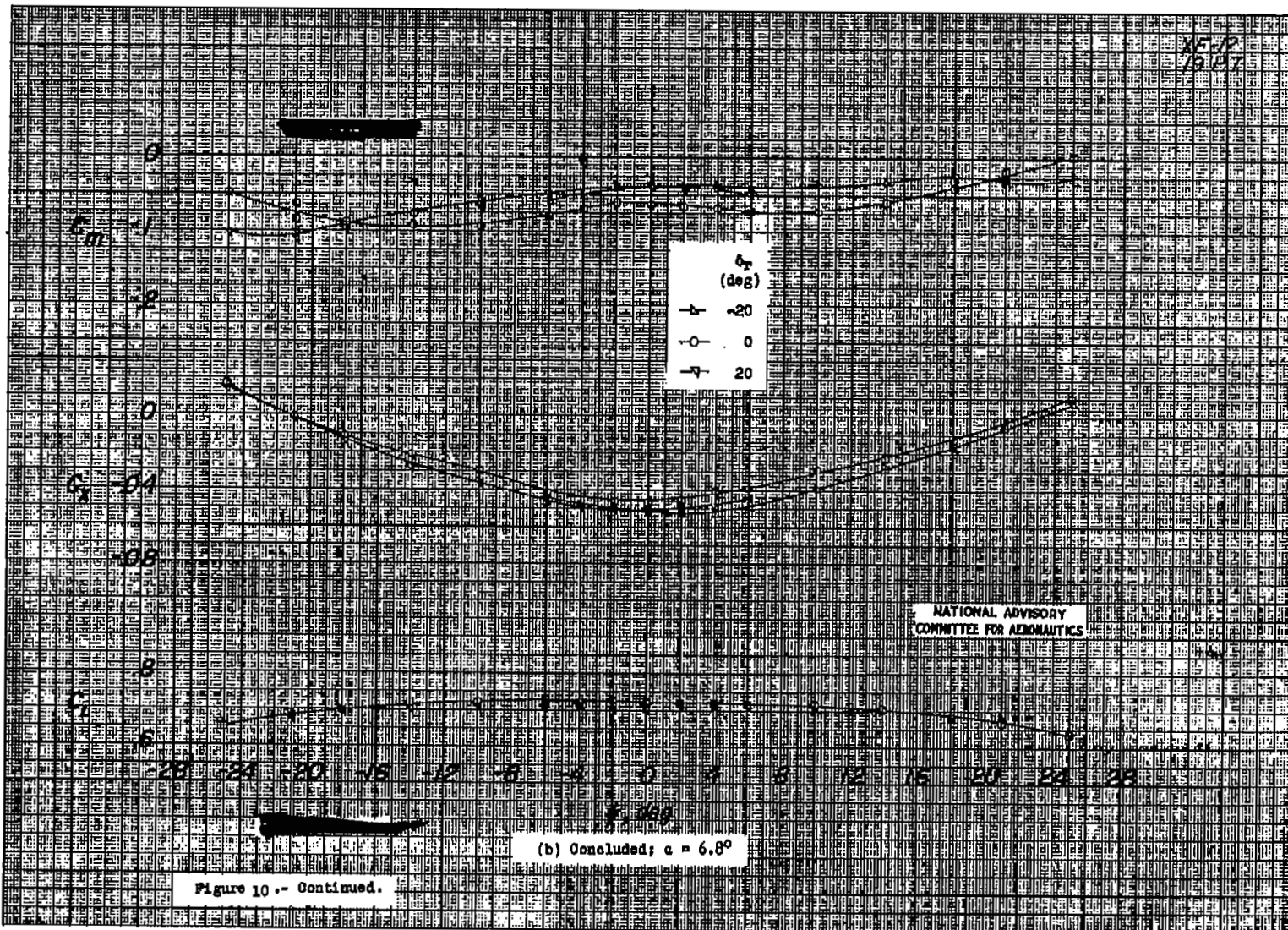


Fig. 10b conc.

20470

NACA RM No. L7B21

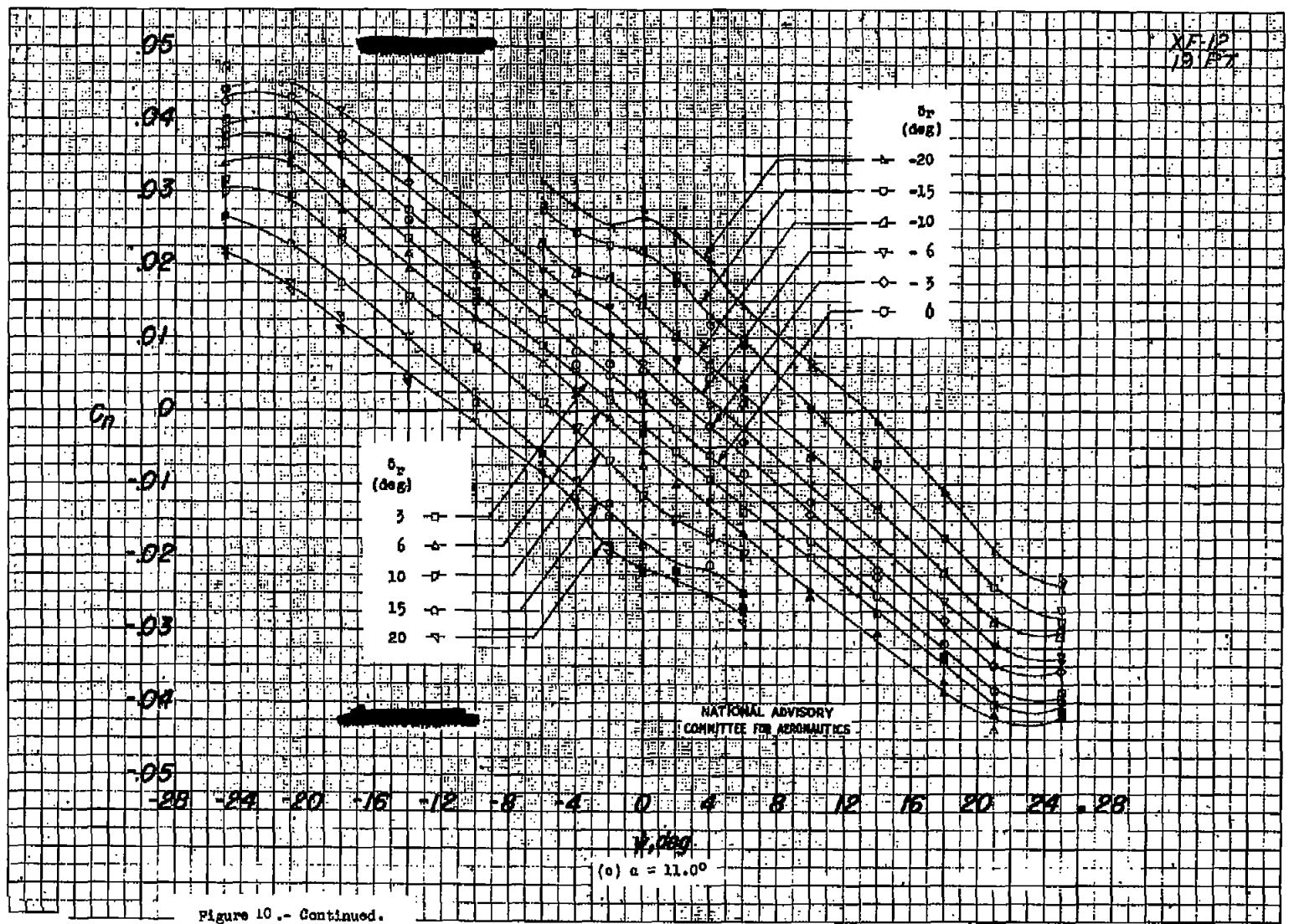


Figure 10.- Continued.

Fig. 10c

20470

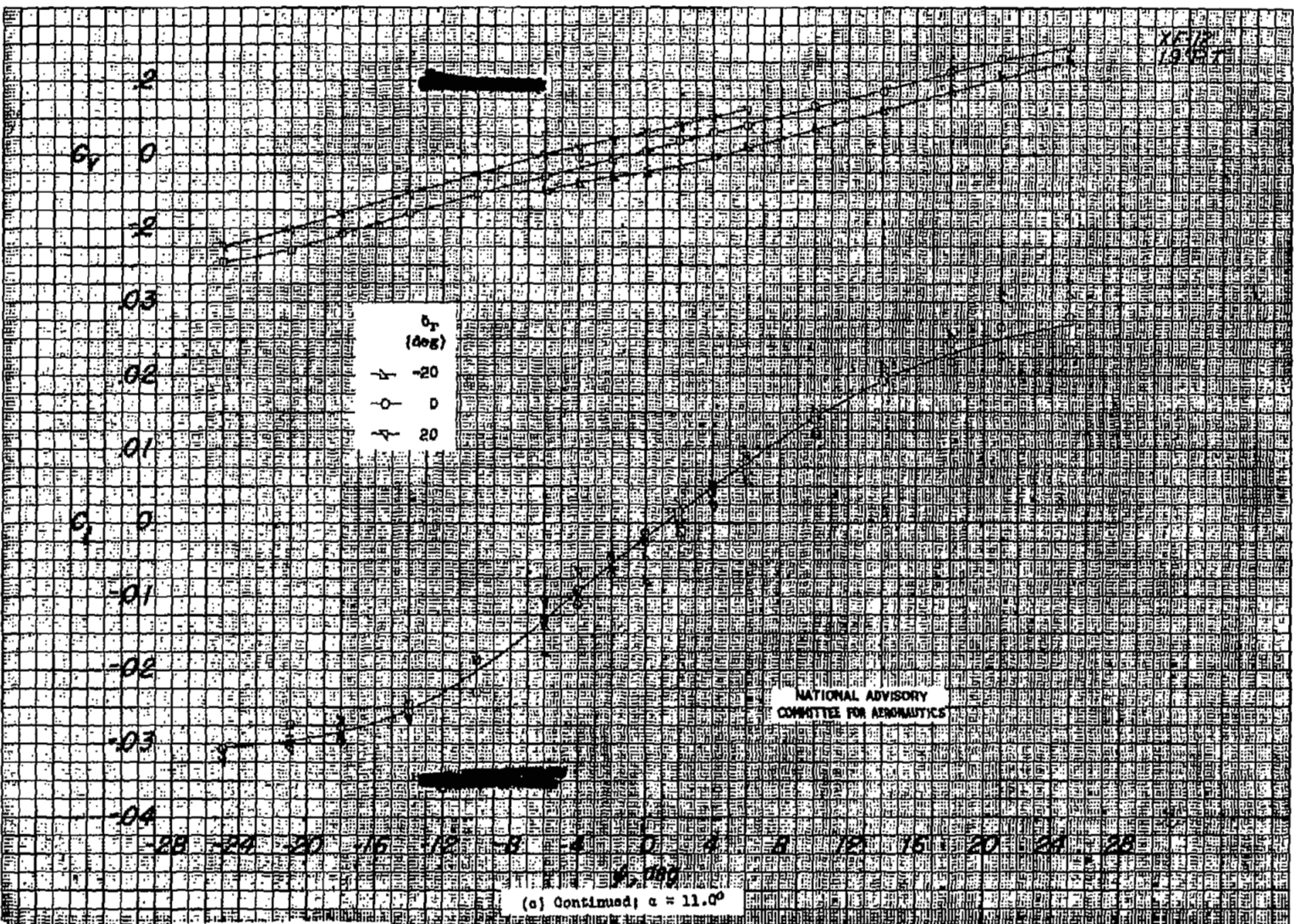


Figure 10.- Continued.

204710

NACA RM No. L7B21

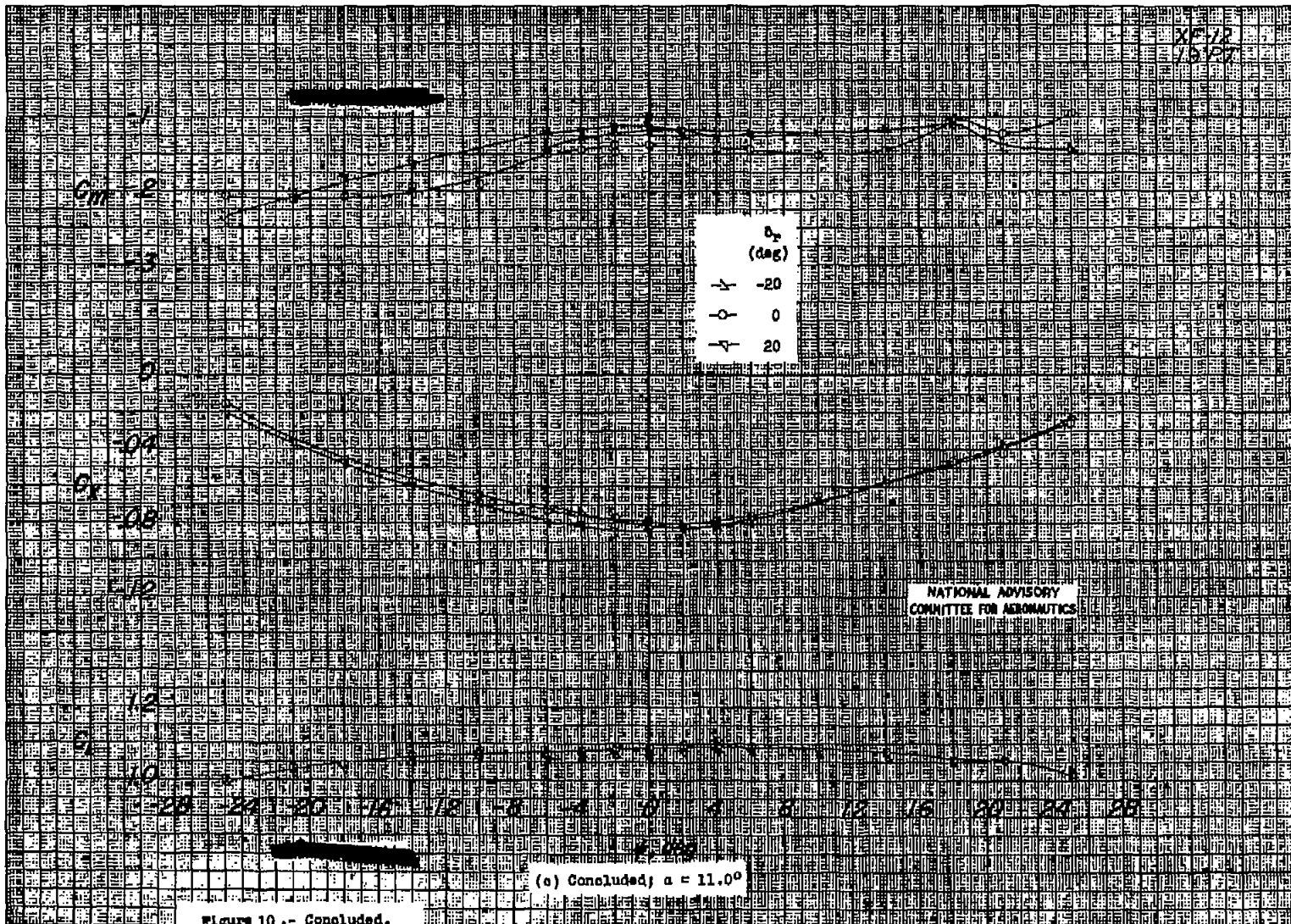
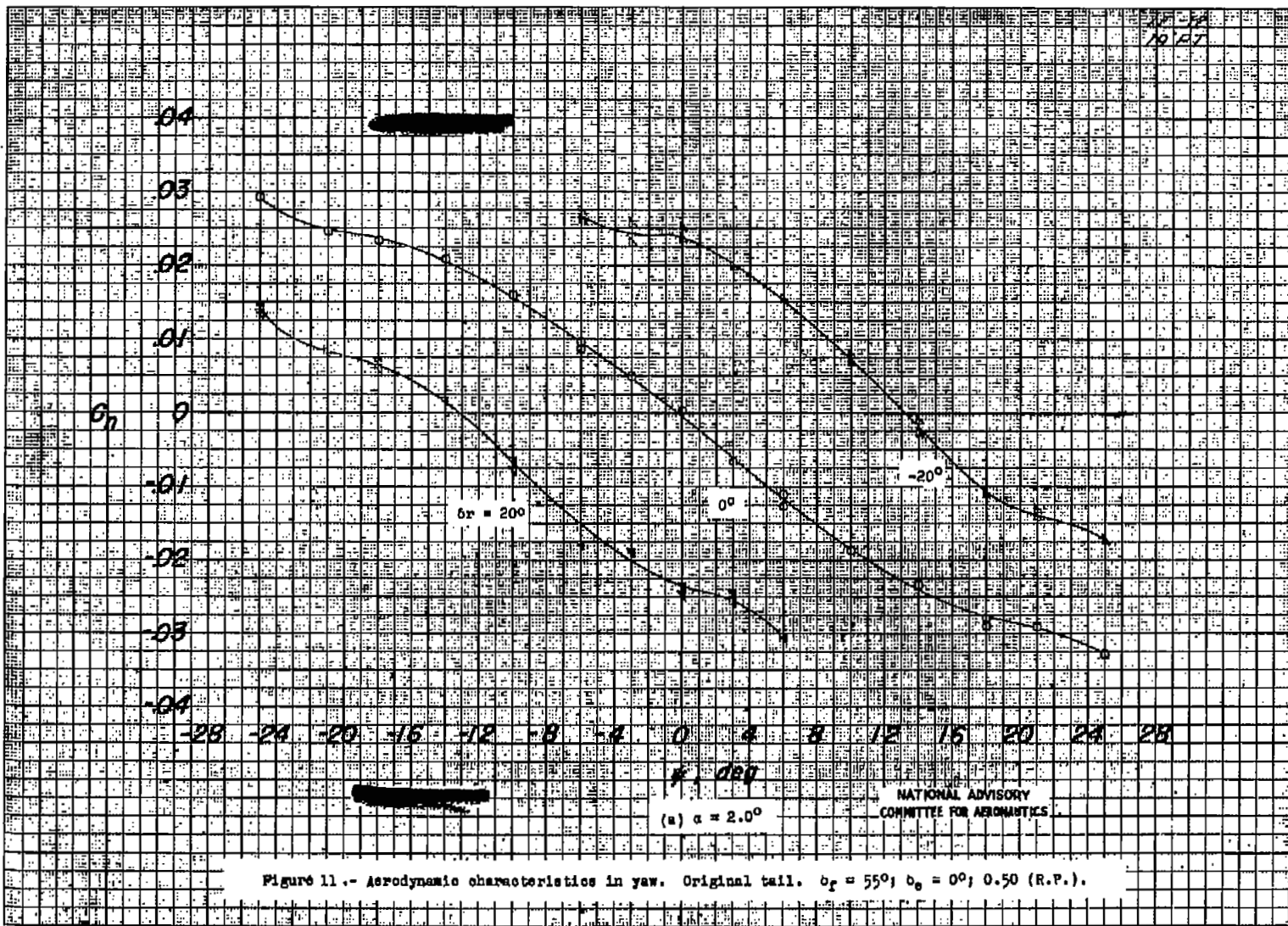


Fig. 10c conc.

20471



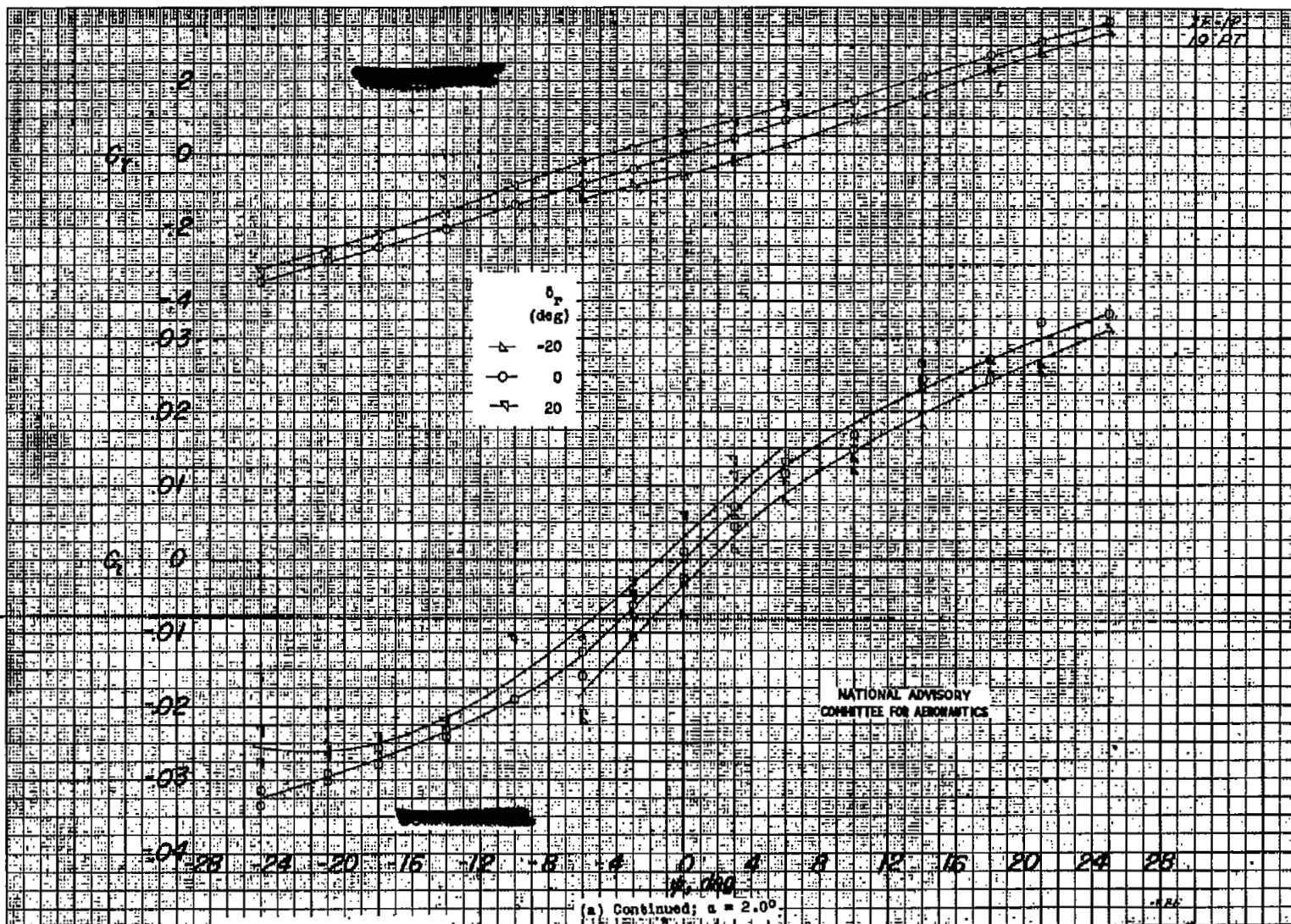


Figure 11.- Continued.

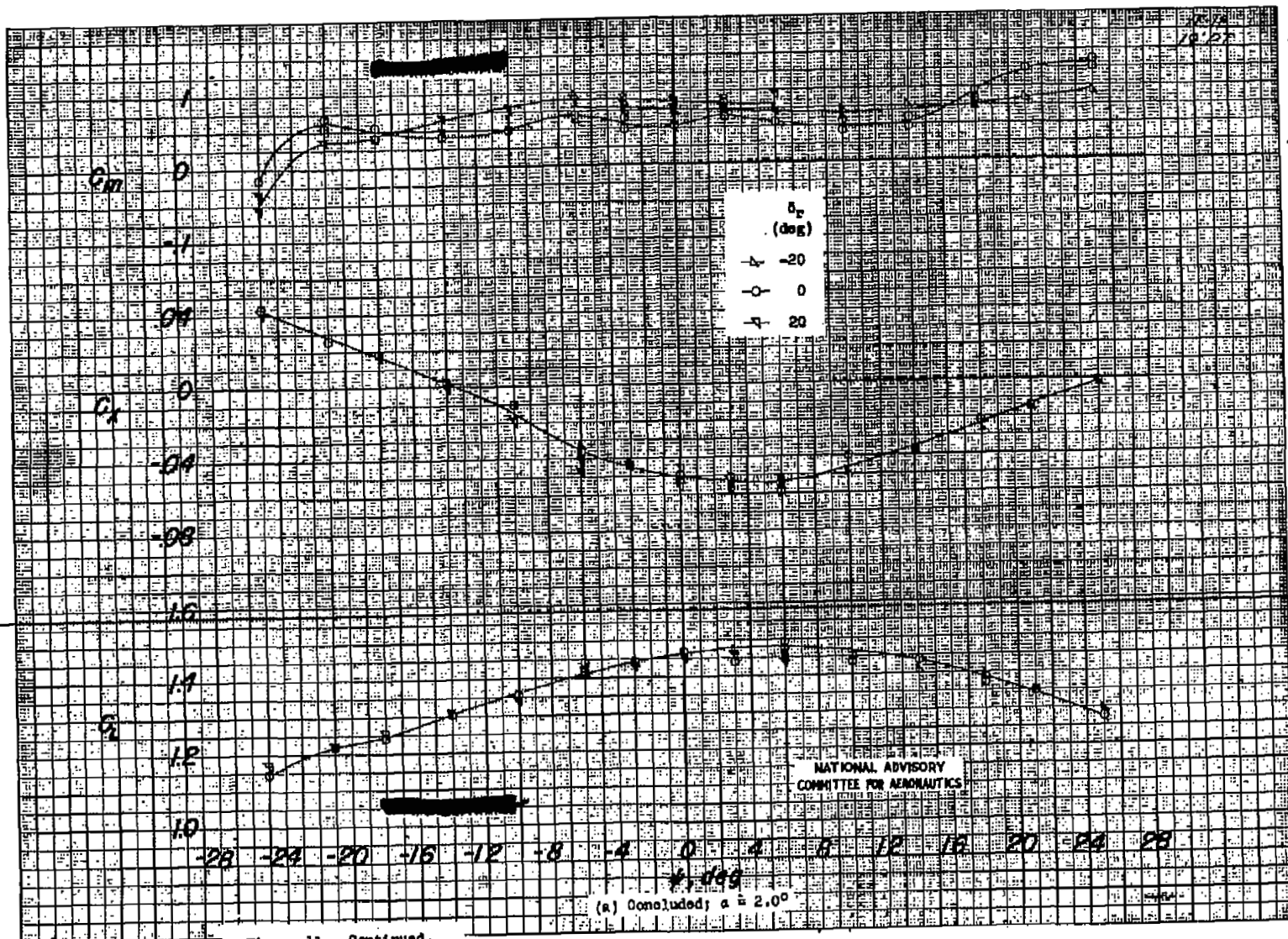
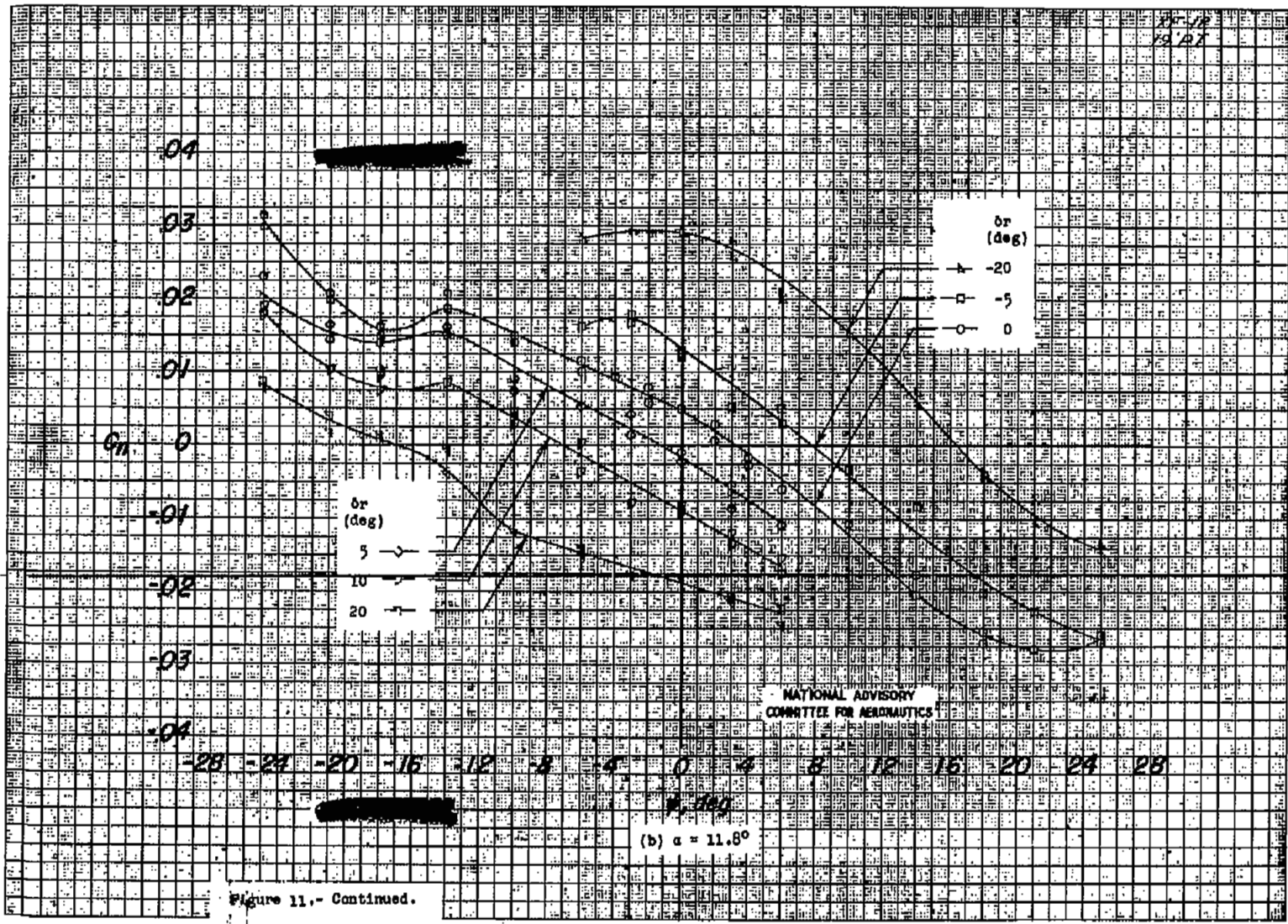


Figure 11.- Continued.

Fig. 11a contc.

20471



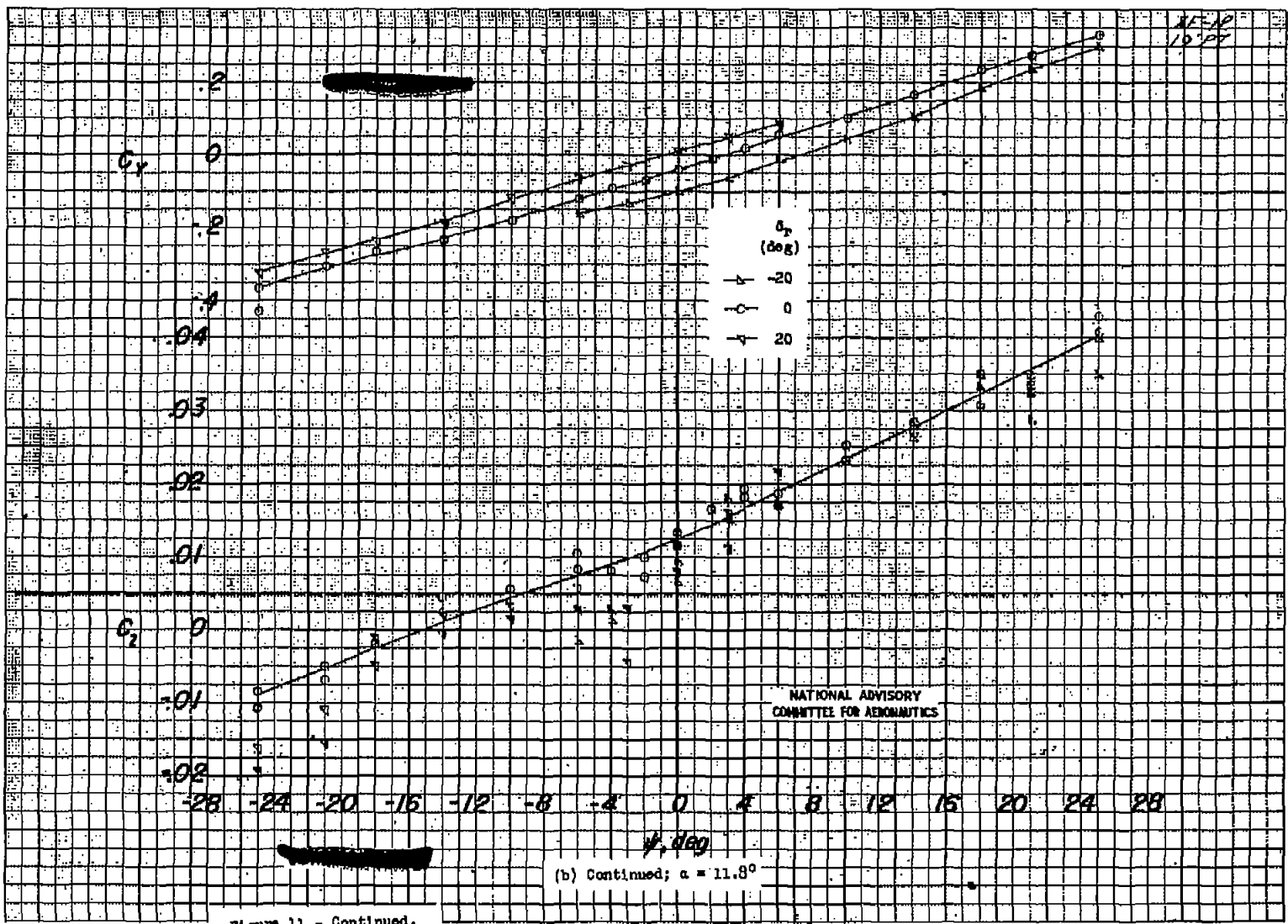


Figure 11.- Continued.

(b) Continued; $\alpha = 11.8^\circ$

FIG. 11b cont.

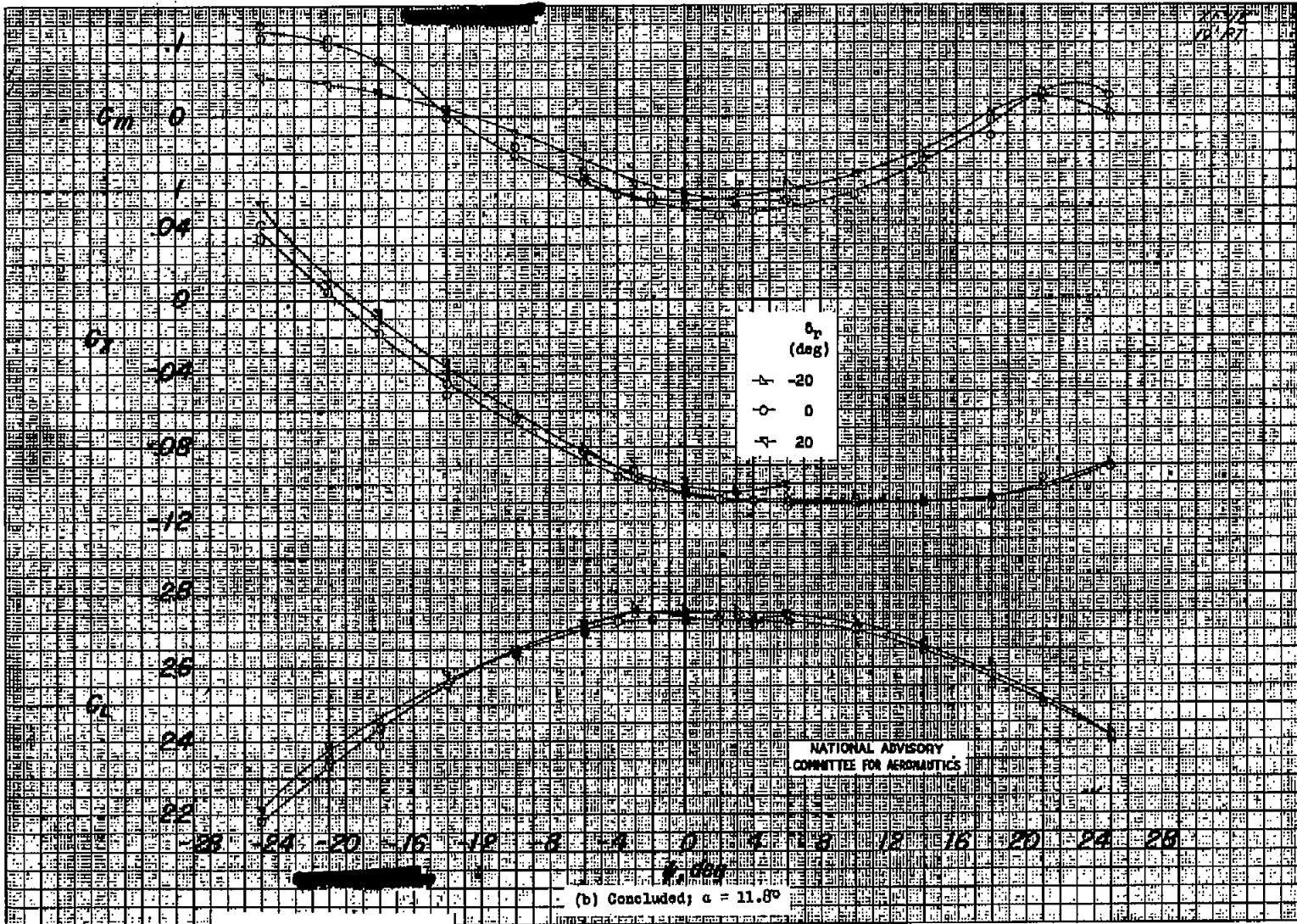
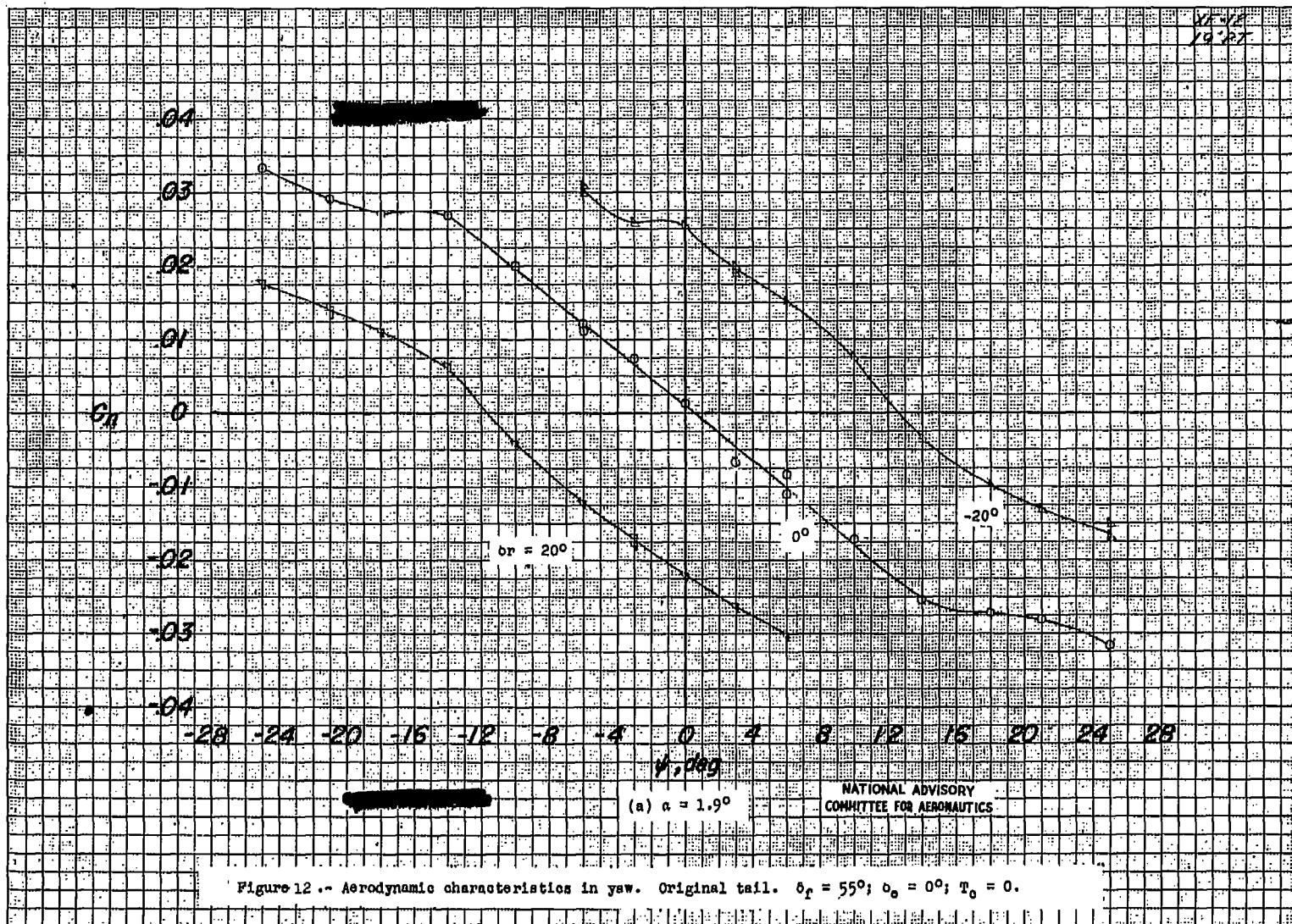


Figure 11.- Concluded.



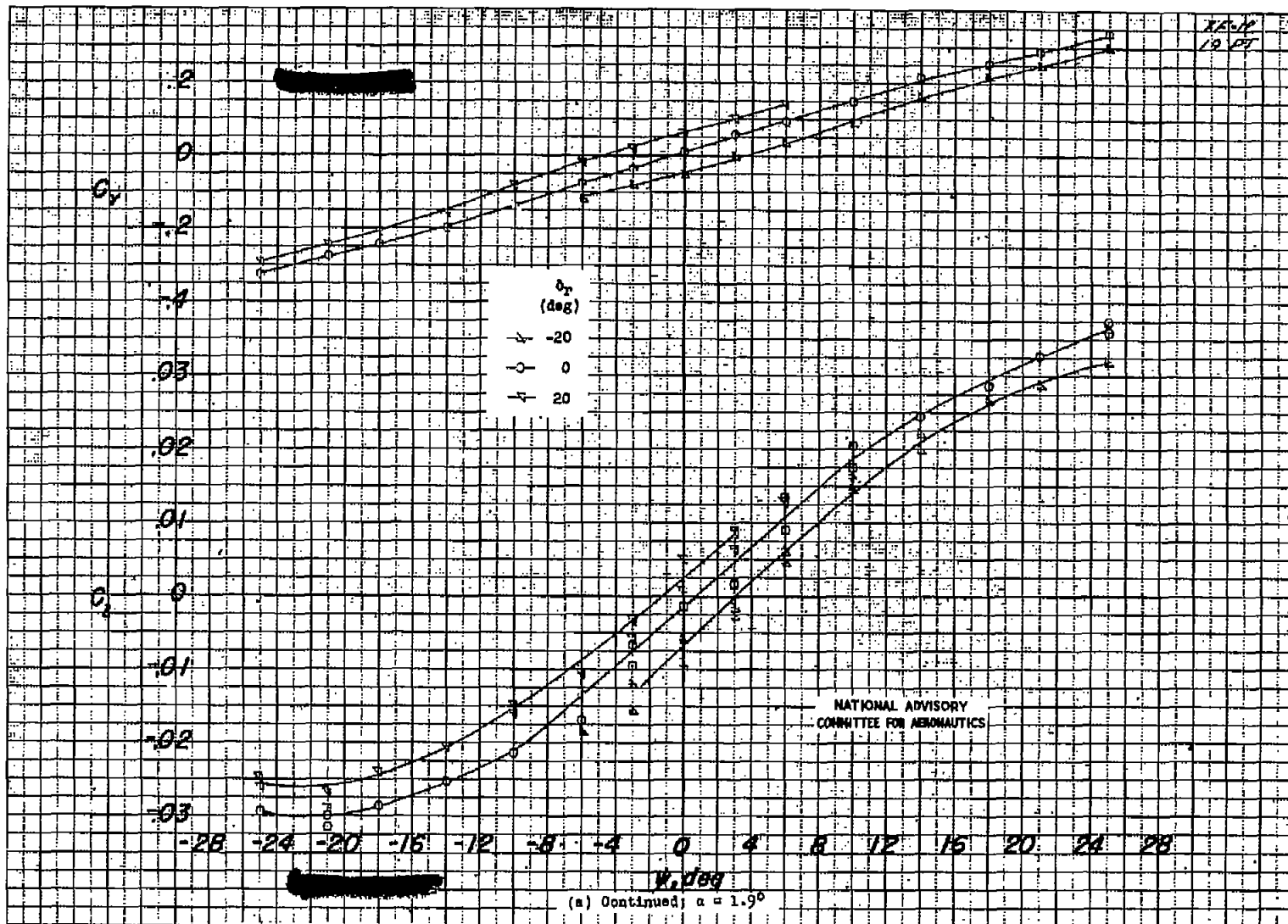


Figure 12.- Continued.

20475

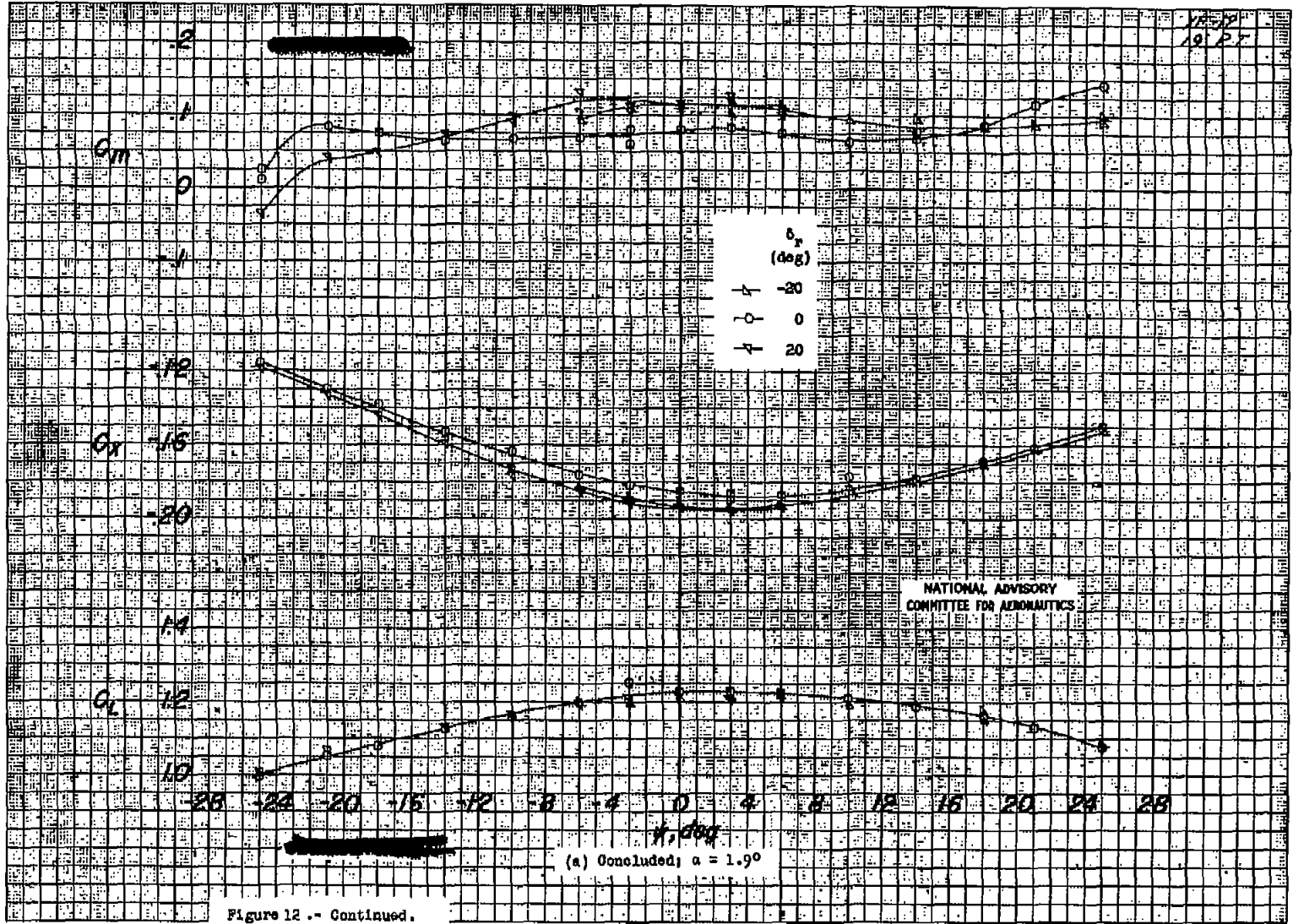


Figure 12 -- Continued.

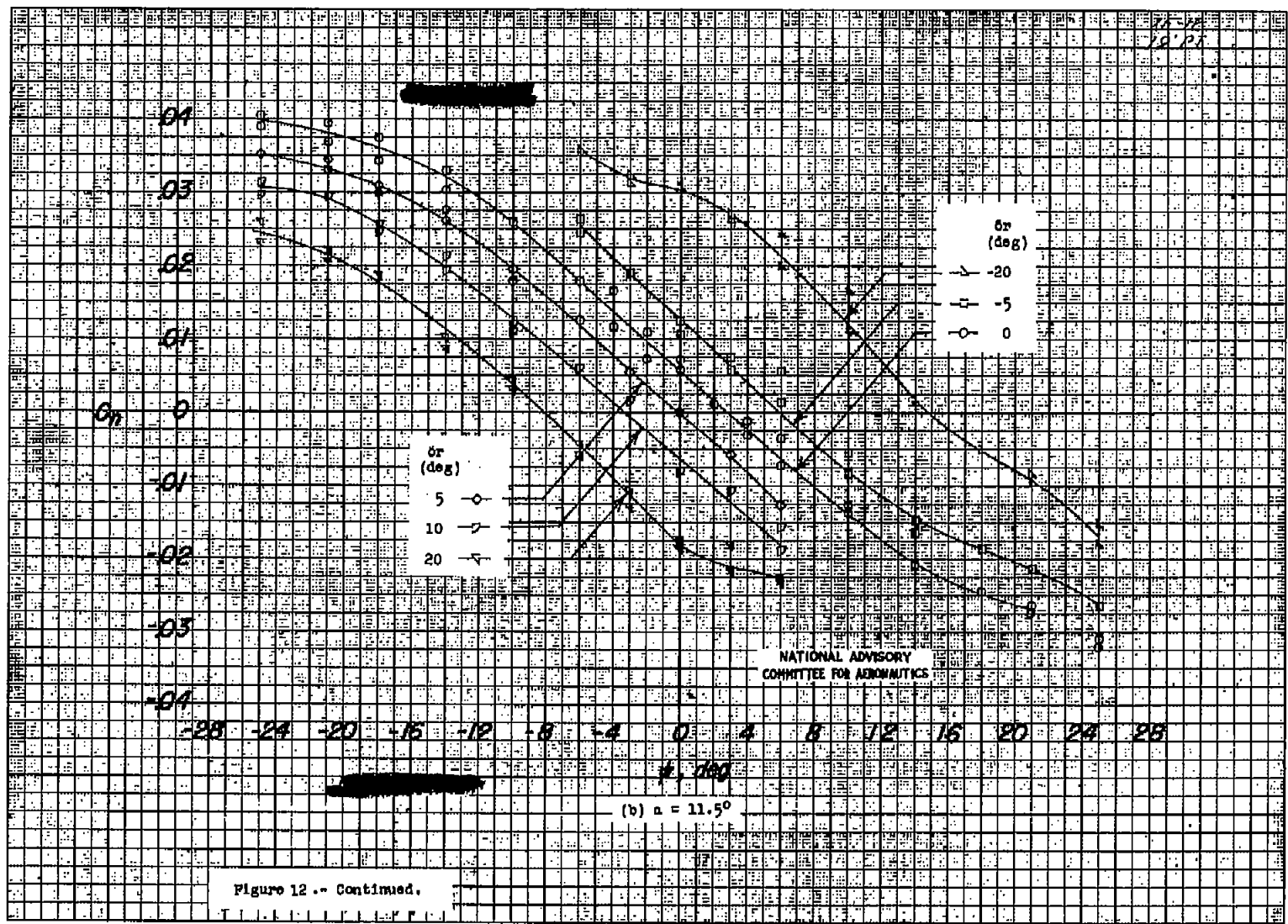


Figure 12 -- Continued.

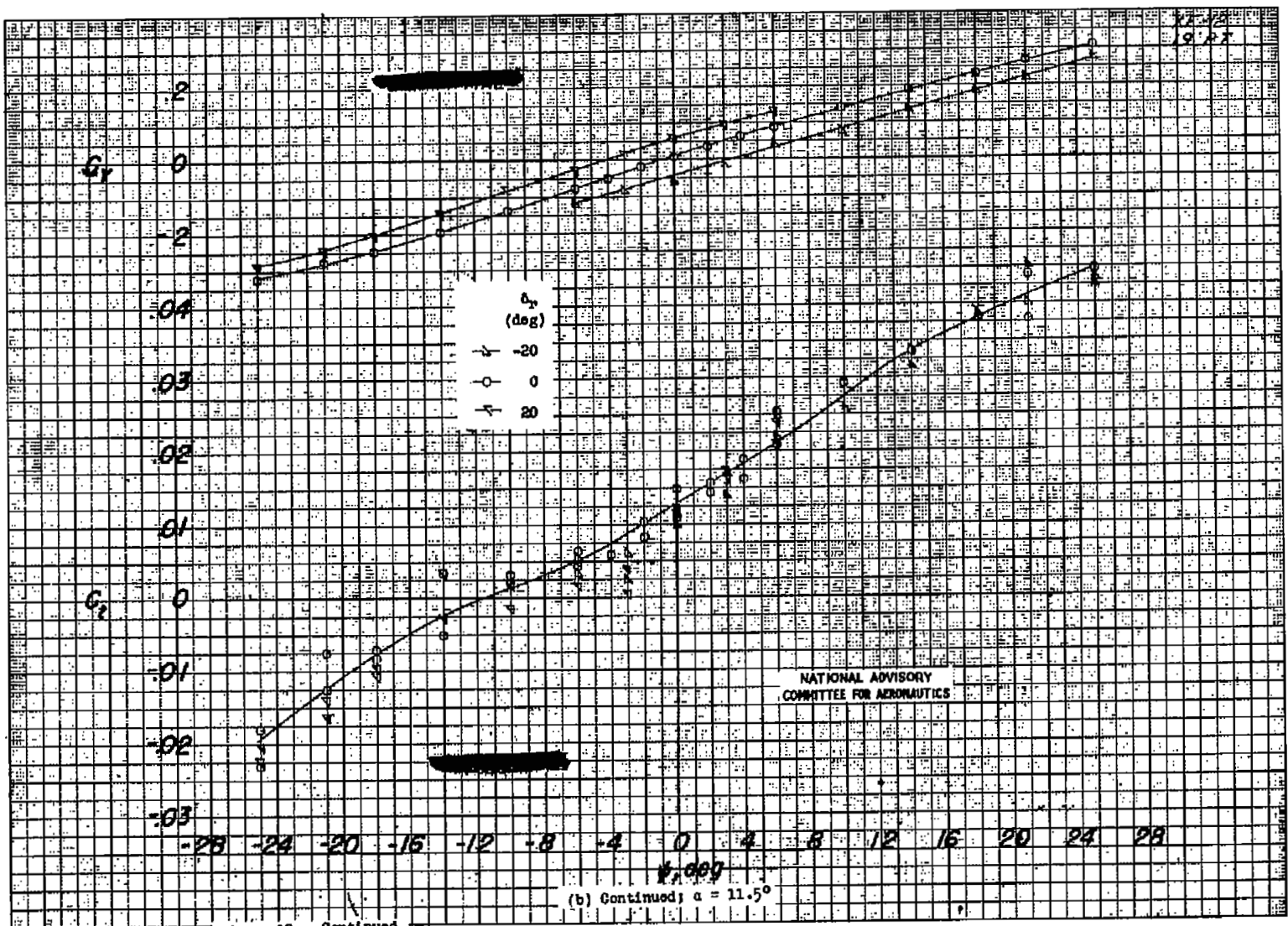


Figure 12 -- Continued.

Fig. 12b cont.

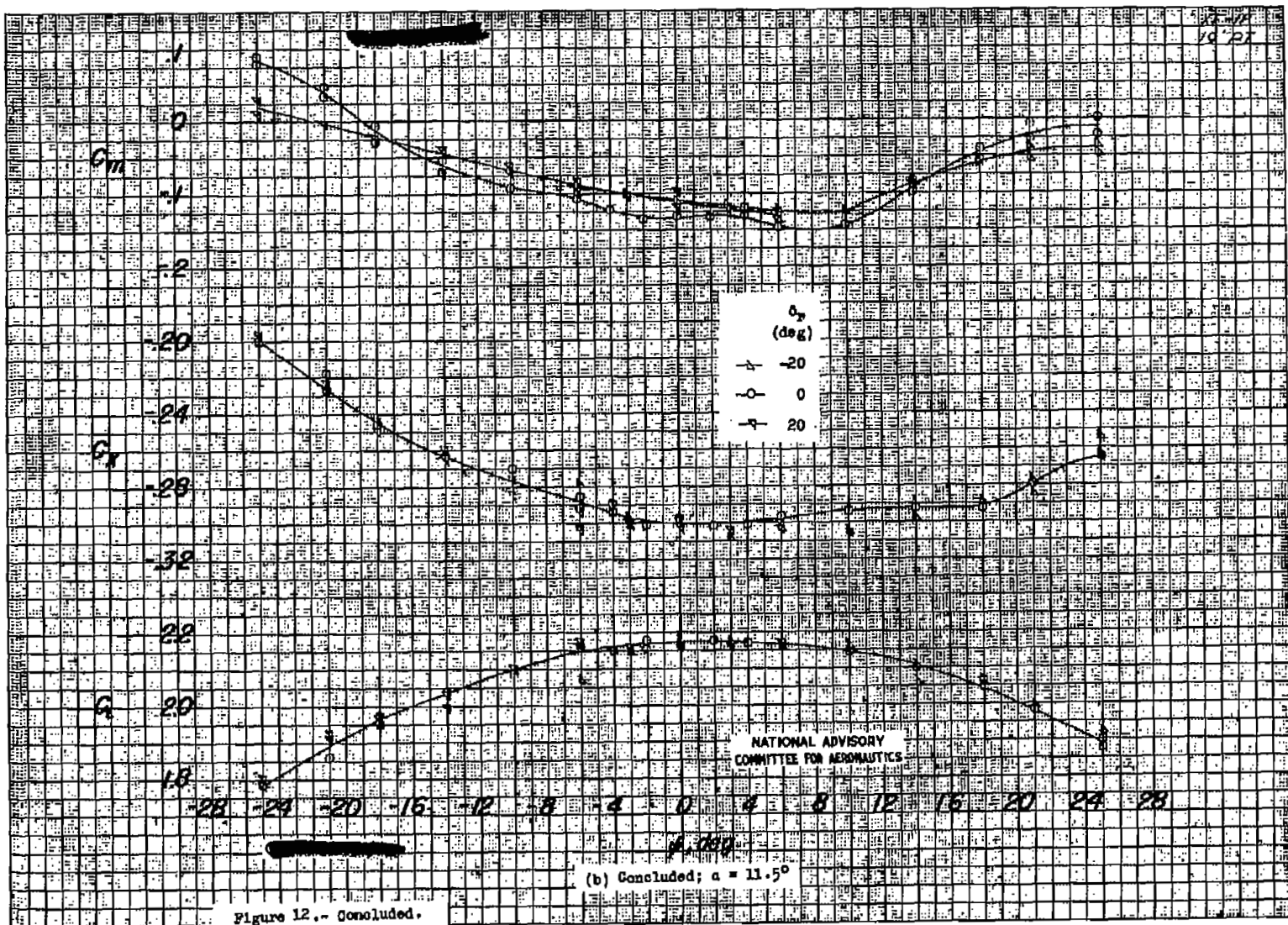
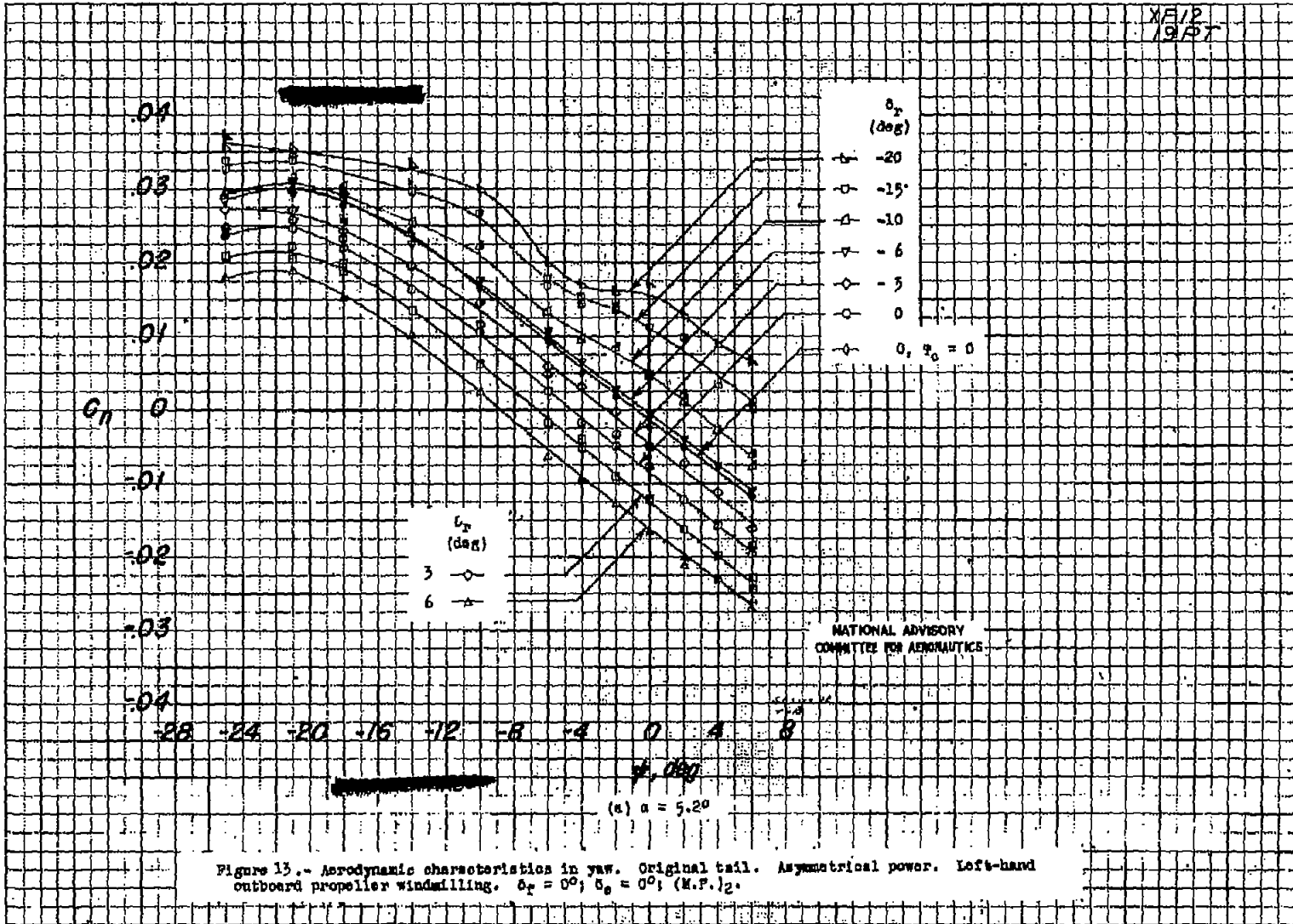
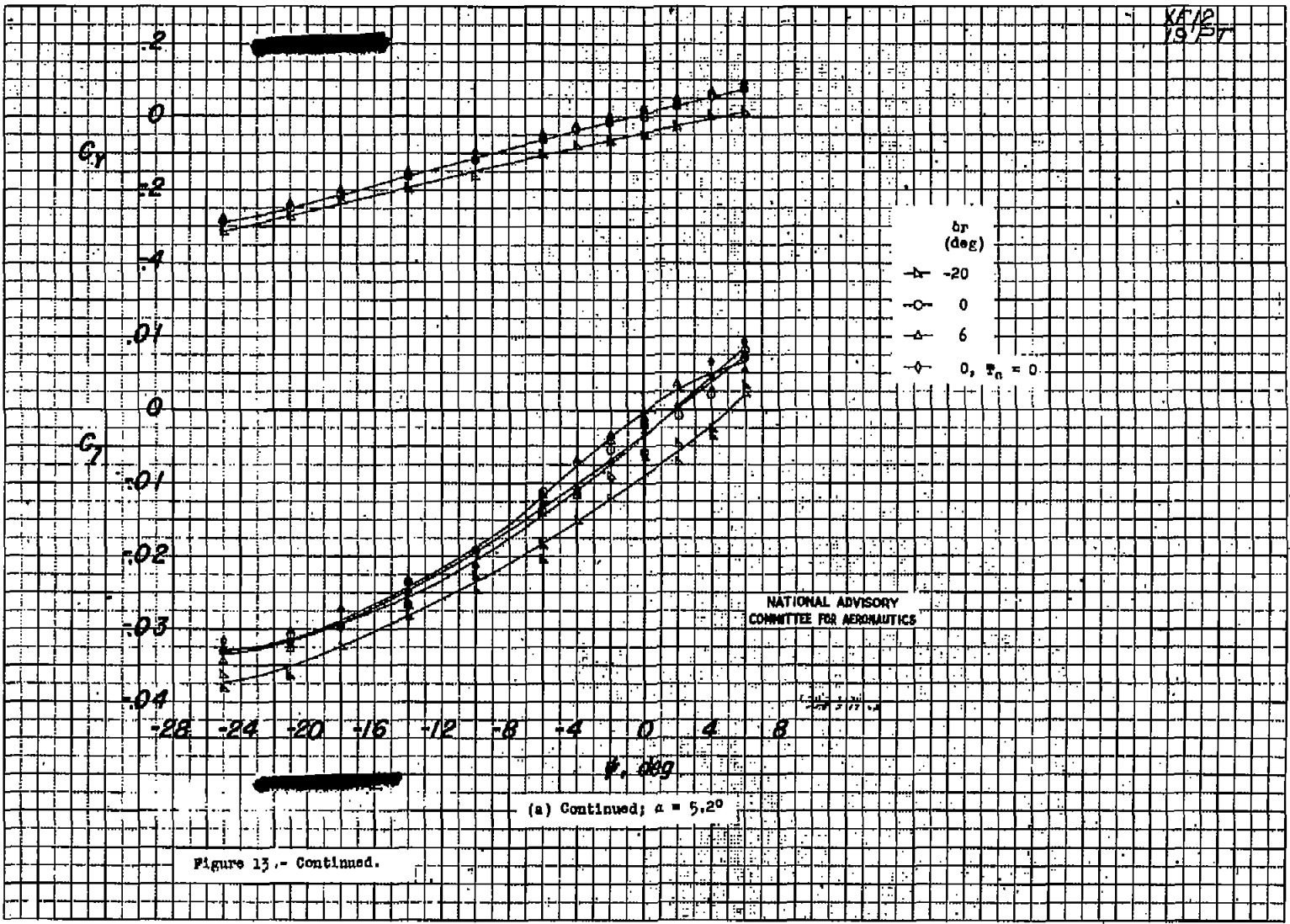


Fig. 12b conc.





20475

NACA RM No. L7B21

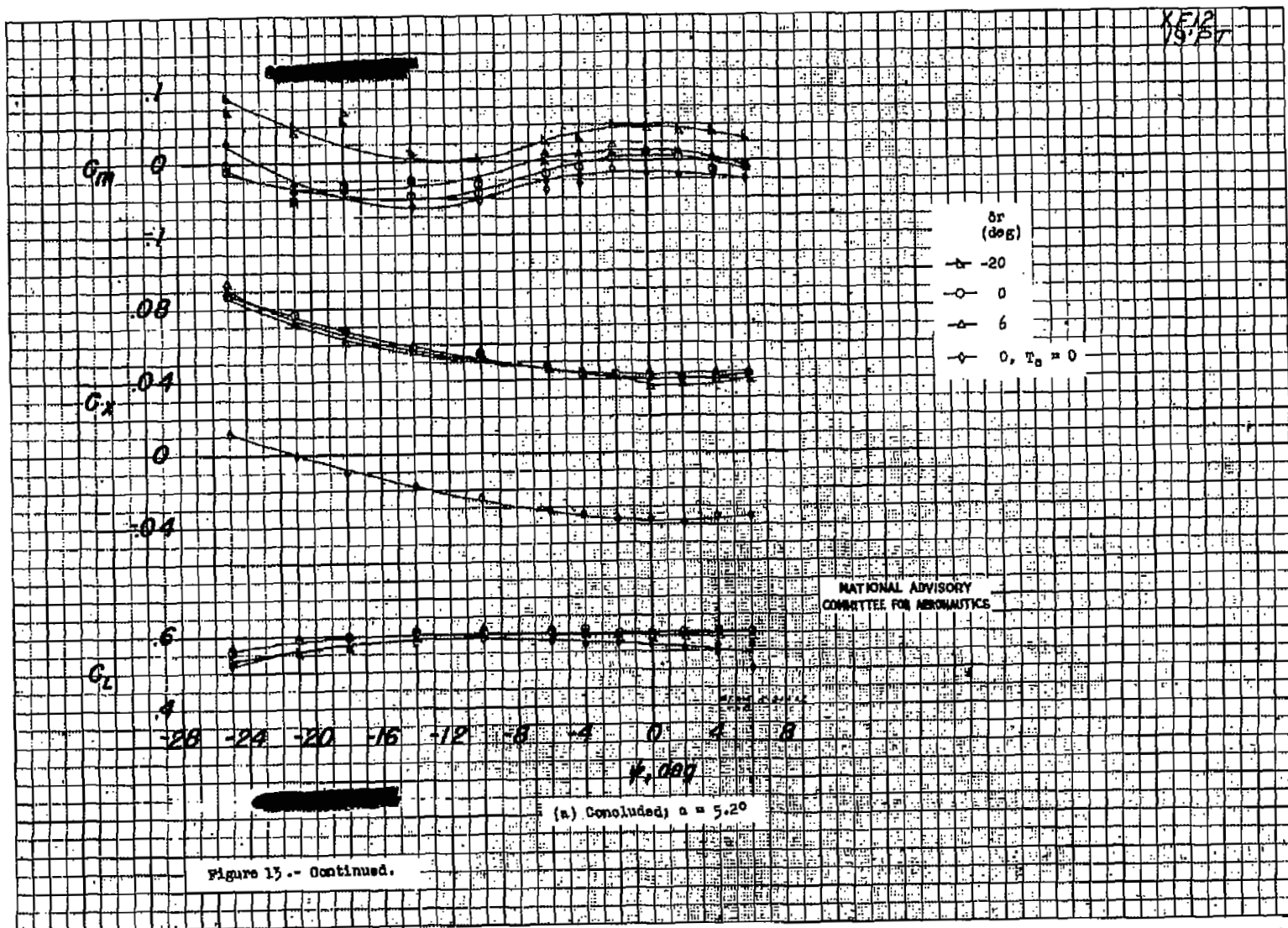


Fig. 13a contc.

20475

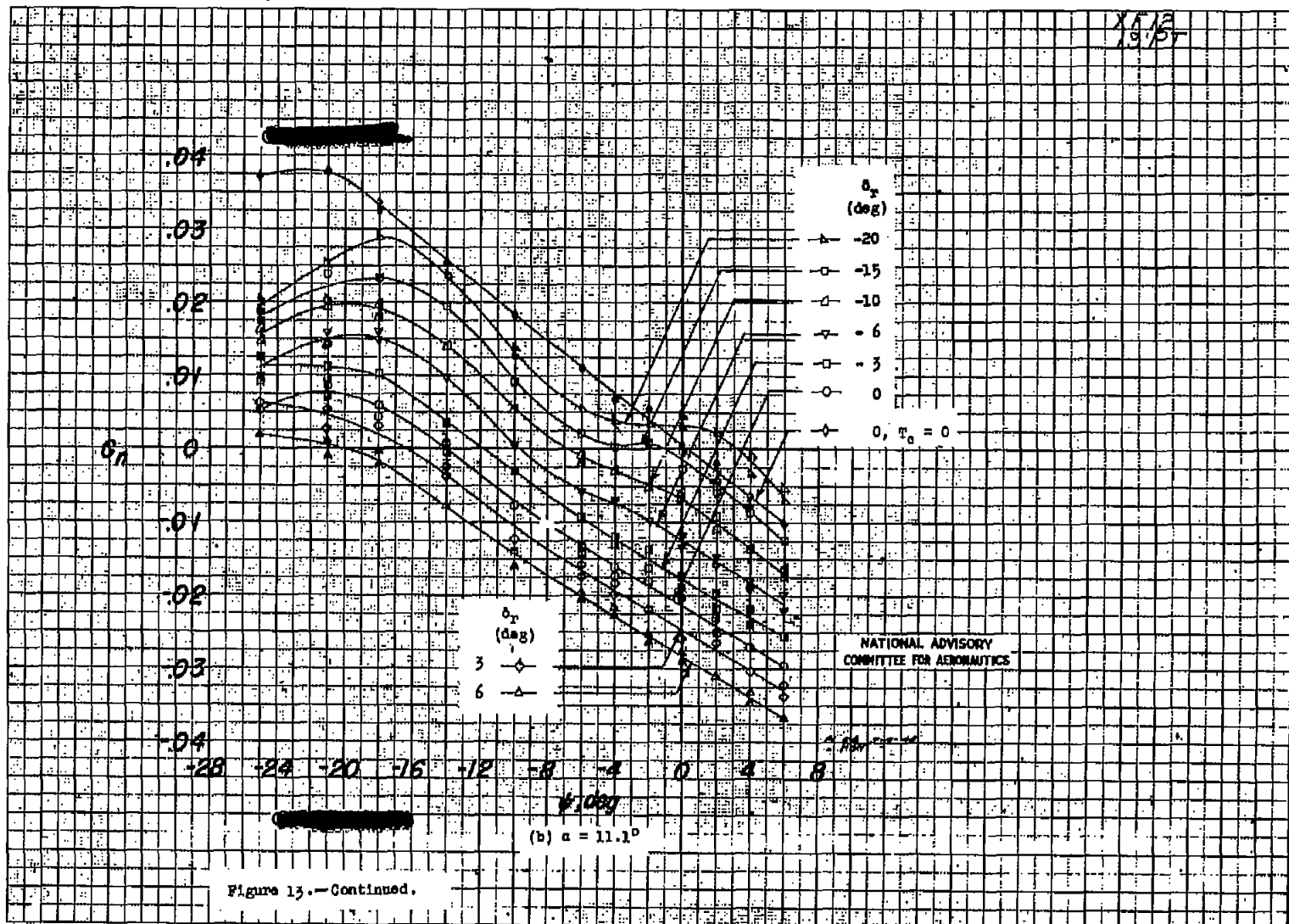


Figure 13.-Continued.

4/12
1947

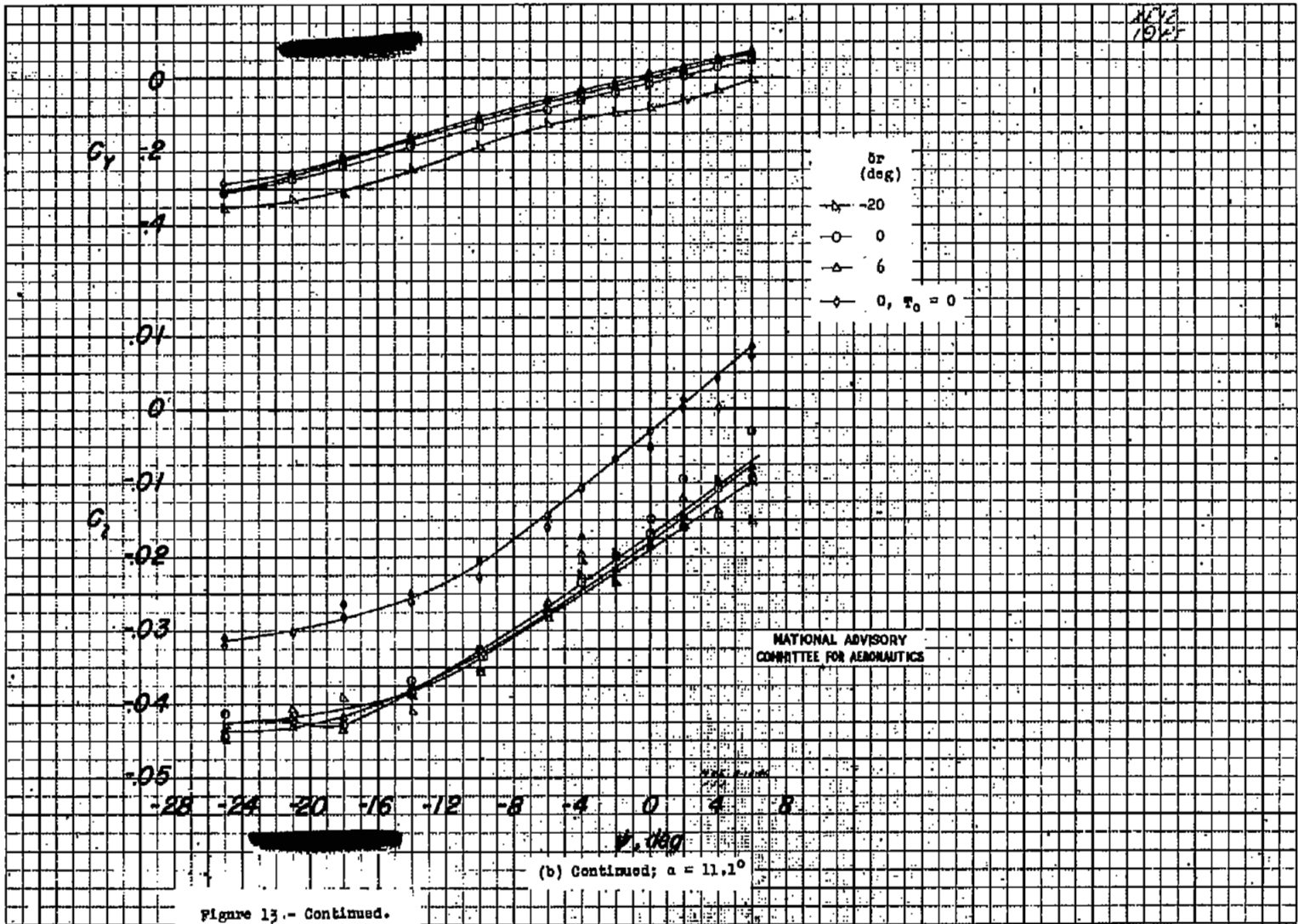


Figure 13.- Continued.

(b) Continued; $\alpha = 11.1^\circ$

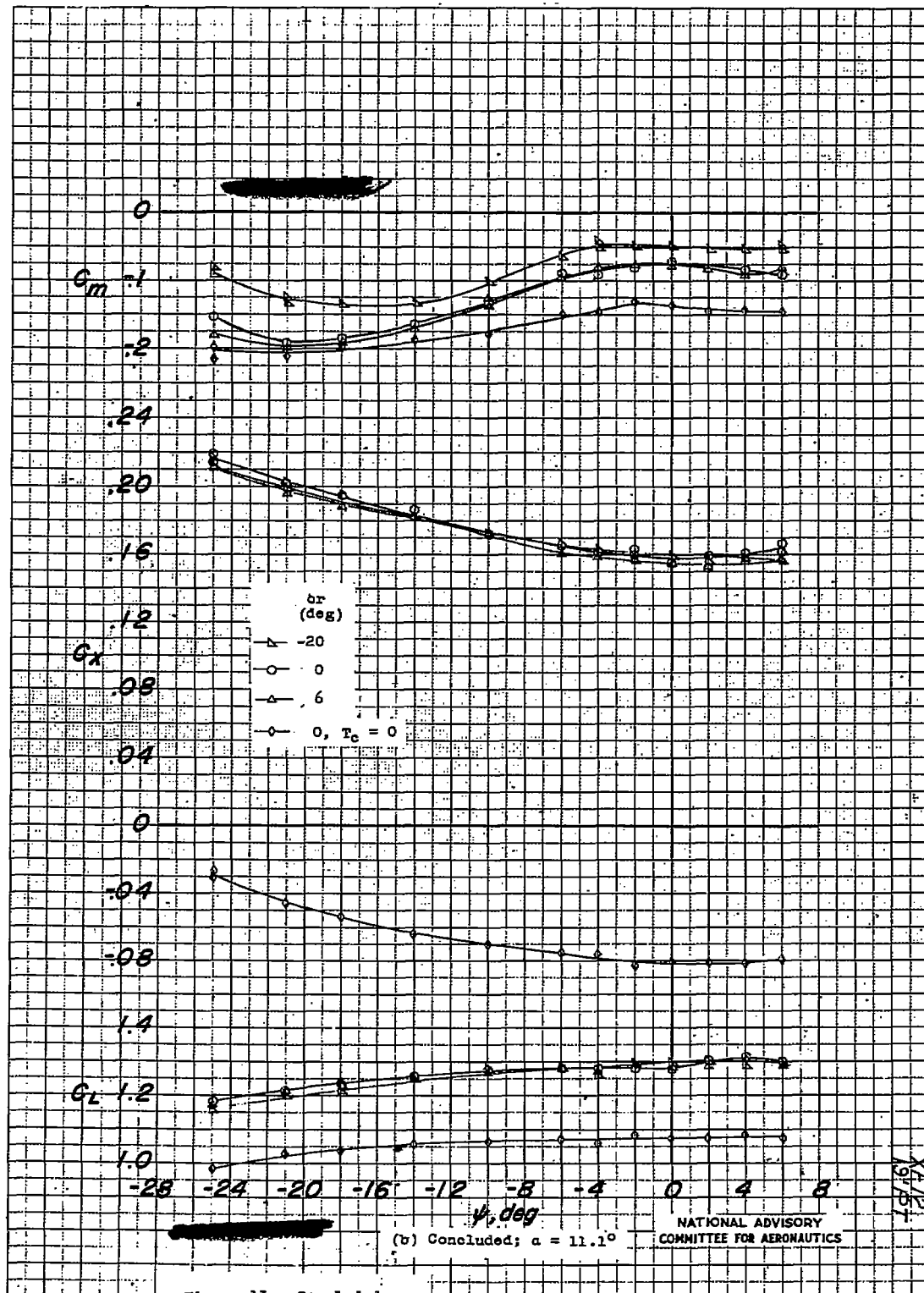


Figure 13.- Concluded.

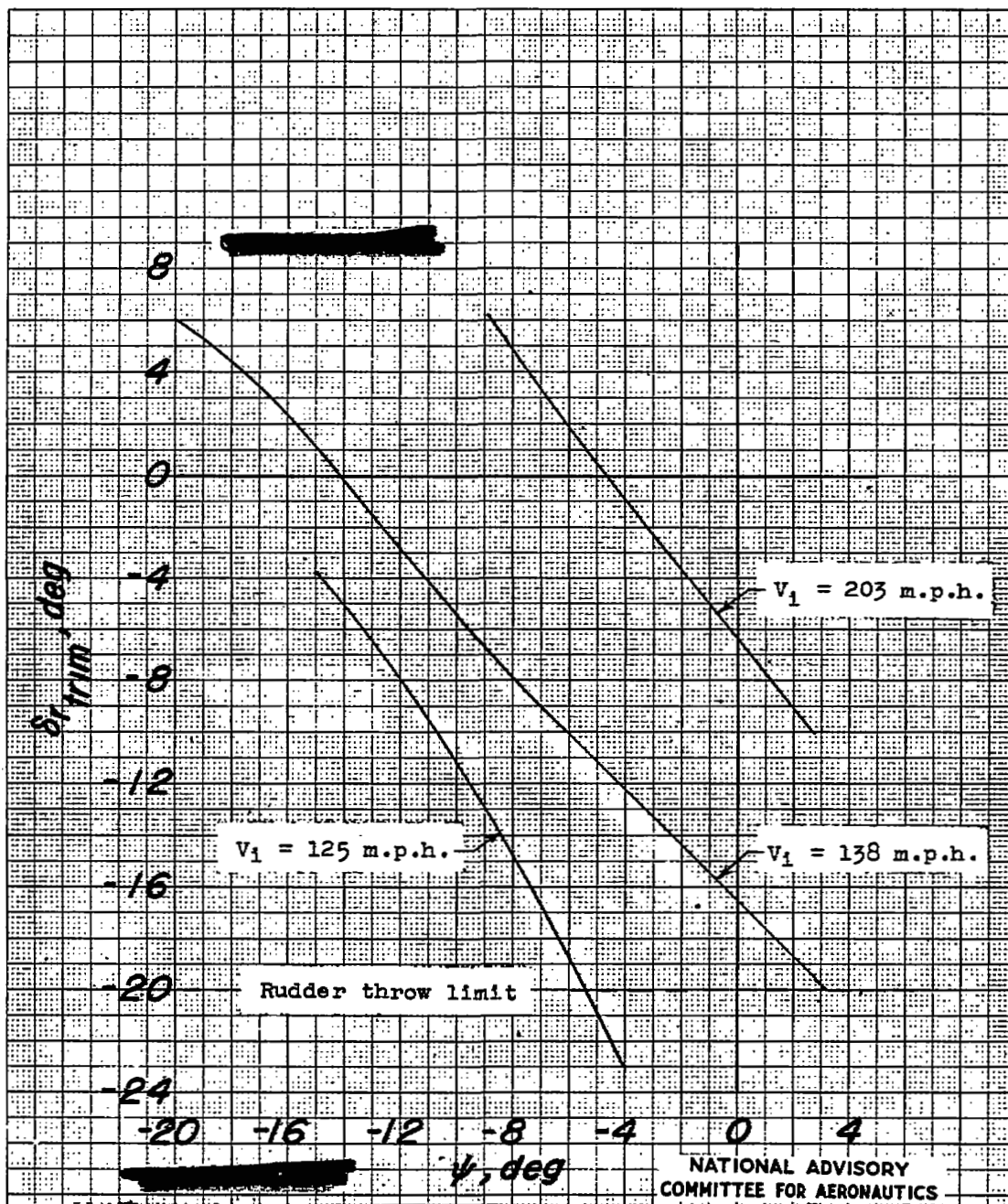


Figure 14.- Variation of rudder deflection required for trim with ψ for several speeds. Original tail. Asymmetrical power. $\delta_f = 0^\circ$; $\delta_e = 0^\circ$; (M.P.)₂

NATIONAL ADVISORY
COMMITTEE FOR AERONAUTICS

20475

NACA RM No. L7B21

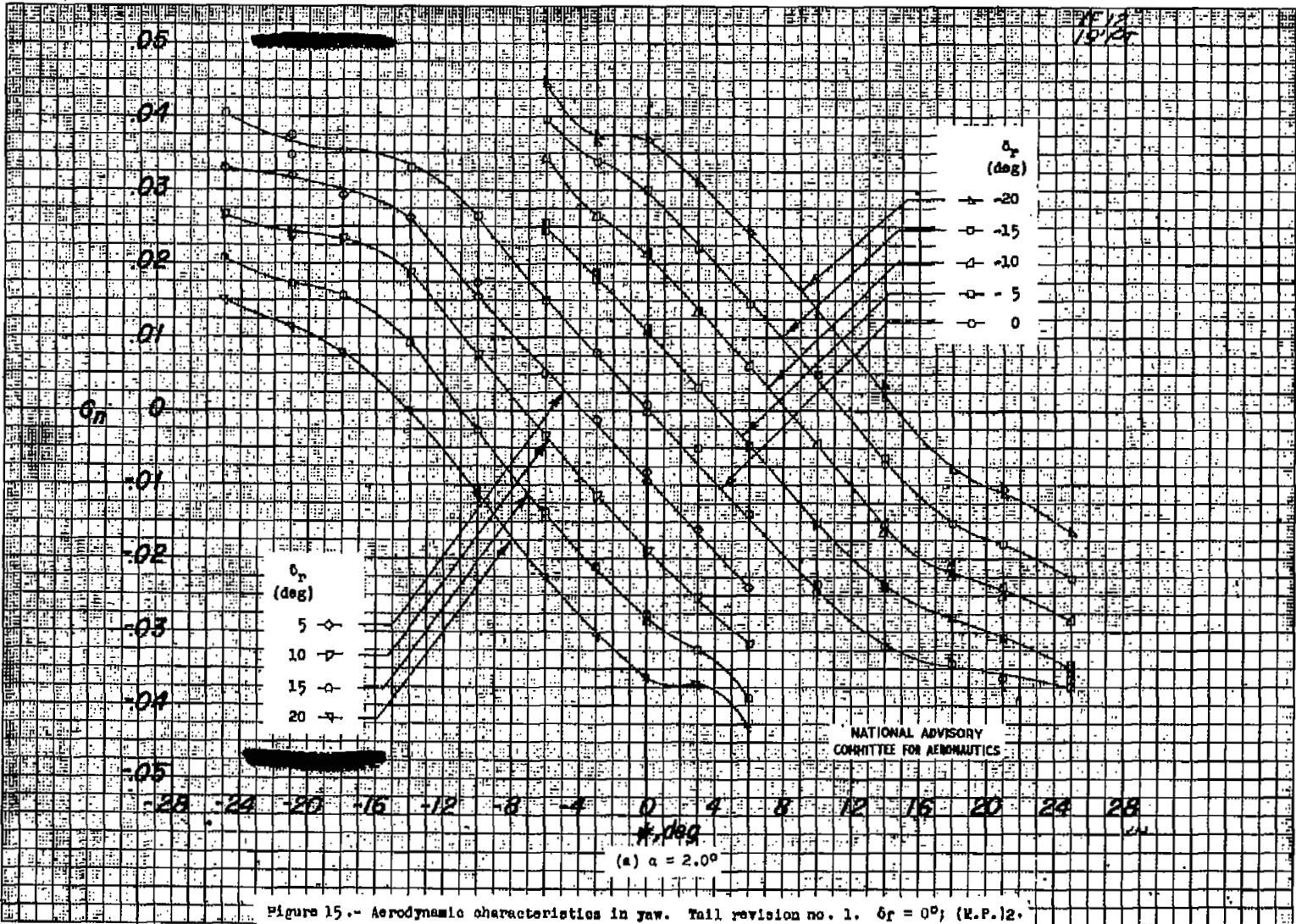


Figure 15.- Aerodynamic characteristics in yaw. Tail revision no. 1. $\delta_r = 0^\circ$; (M.P.12).

Fig. 15a

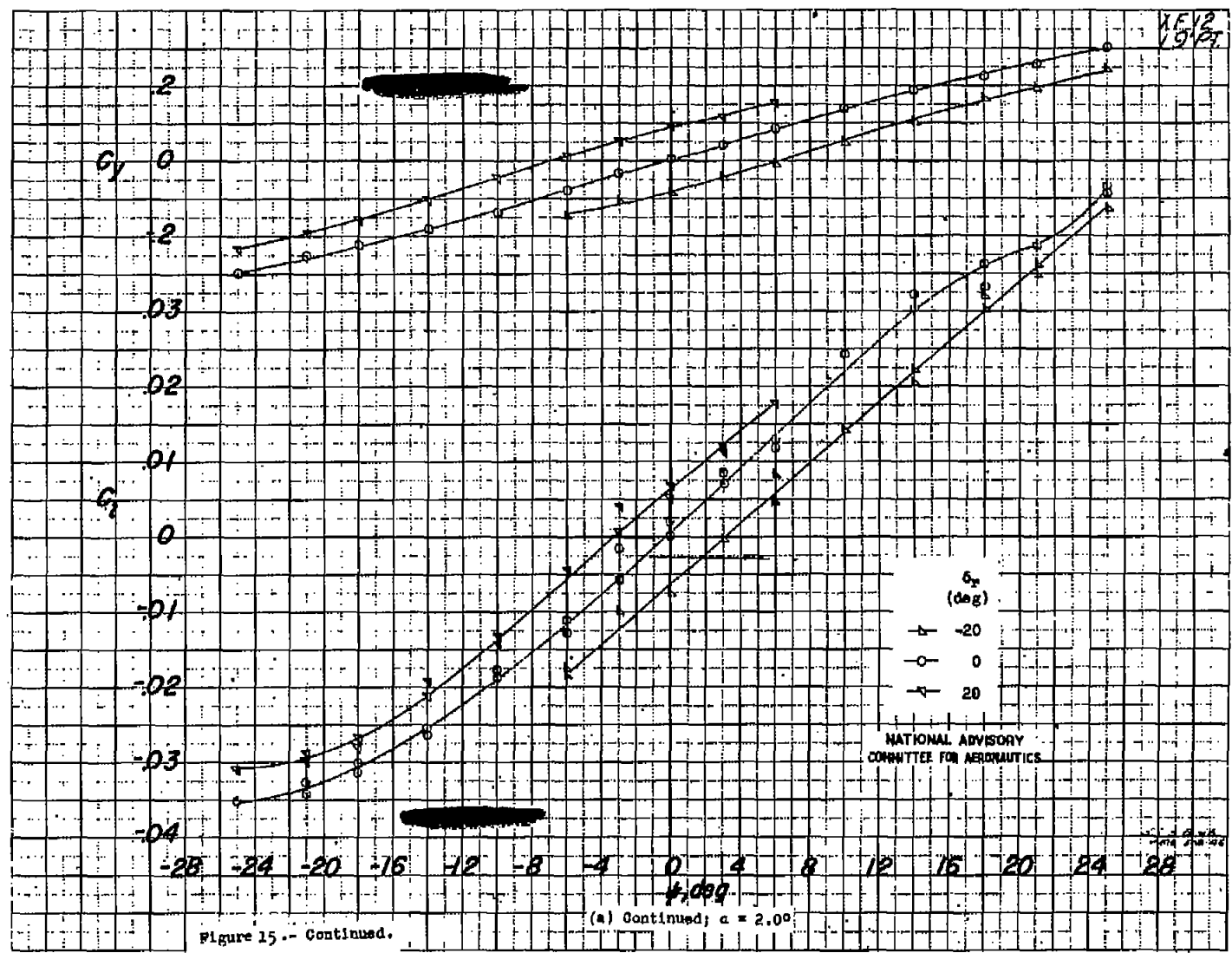


Figure 15.-- Continued.

(a) Continued; $\alpha = 2.0^\circ$

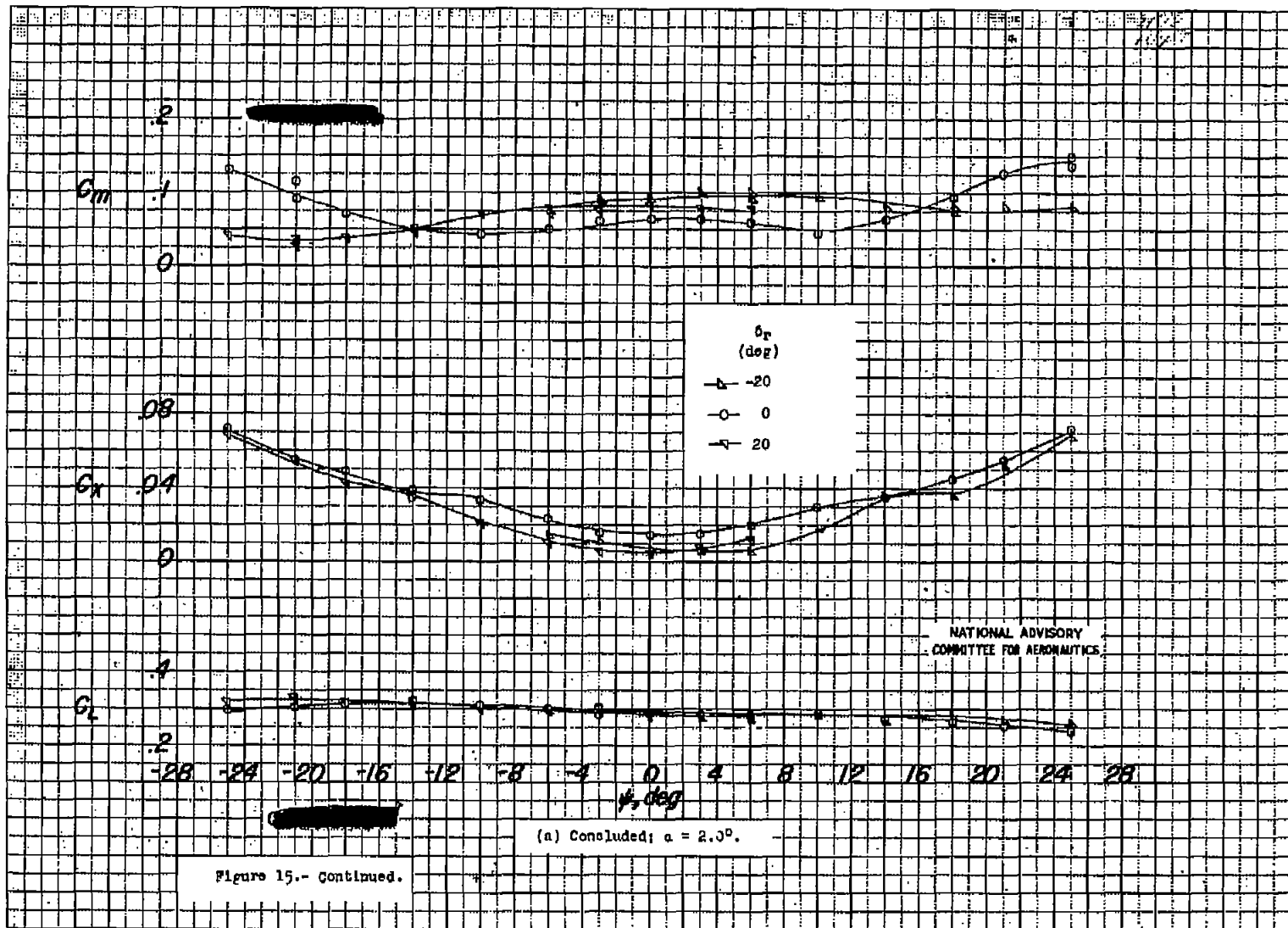


Figure 15.- Continued.

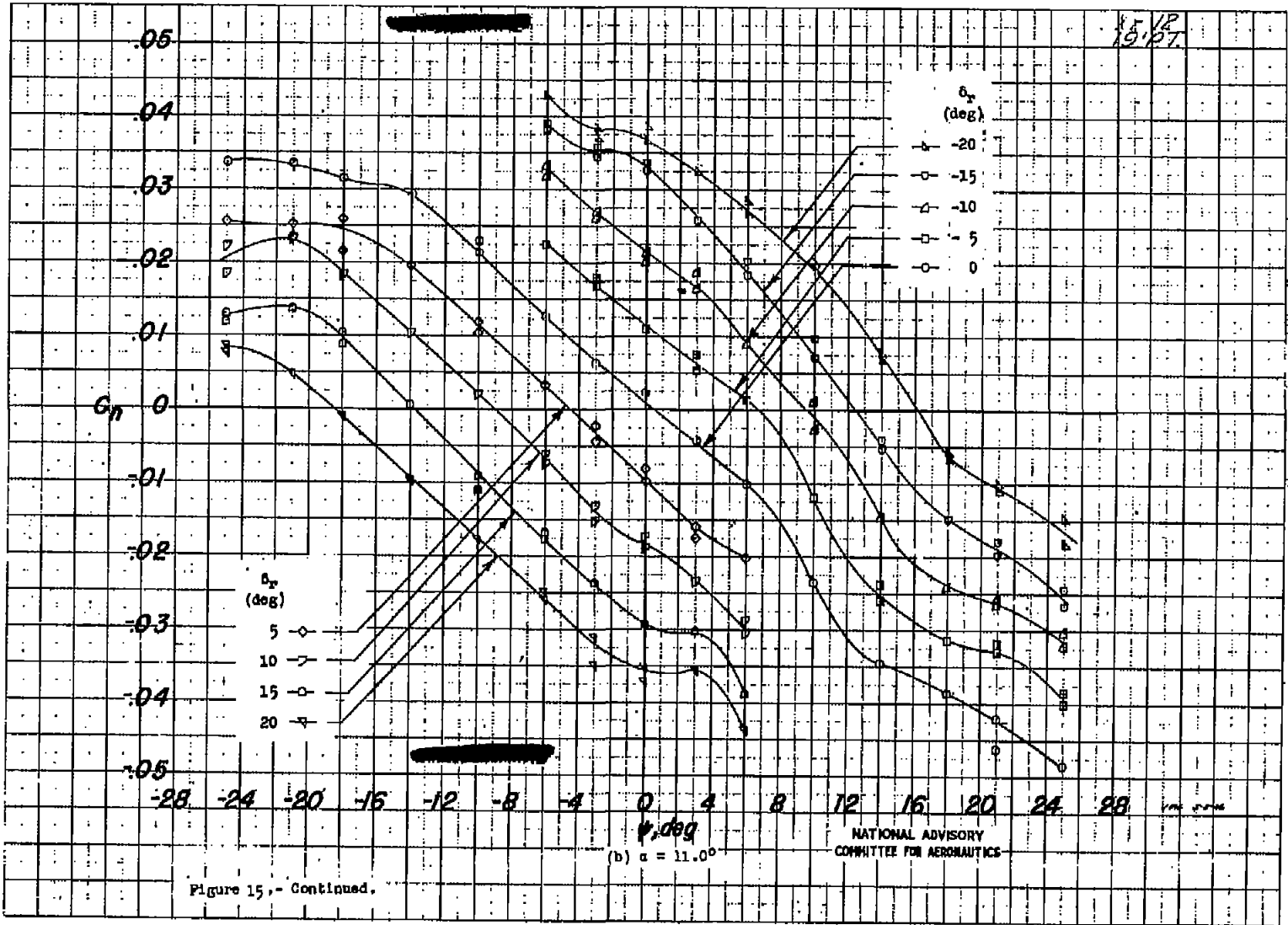


Figure 15, - Continued.

(b) $\alpha = 11.0^\circ$

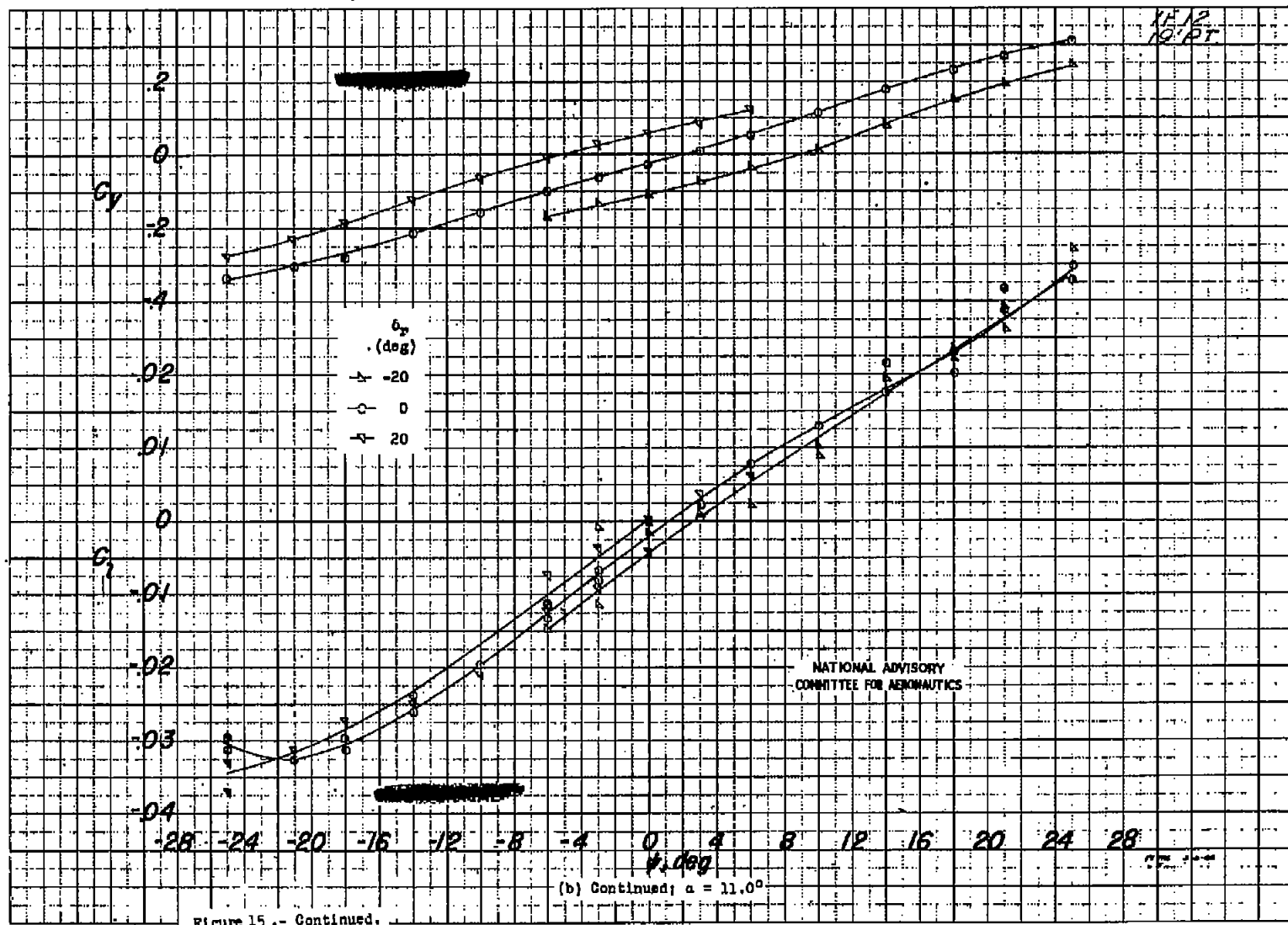


Figure 15 -- Continued.

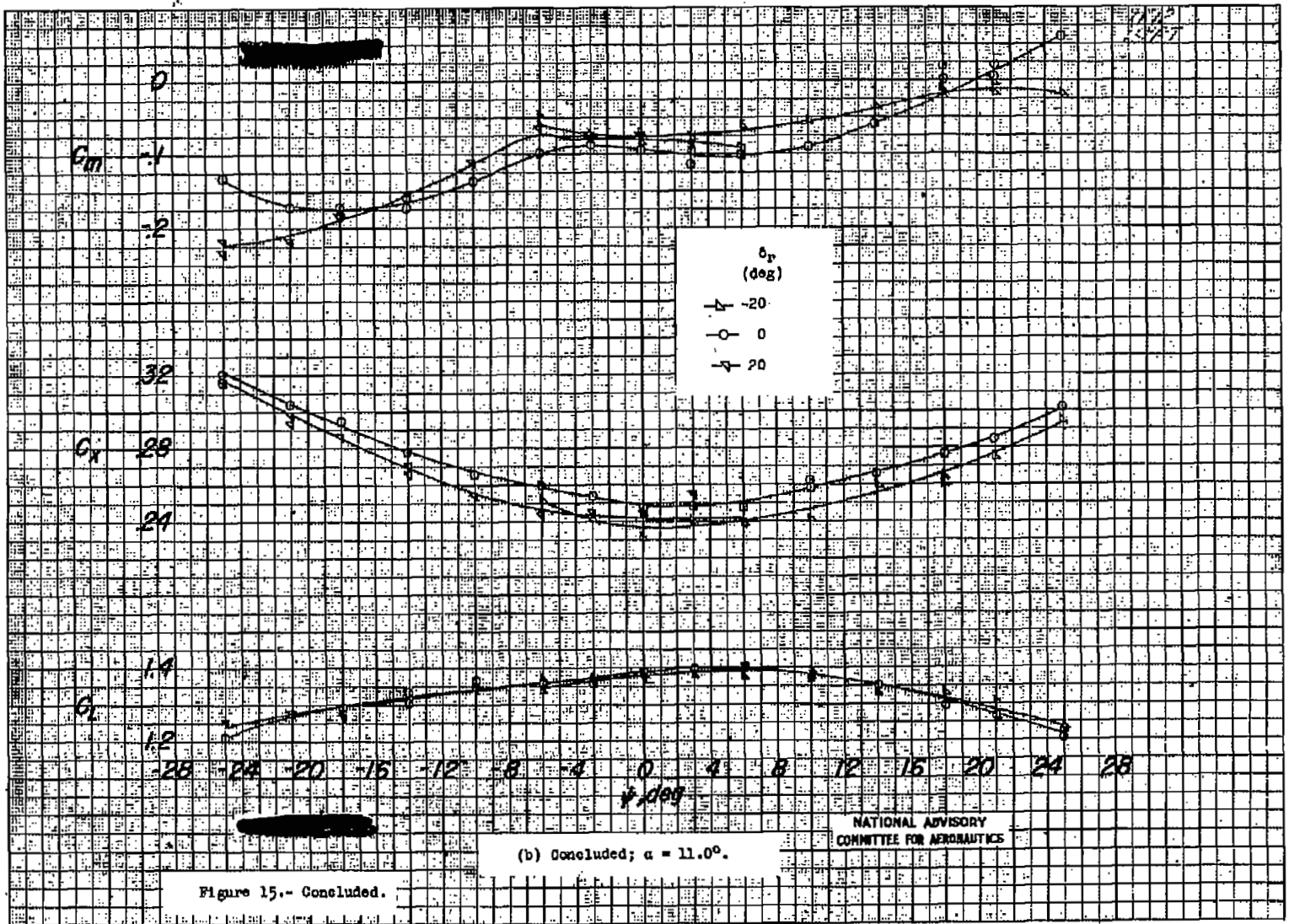
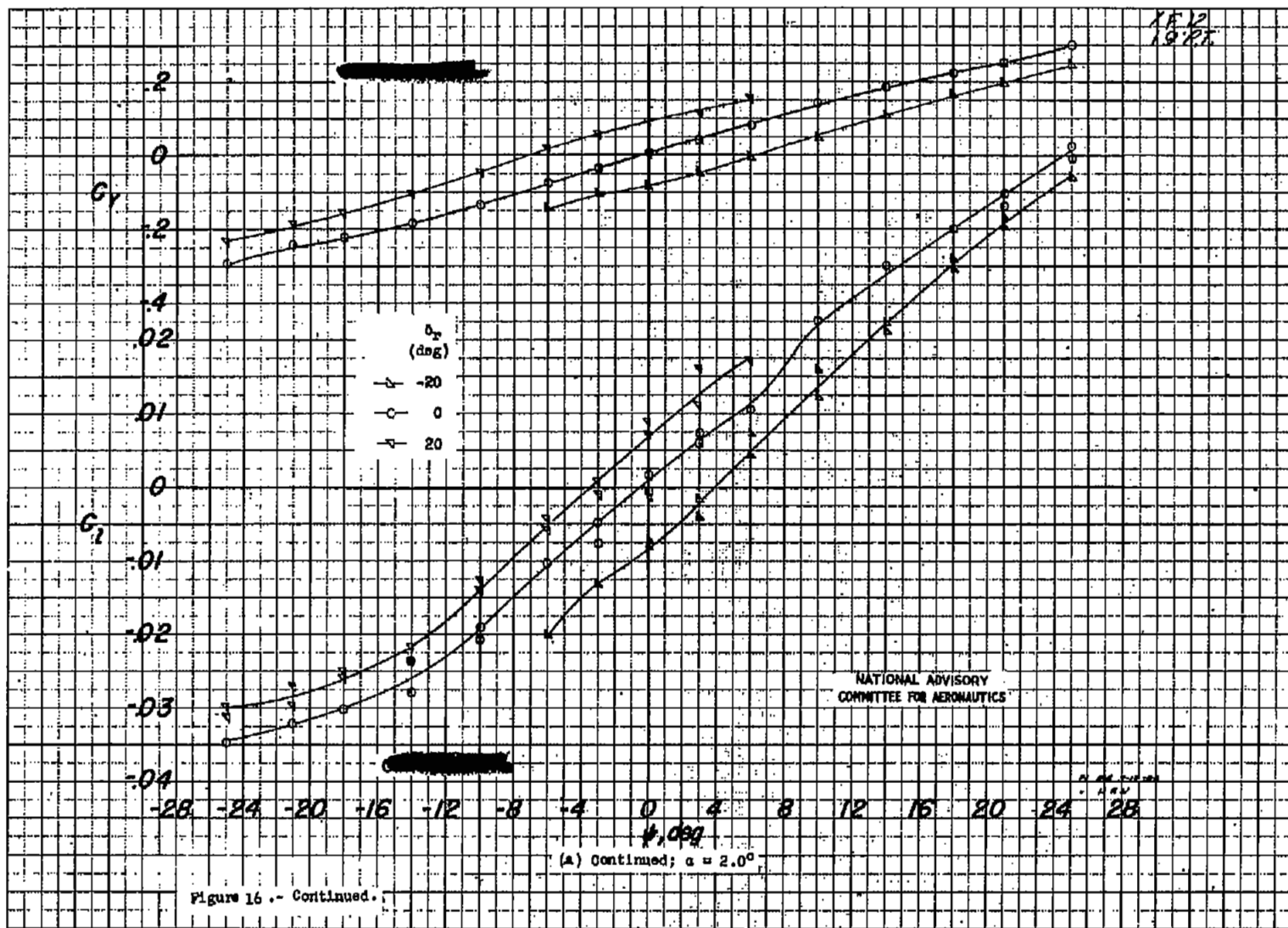


Figure 15.- Concluded.

(b) Concluded; $\alpha = 11.0^\circ$.

NATIONAL ADVISORY
COMMITTEE FOR AERONAUTICS



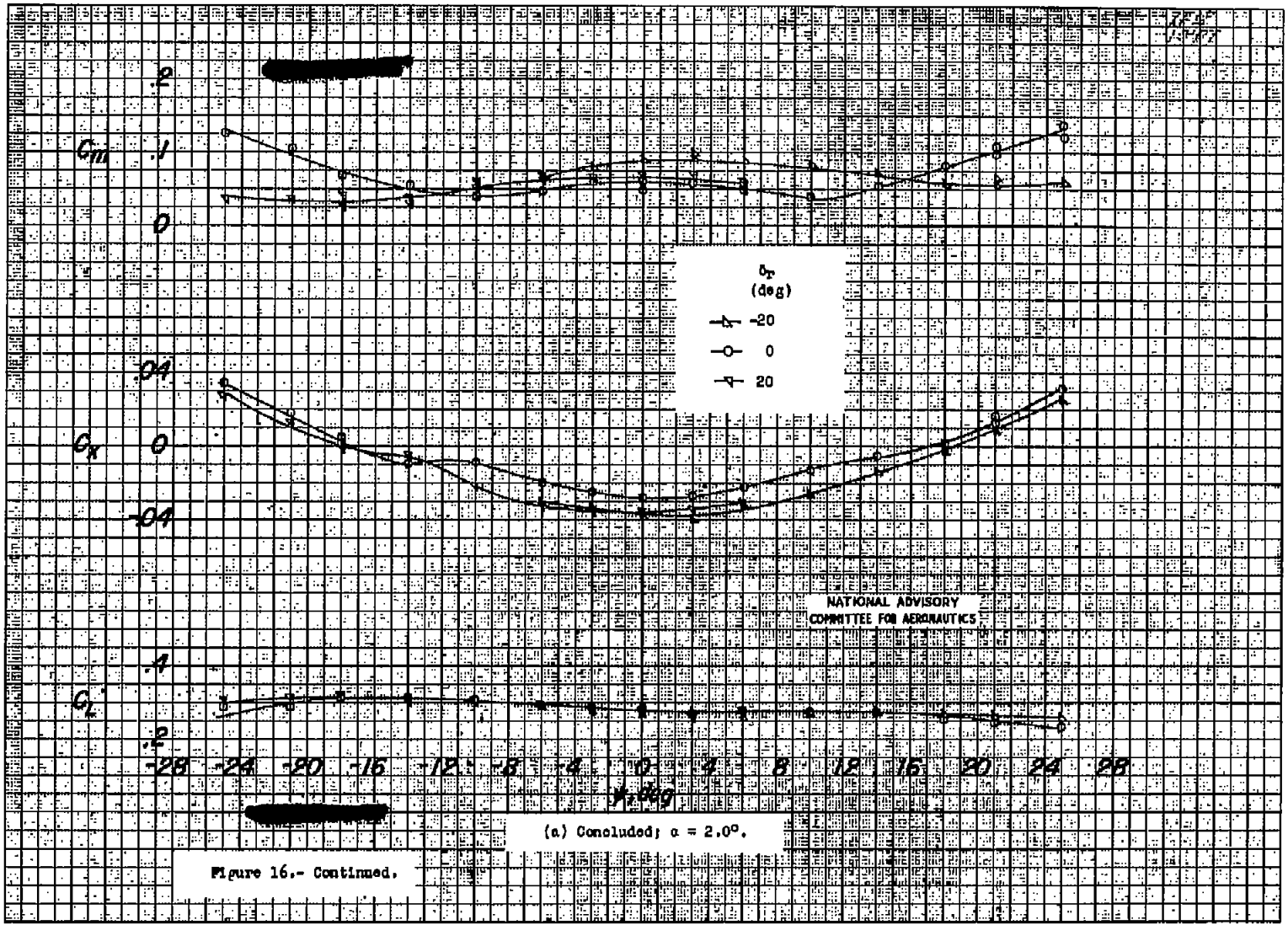


Figure 16.- Continued.

Fig. 16a conc.

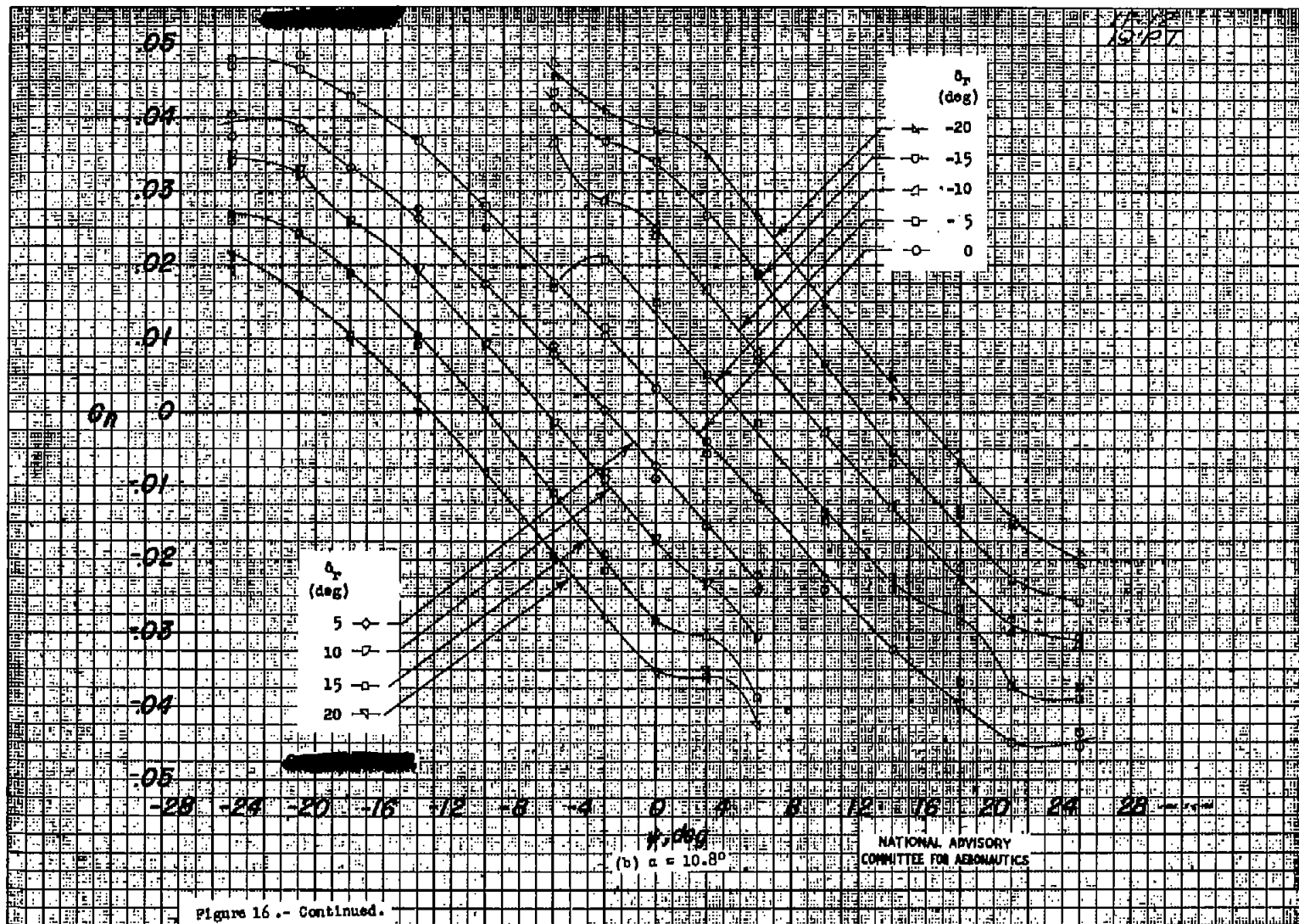


Figure 16.- Continued.

Fig. 16b

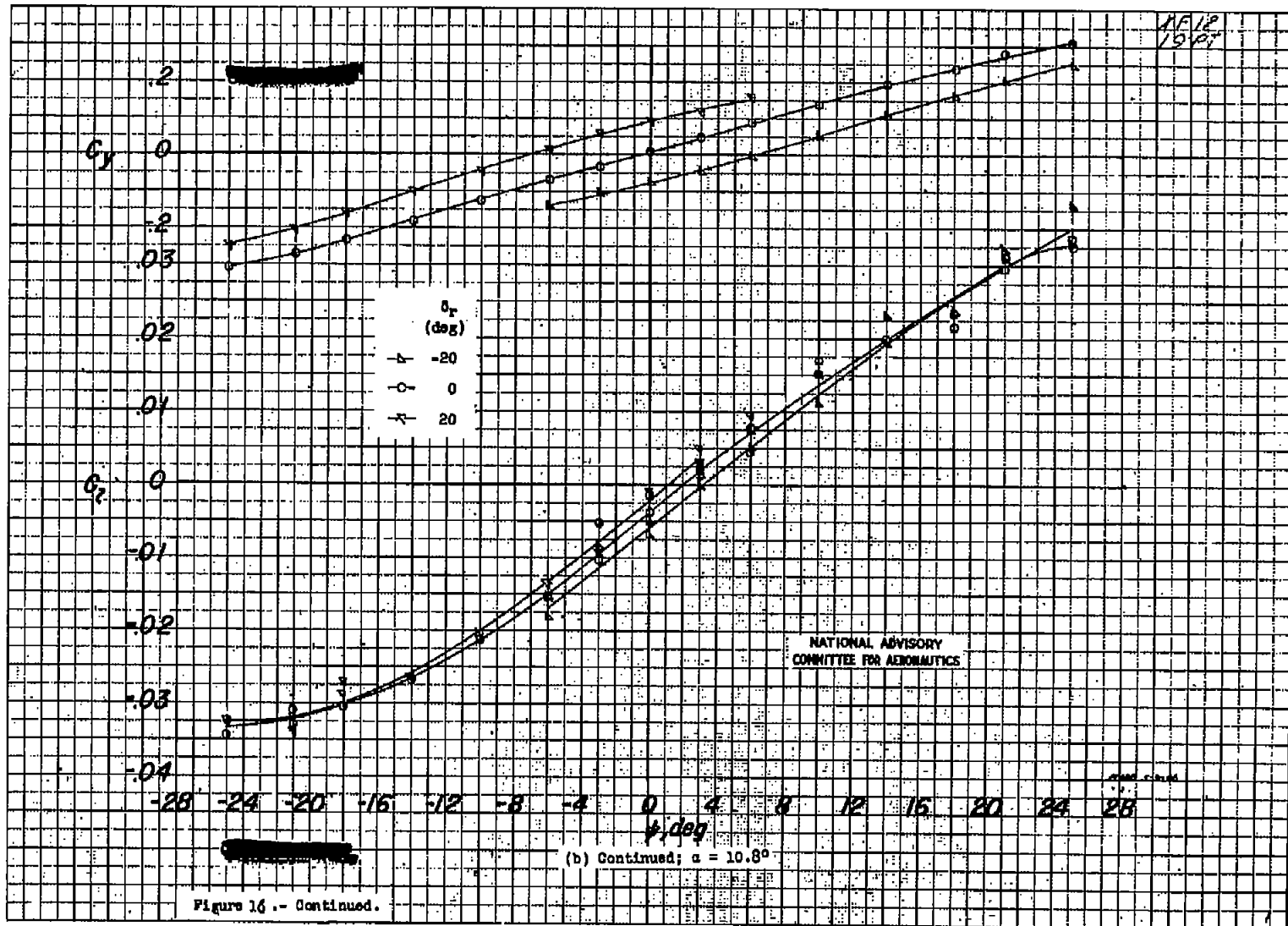


Fig. 16b cont.

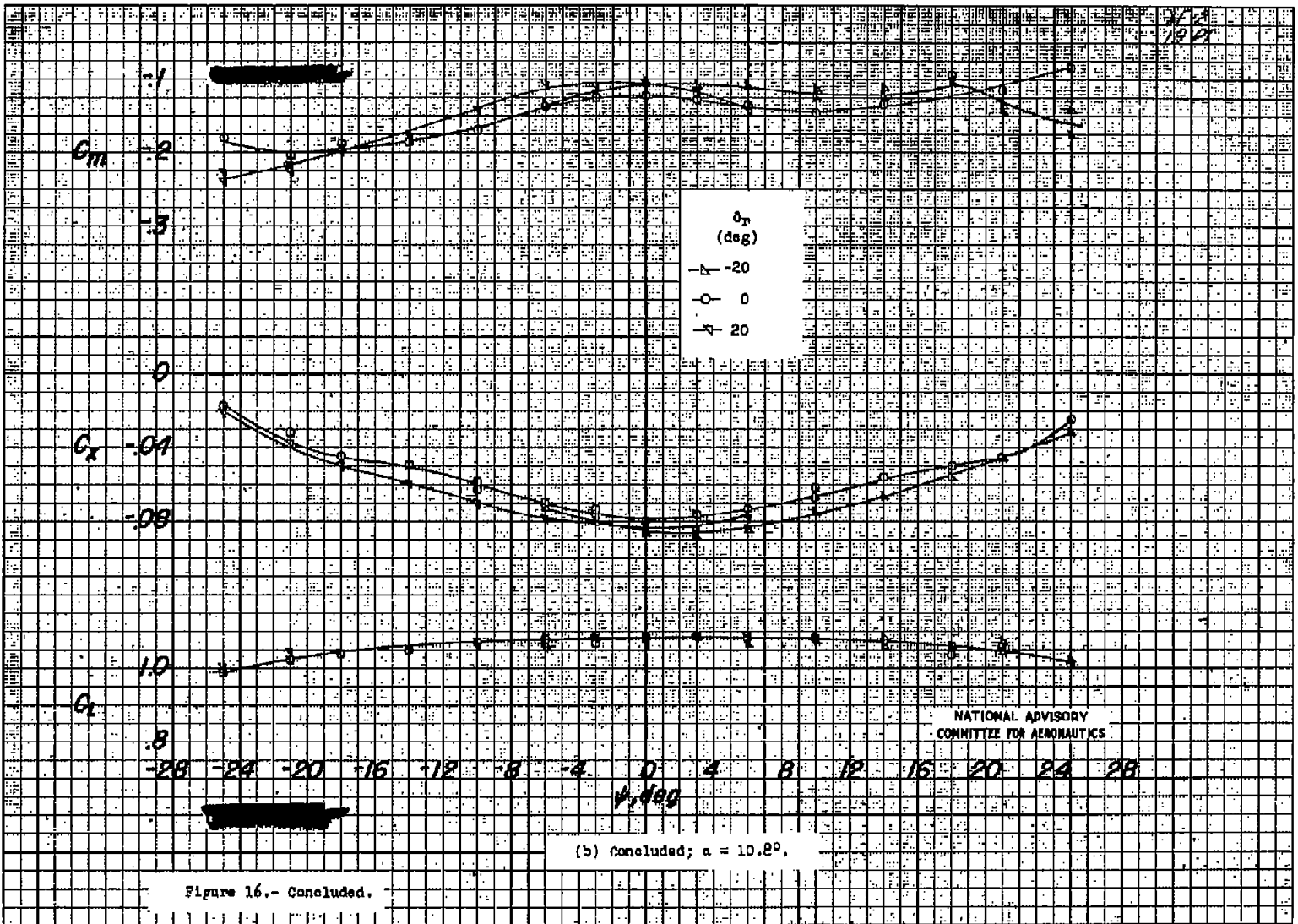


Figure 16.- Concluded.

Fig. 16b conc.

20477

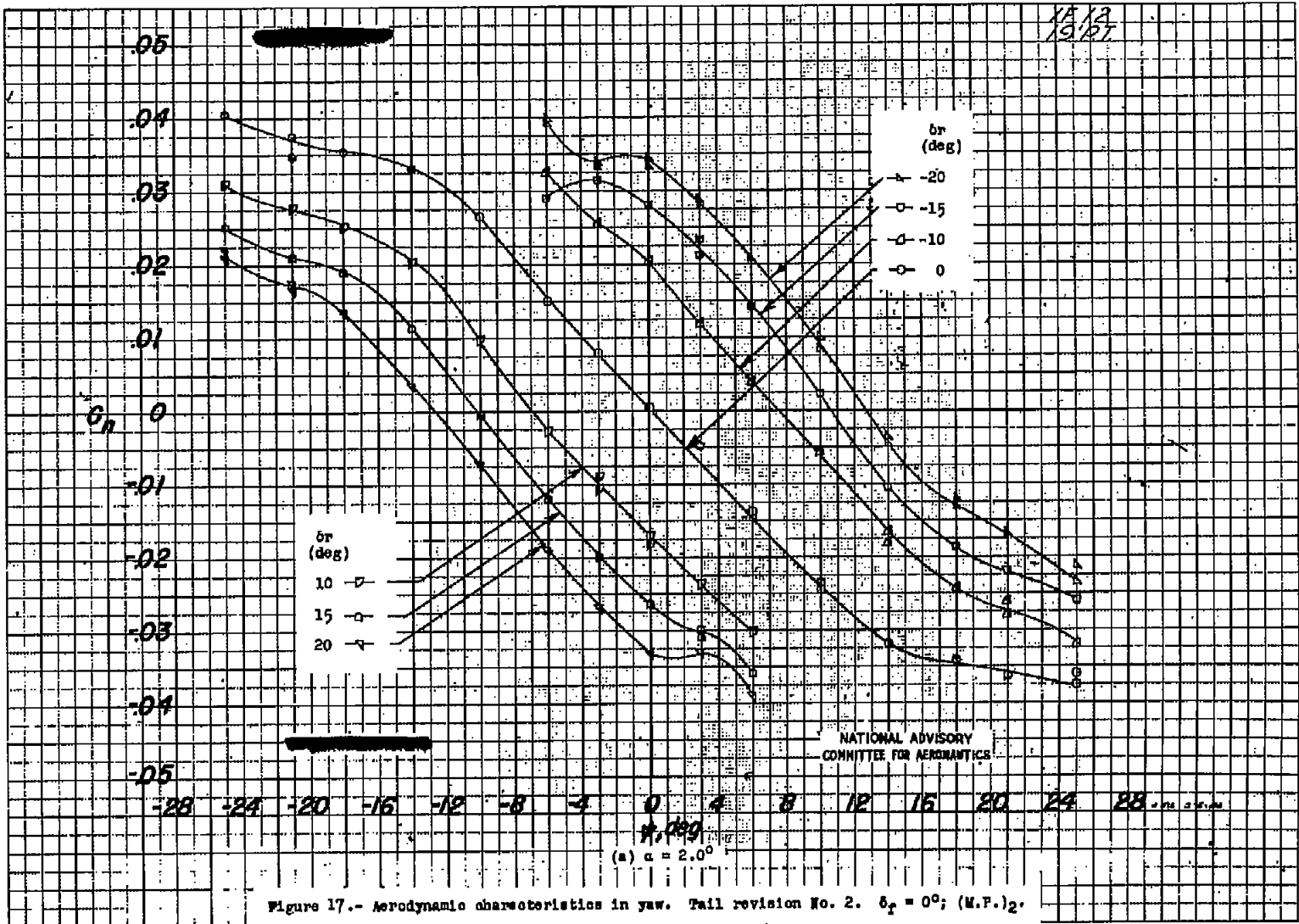


Figure 17.- Aerodynamic characteristics in yaw. Tail revision No. 2. $\delta_r = 0^\circ$; (M.F.)₂.

204717

NACA RM No. L7B21

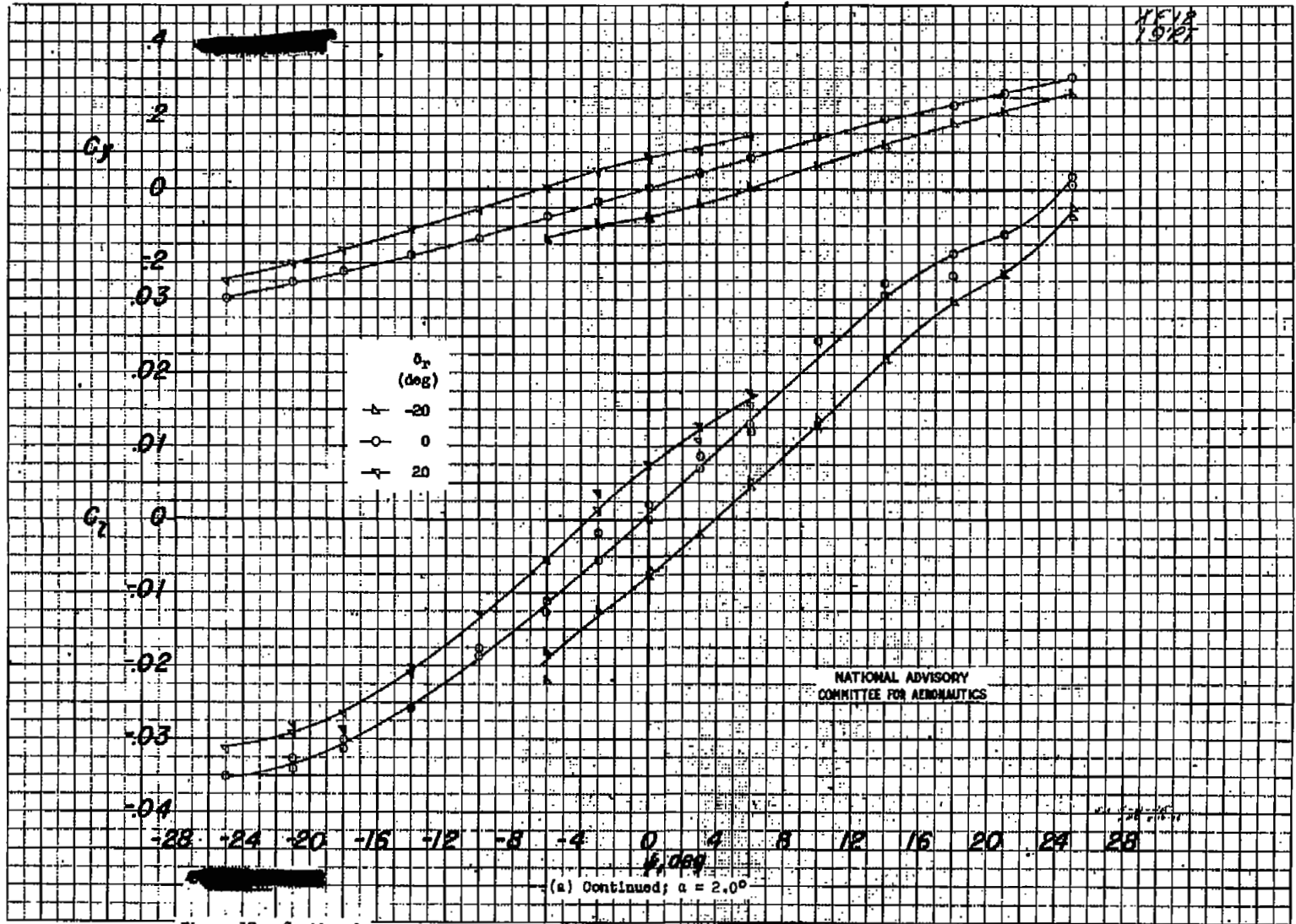
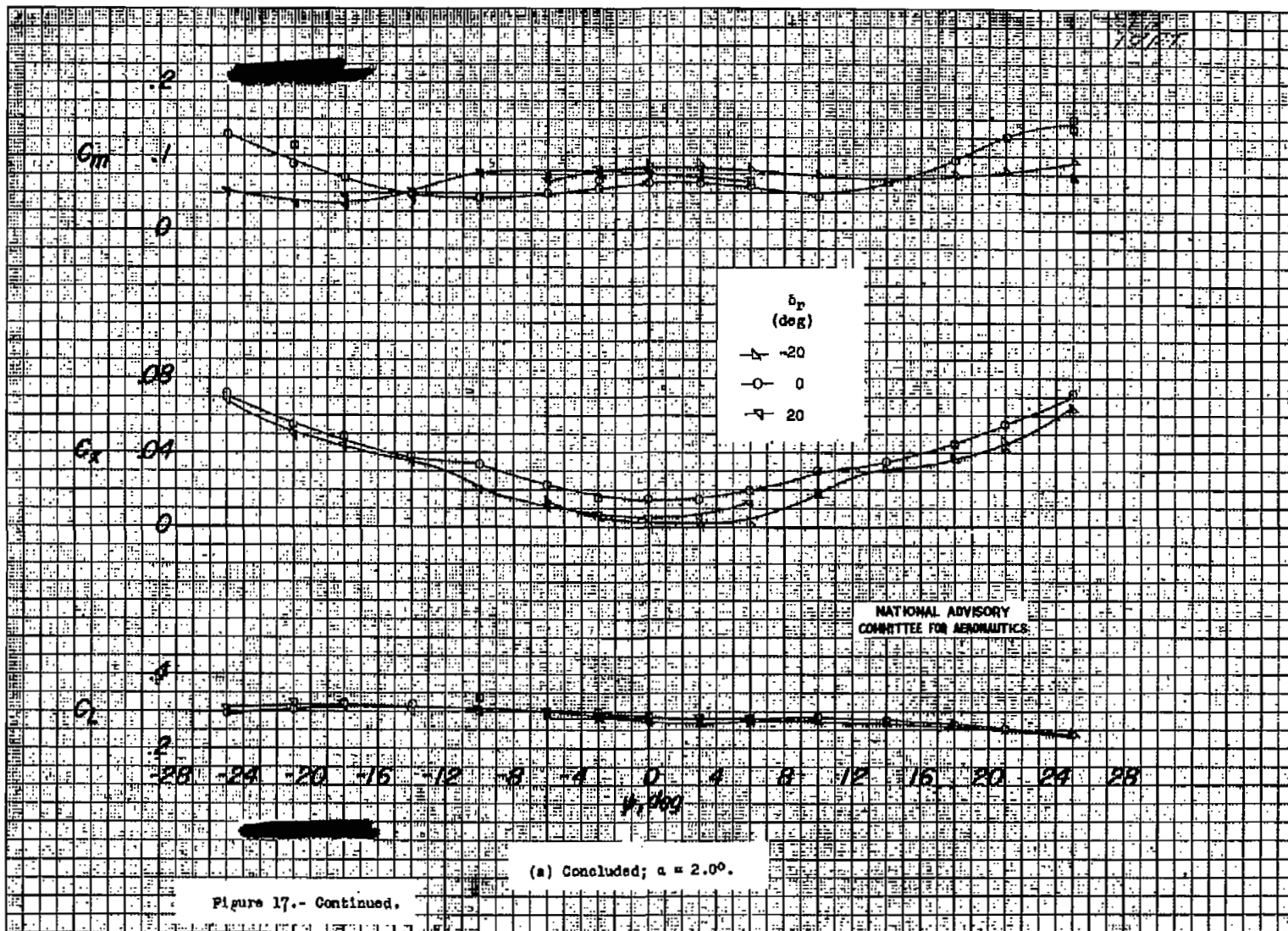


Figure 17.- Continued.

FIG. 17a cont.



20475

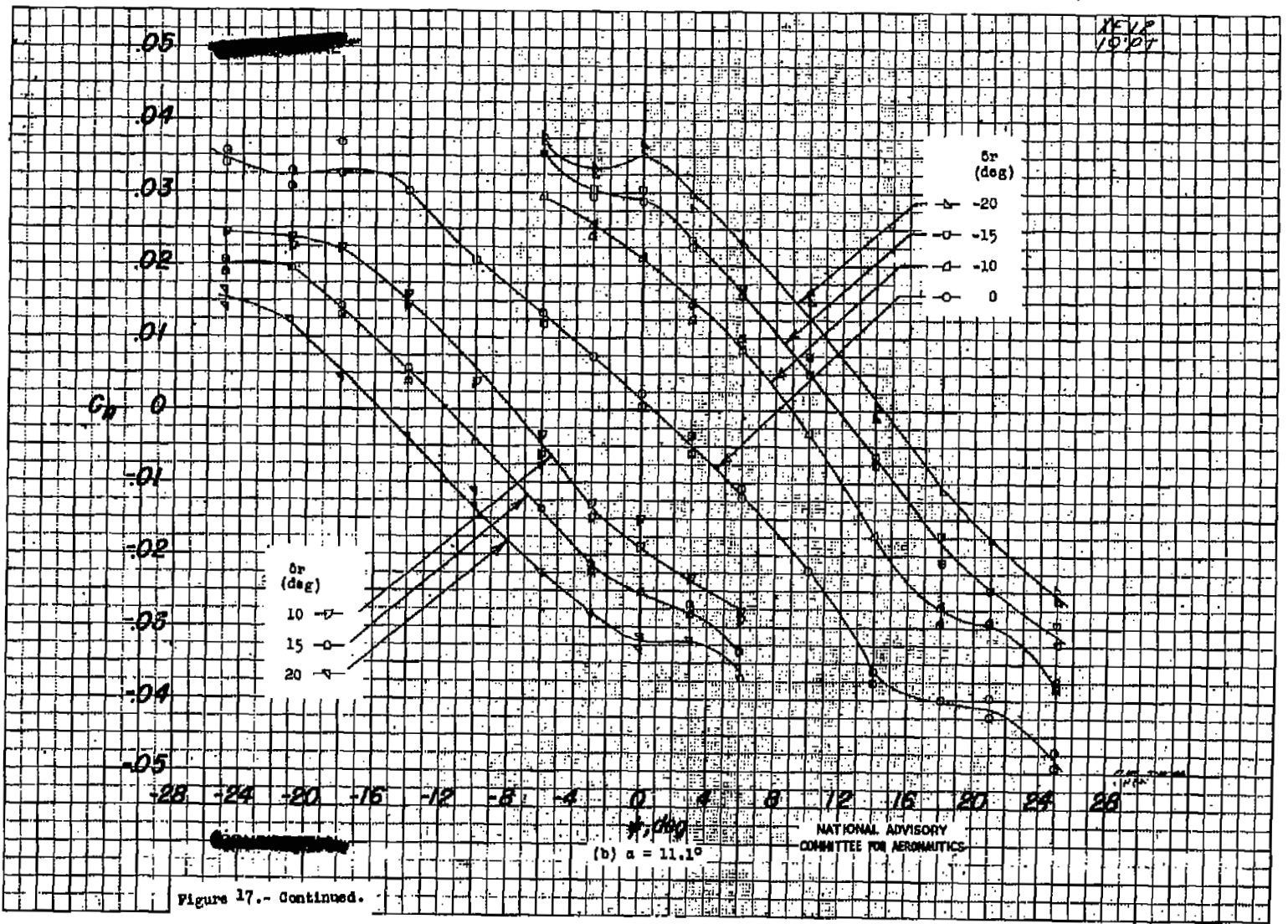


Figure 17.- Continued.

20471

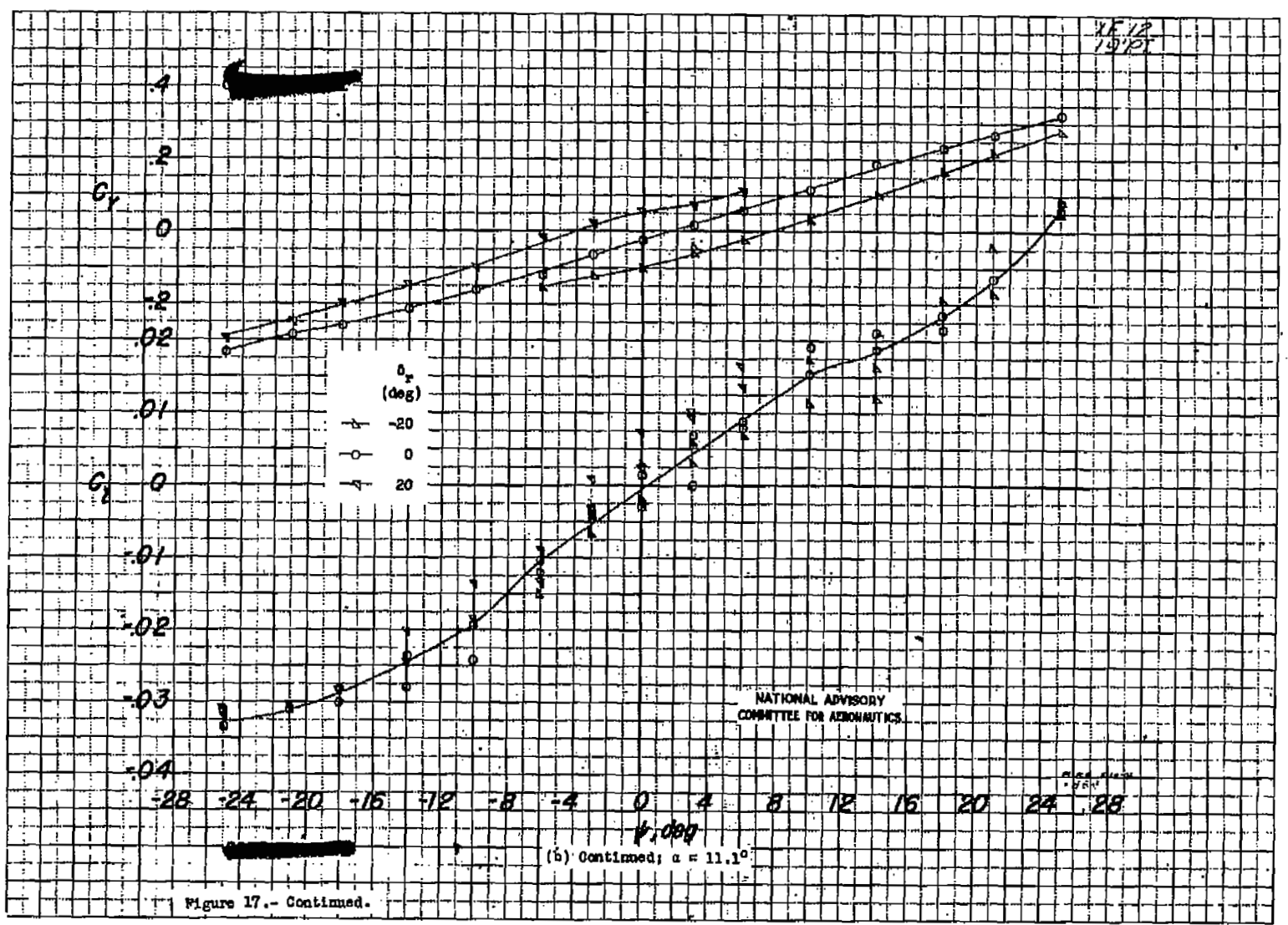


Figure 17.- Continued.

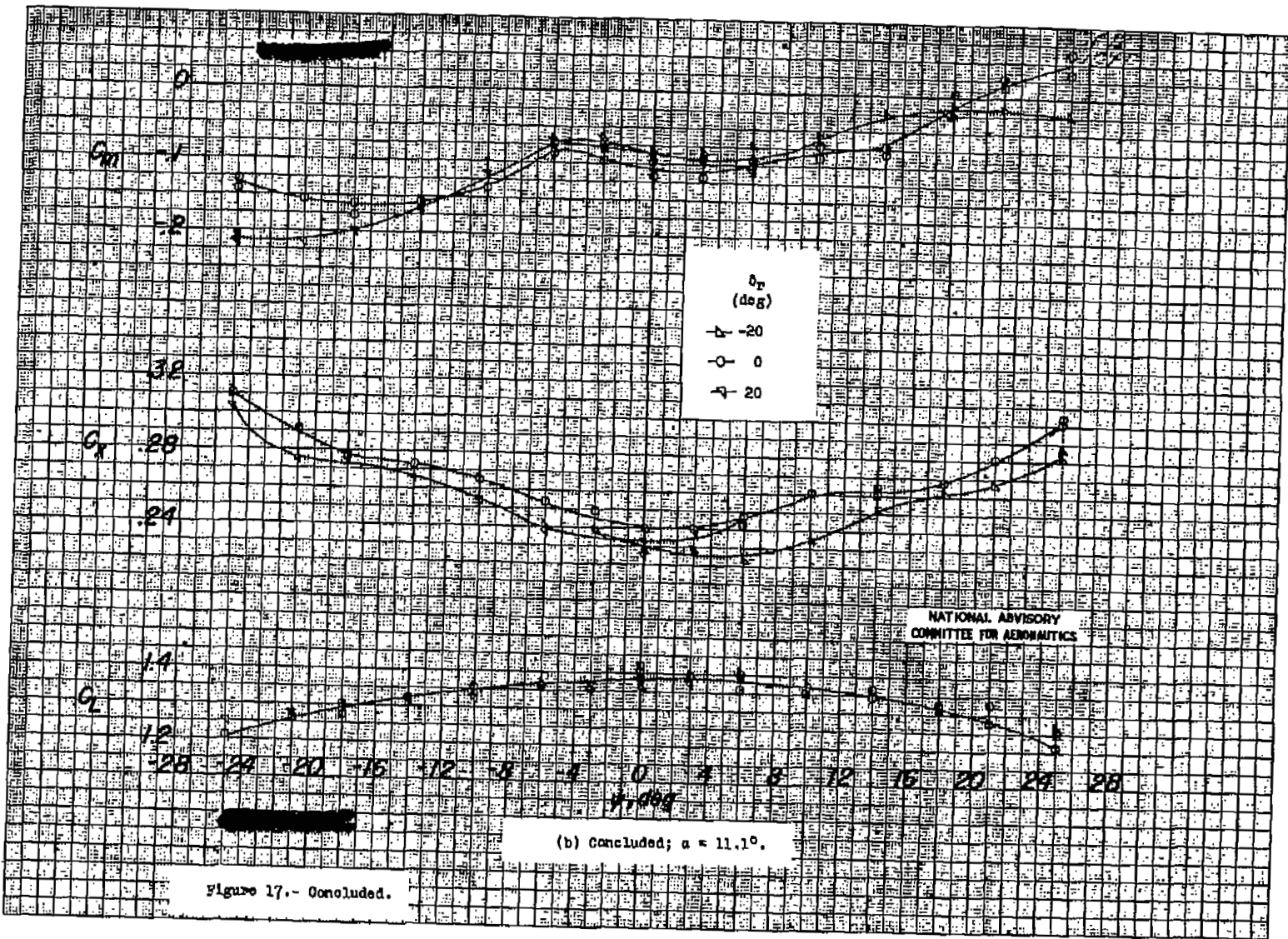


Fig. 17b conc.

NACA – Digidocs

Document processing error

Unreadable tiff image

20470

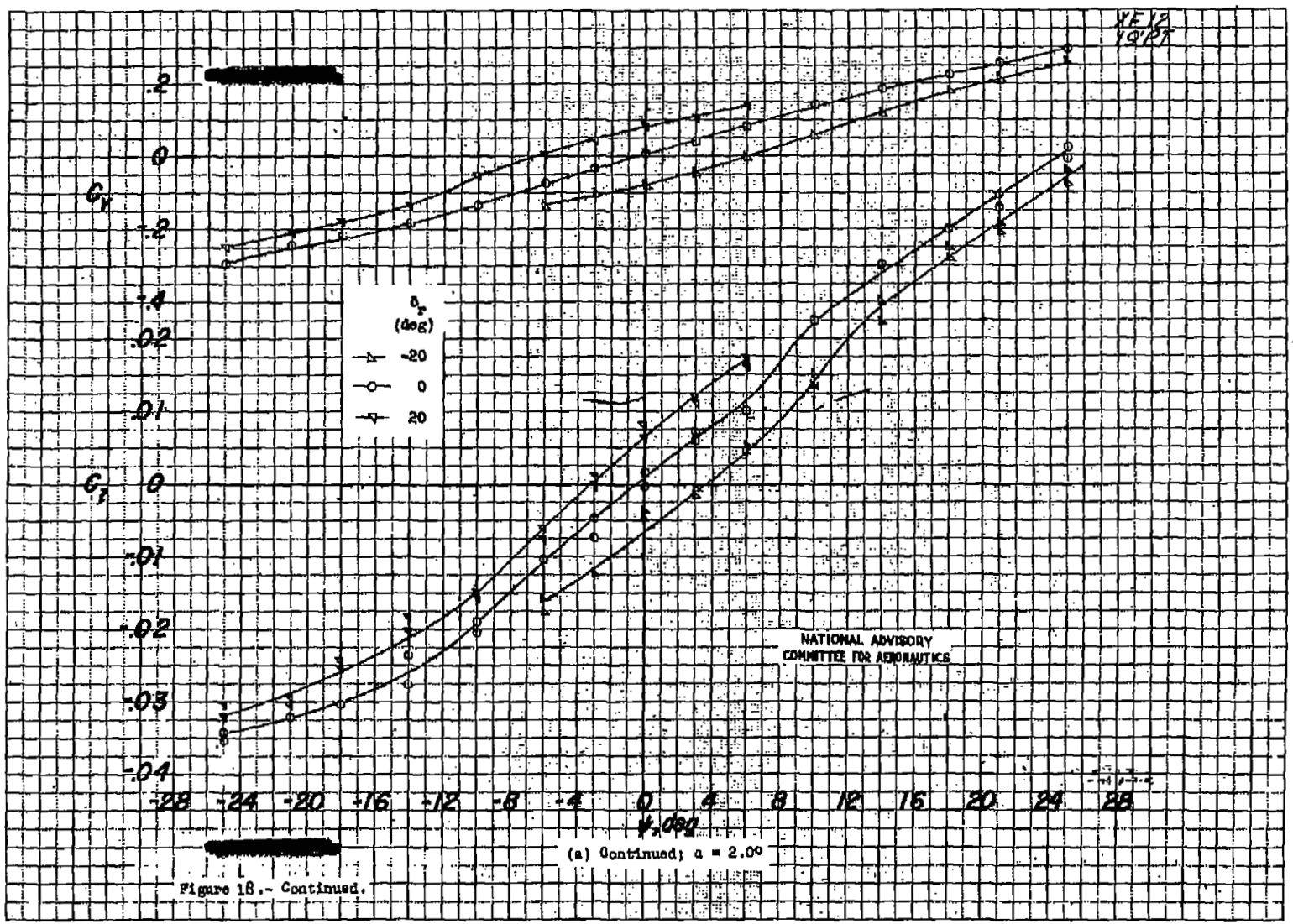


Figure 18a. - Continued.

(a) Continued; a = 2.00

Fig. 18a. cont.

20476

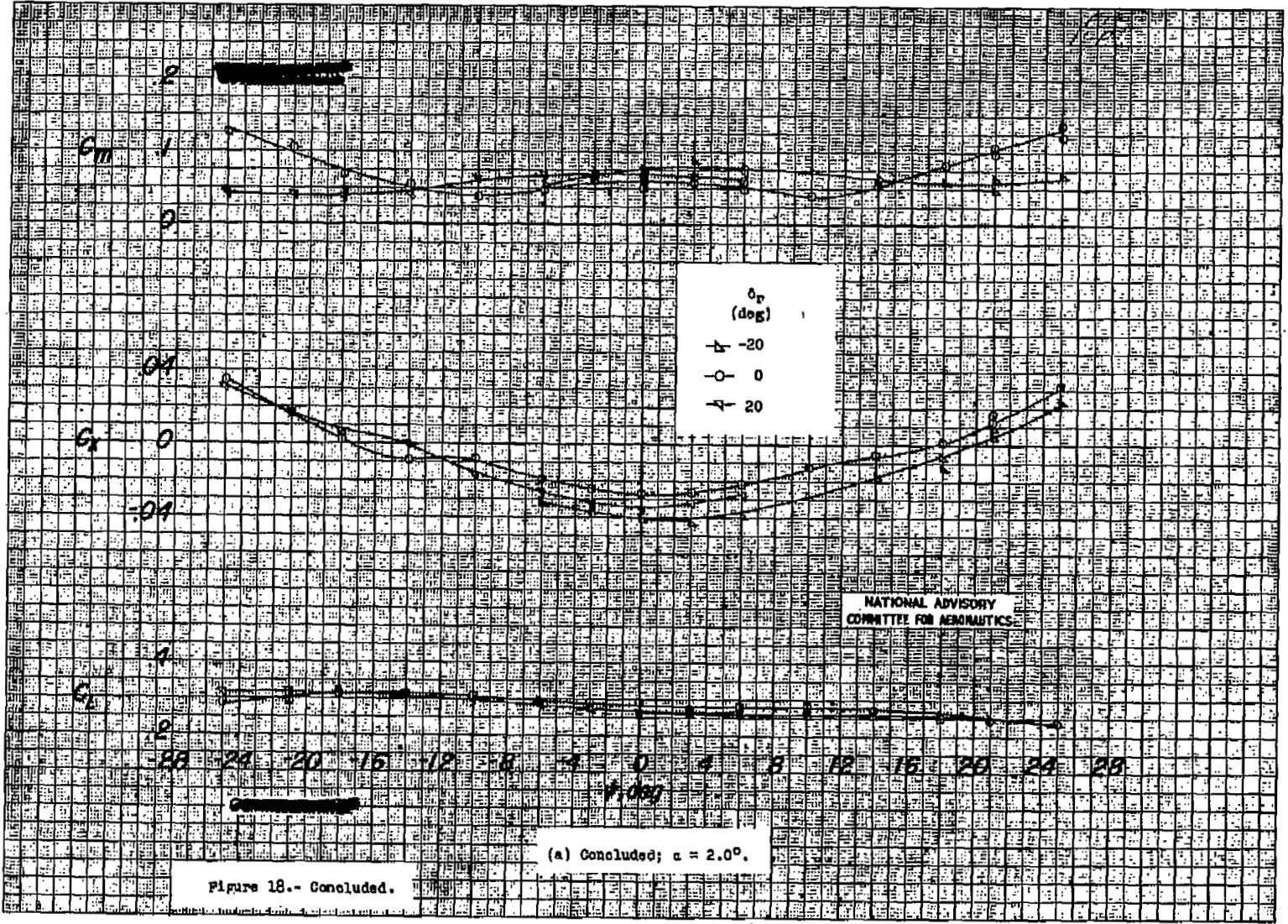
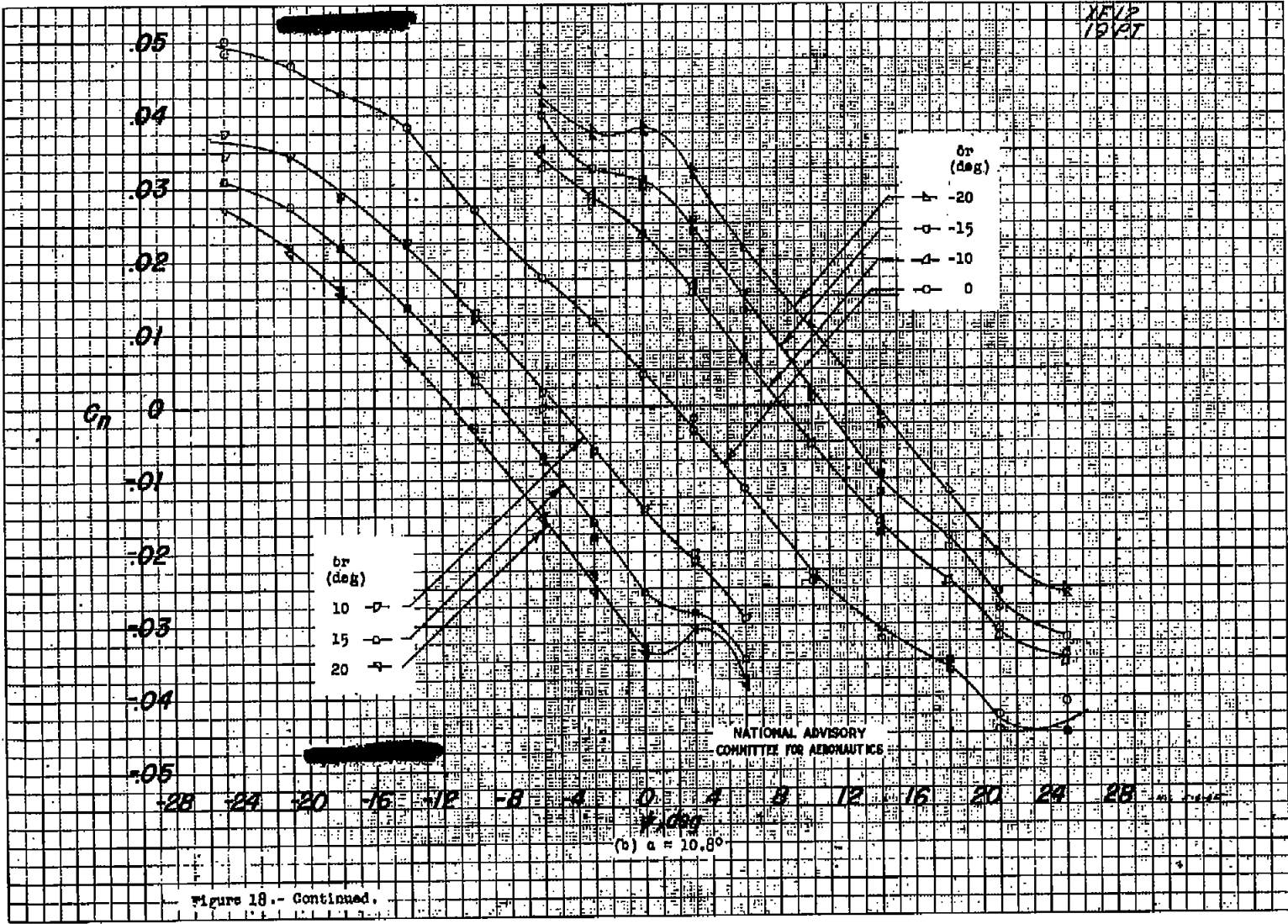


Fig. 18a conc.

20470



20479

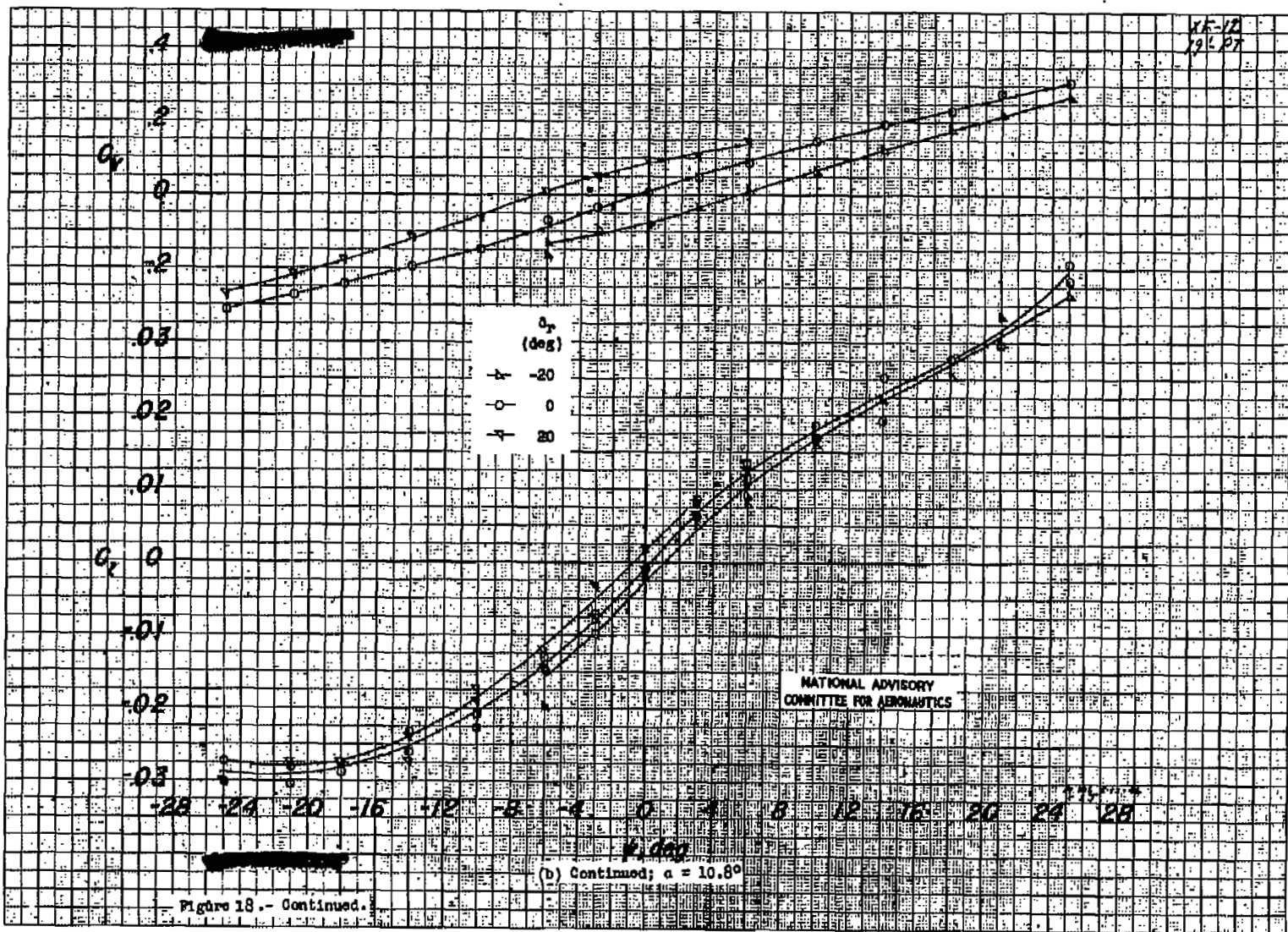


Figure 18.- Continued.

Fig. 18b cont.

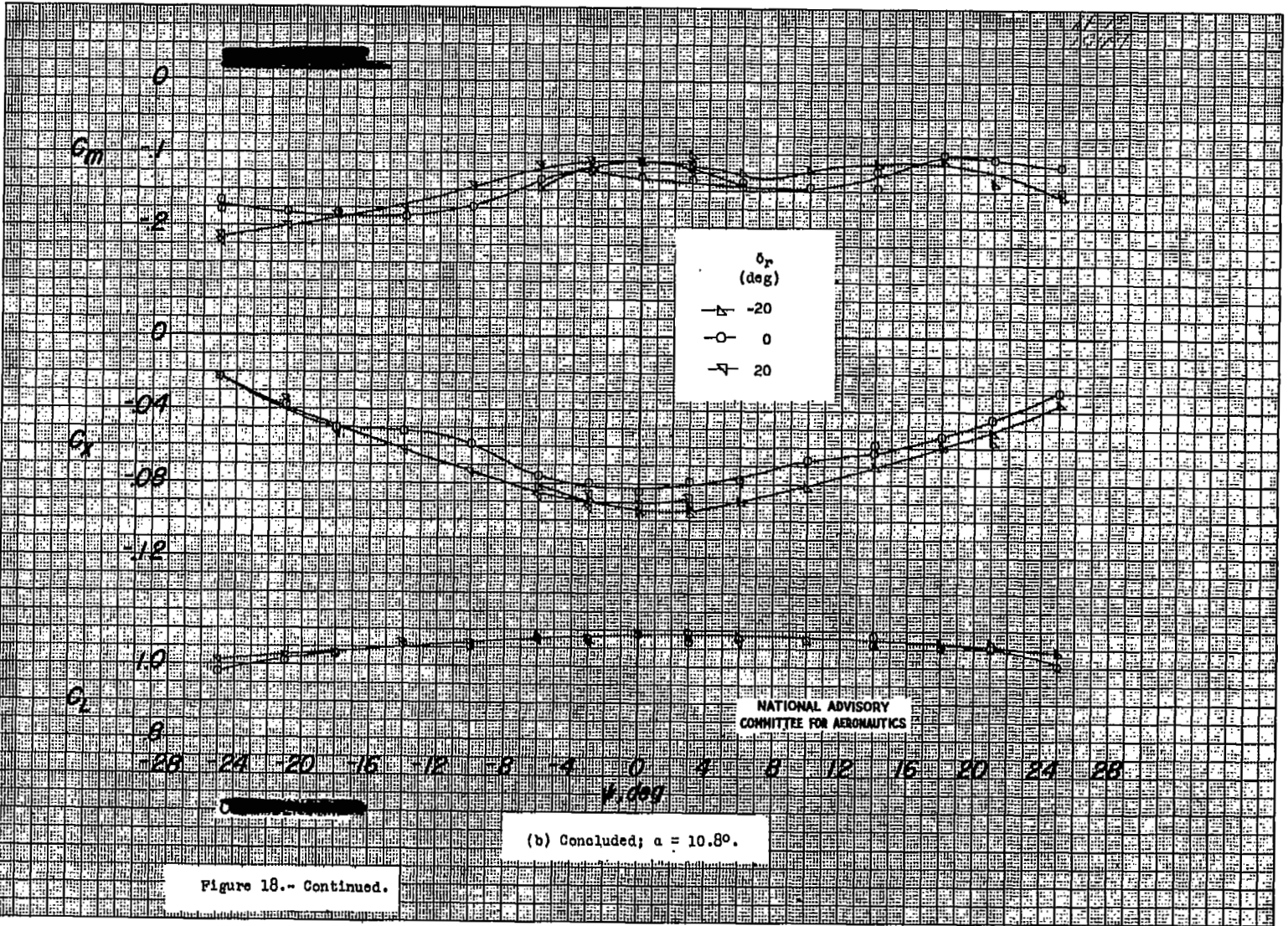


Fig. 18b conc.

20479

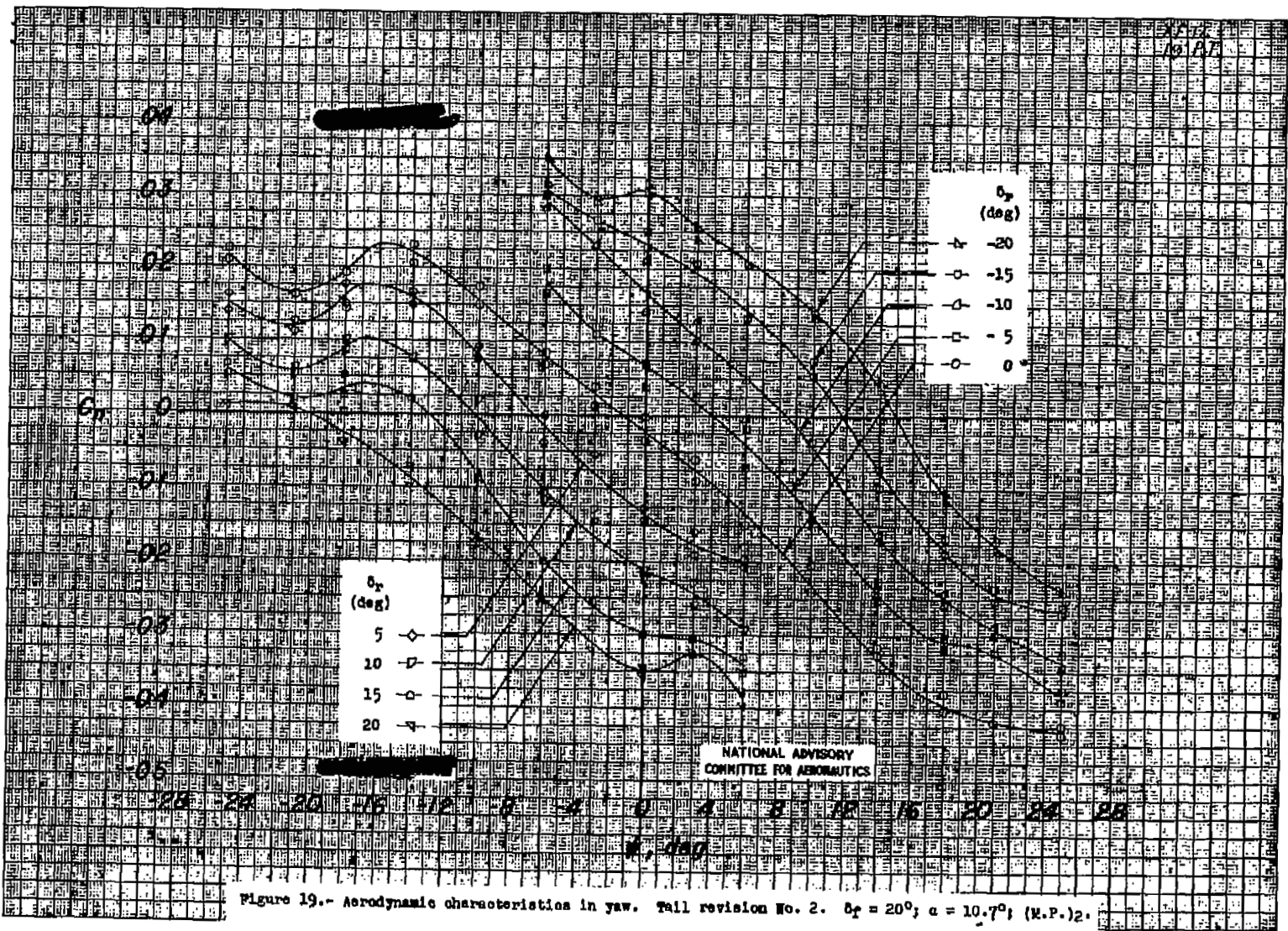


Figure 19.- Aerodynamic characteristics in yaw. Tail revision No. 2. $\delta_r = 20^\circ$; $\alpha = 10.7^\circ$; (N.P.)₂.

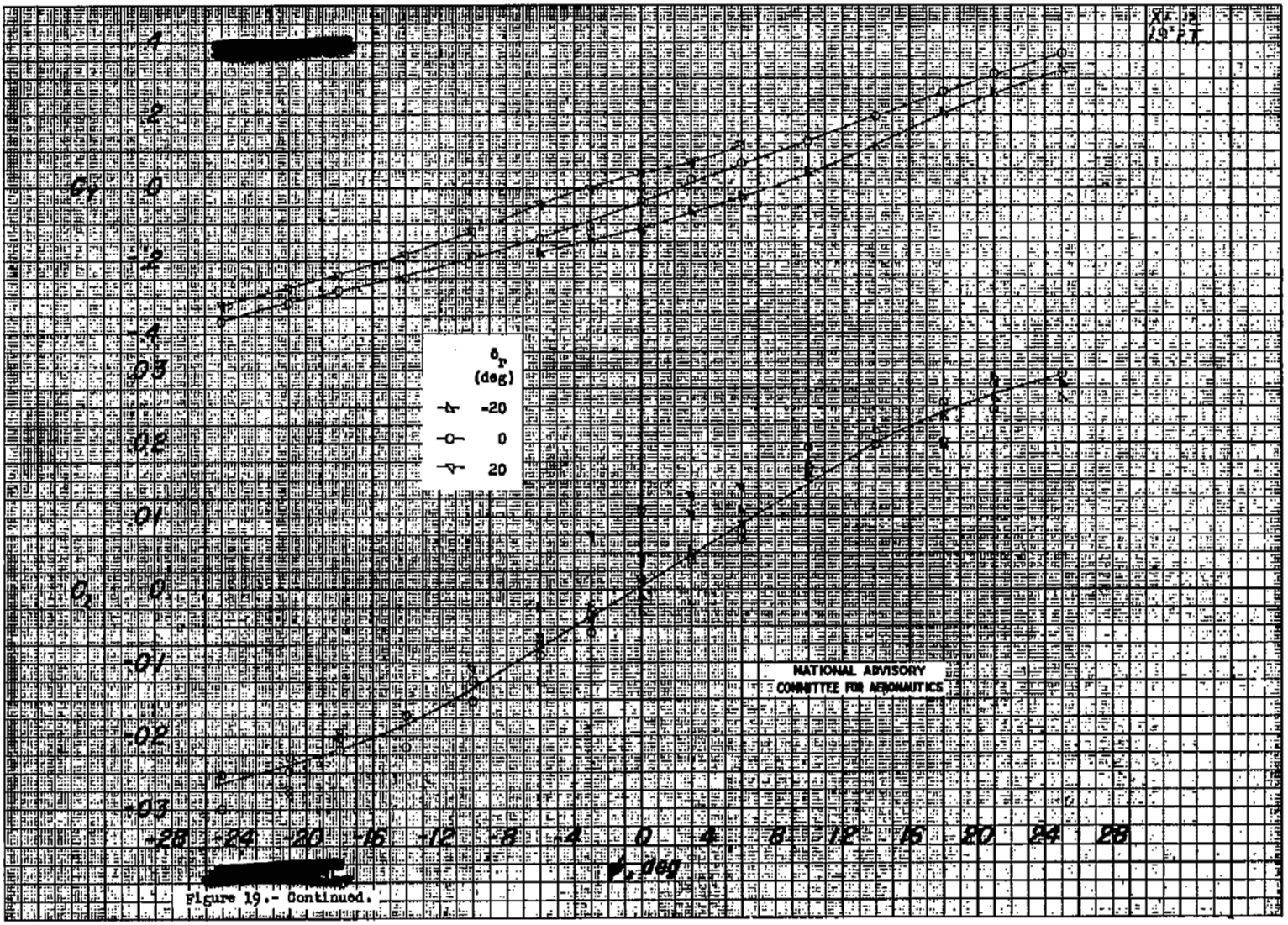


Figure 19.- Continued.

20470

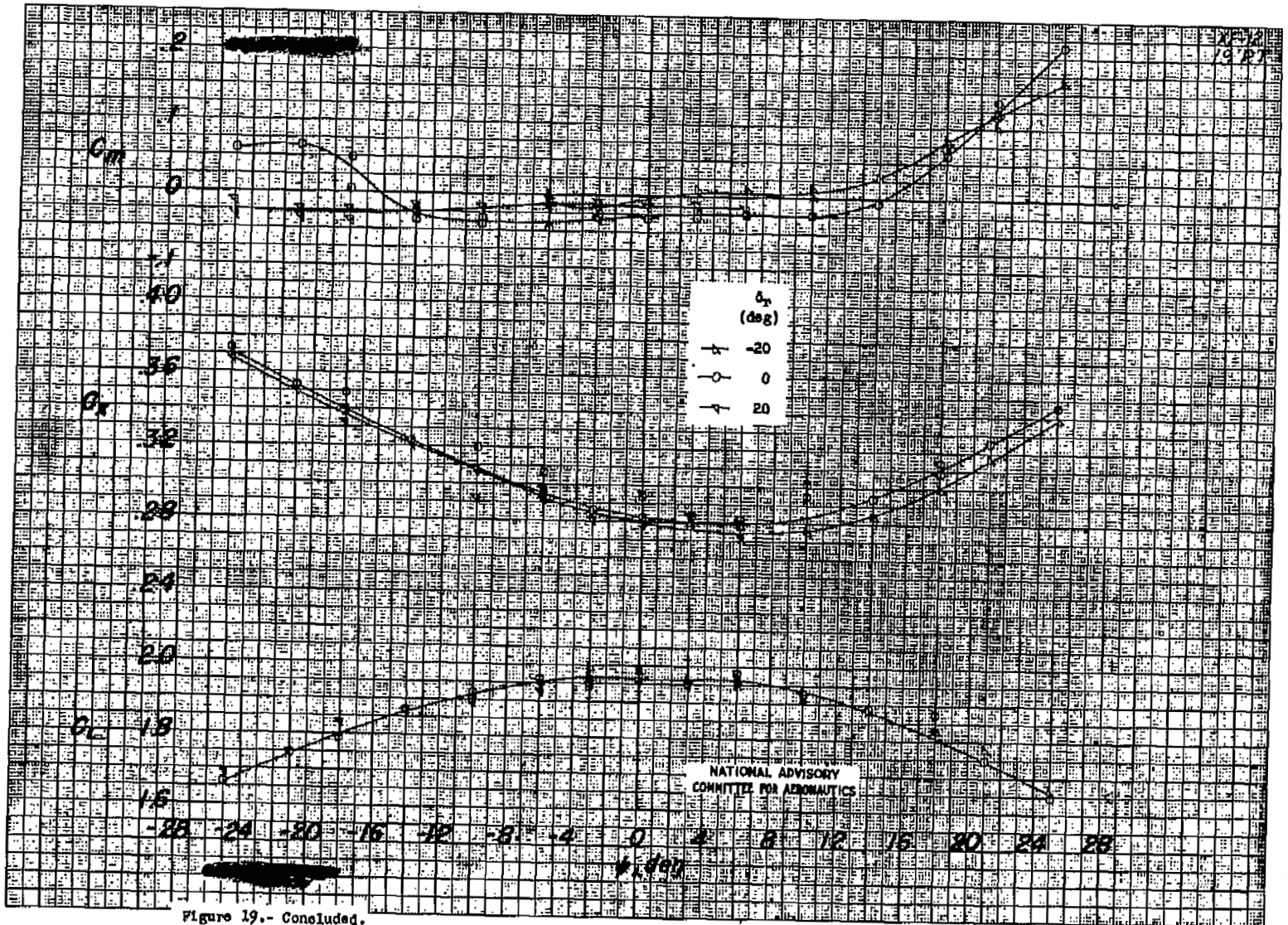


Figure 19.- Concluded.

FIG. 19 conc.

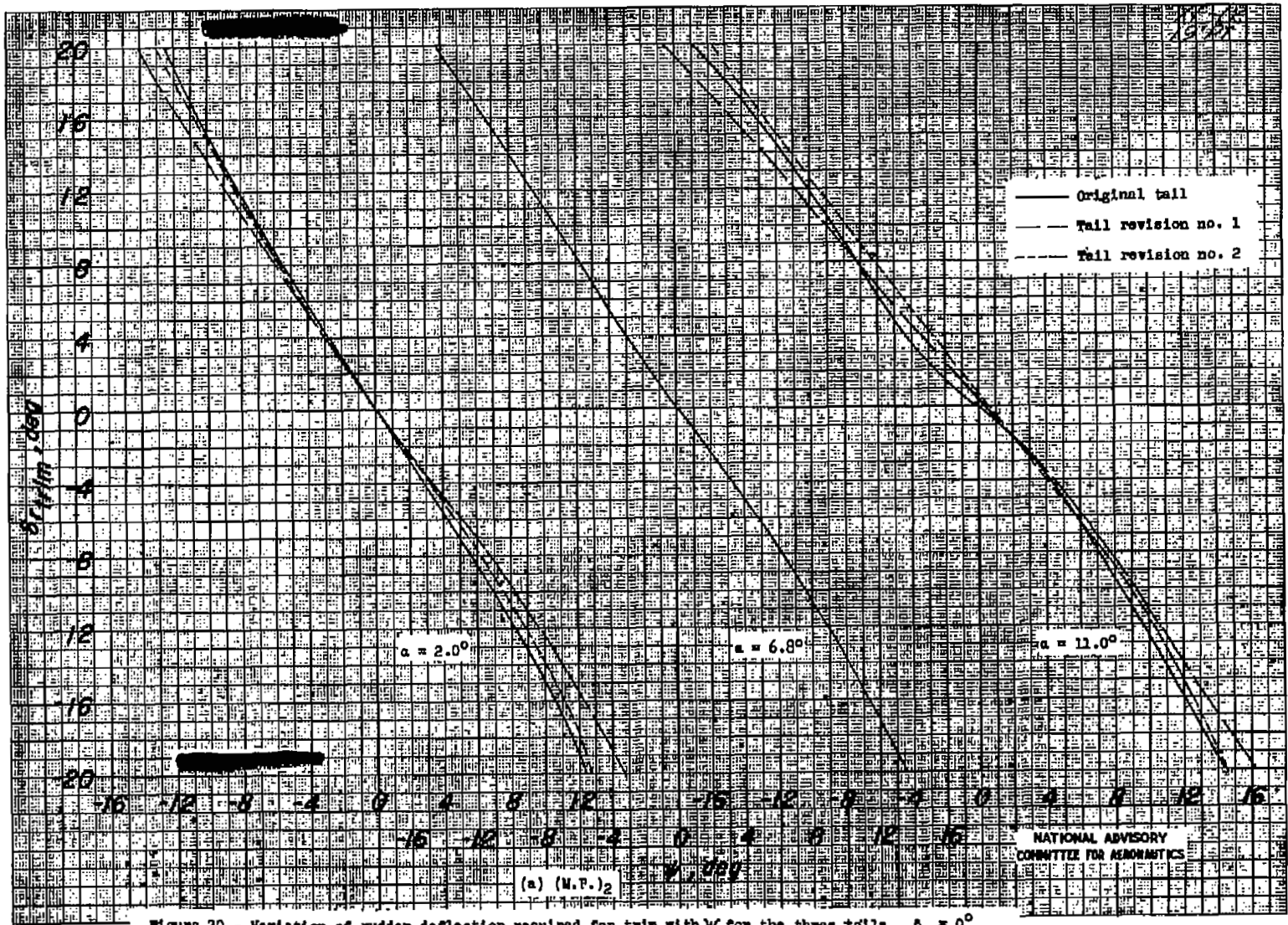


Figure 20.- Variation of rudder deflection required for trim with W for the three tails. $\delta_r = 0^\circ$

204700

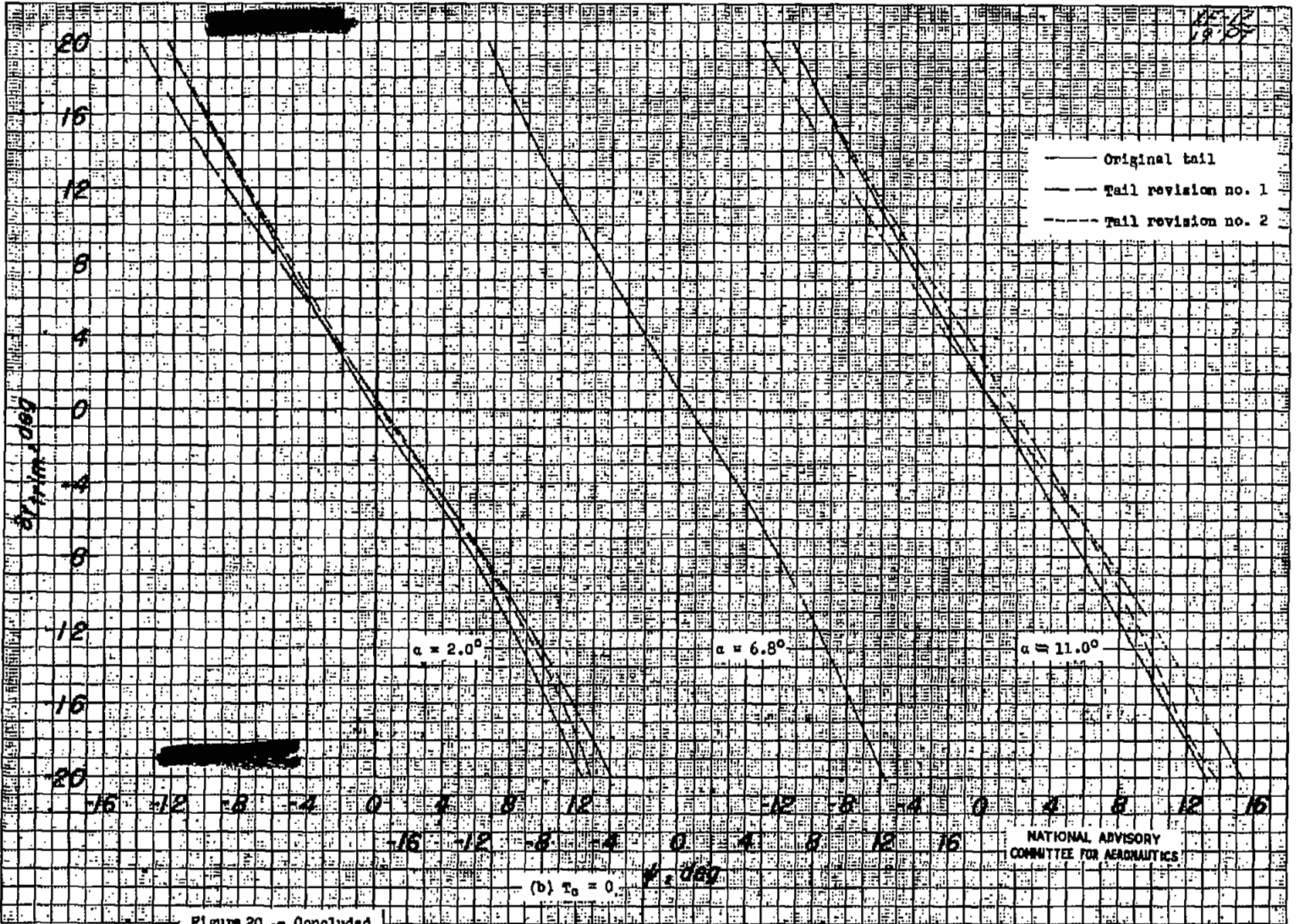


Figure 20 -- Concluded.



Figure 21.- Variation of rudder deflection with C_n ($\psi = 0^\circ$) for the three tails. $\delta_r = 0^\circ$

20475

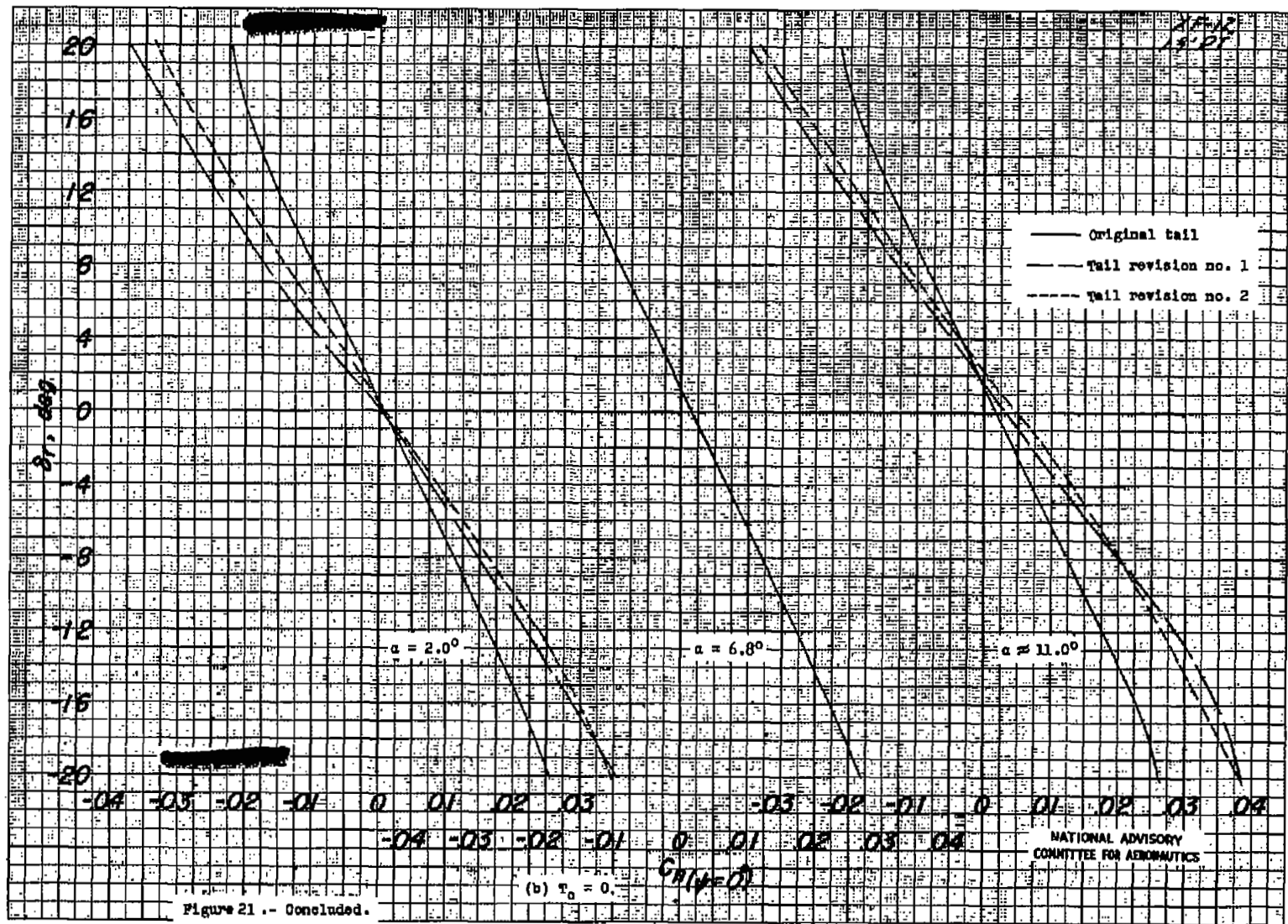


Figure 21 -- Concluded.

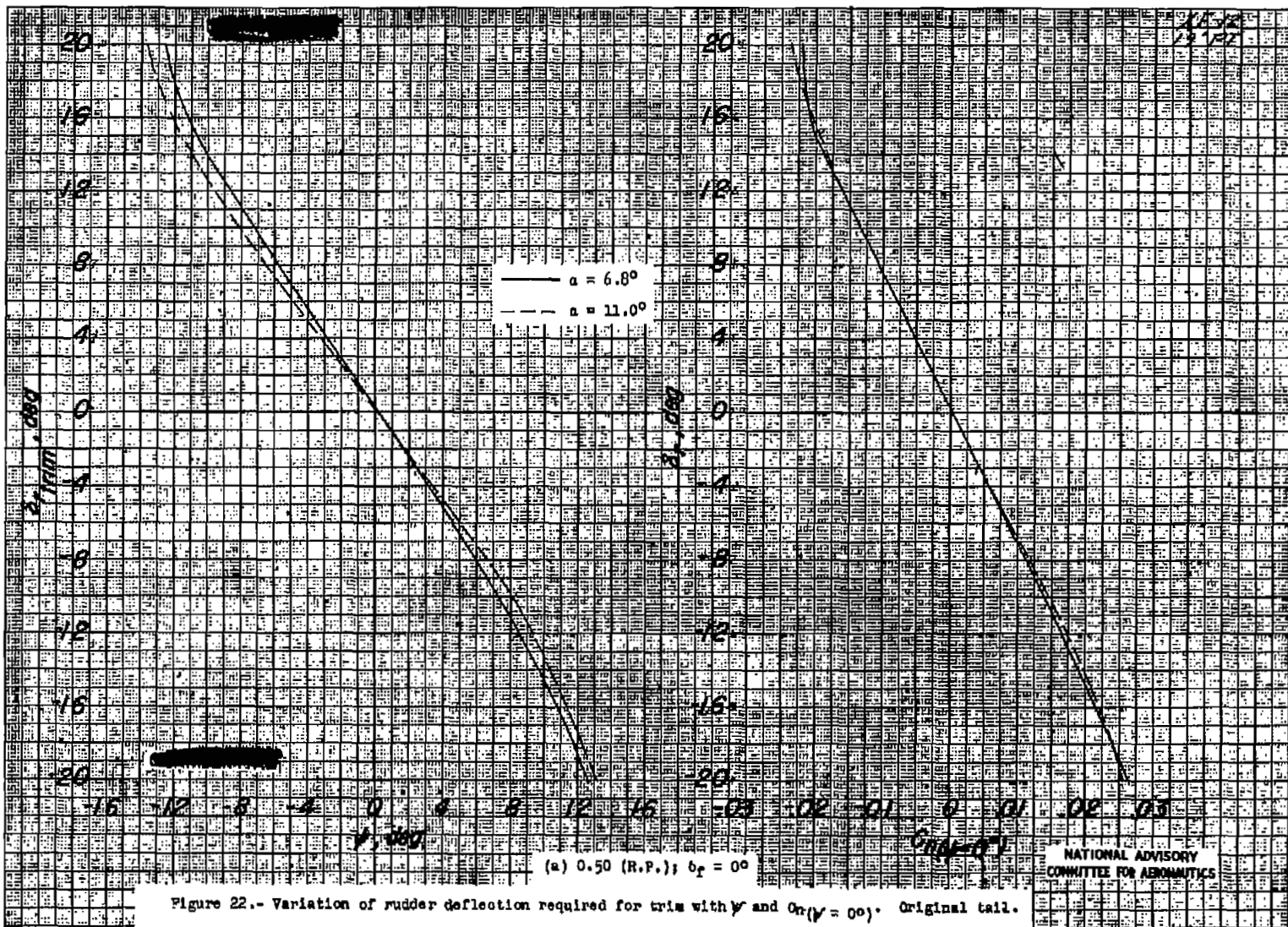
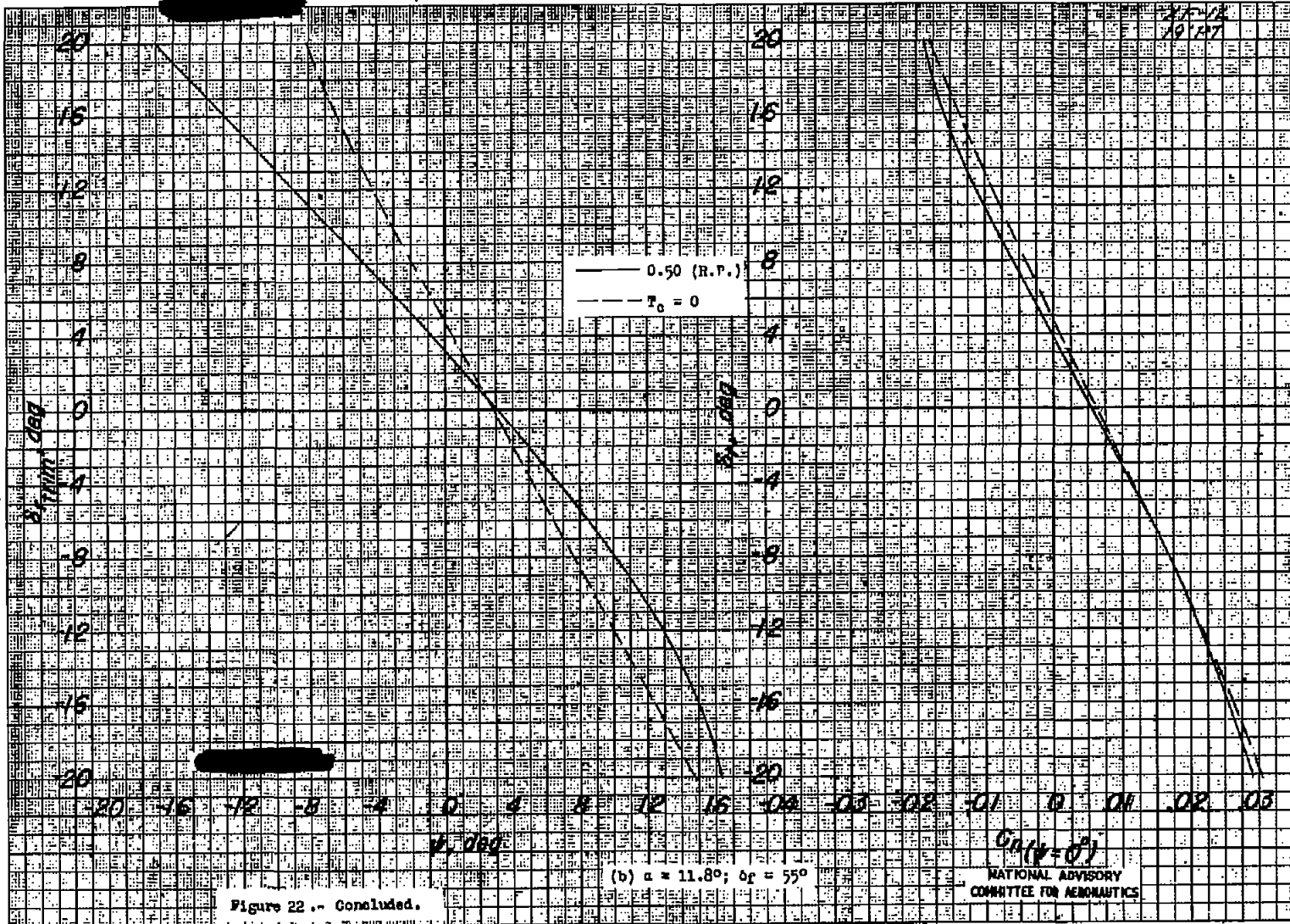


Figure 22.- Variation of rudder deflection required for trim with α and δ_r ($\alpha = 0^\circ$). Original tail.



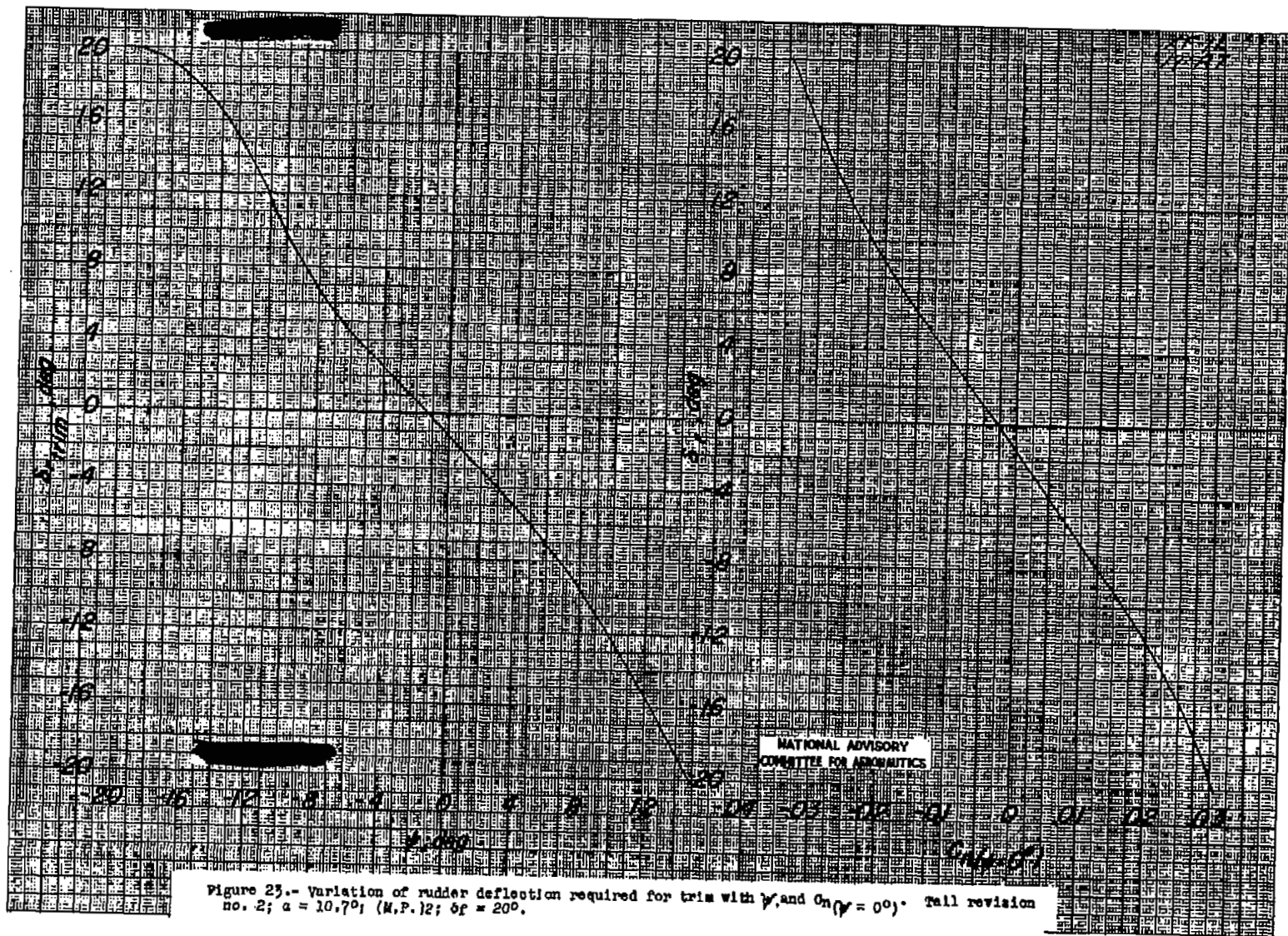


Figure 25.- Variation of rudder deflection required for trim with β , and $C_{n\beta} = 0$. Tail revision no. 2; $\alpha = 10.7^\circ$; (M.P. 12; $\delta_f = 20^\circ$).

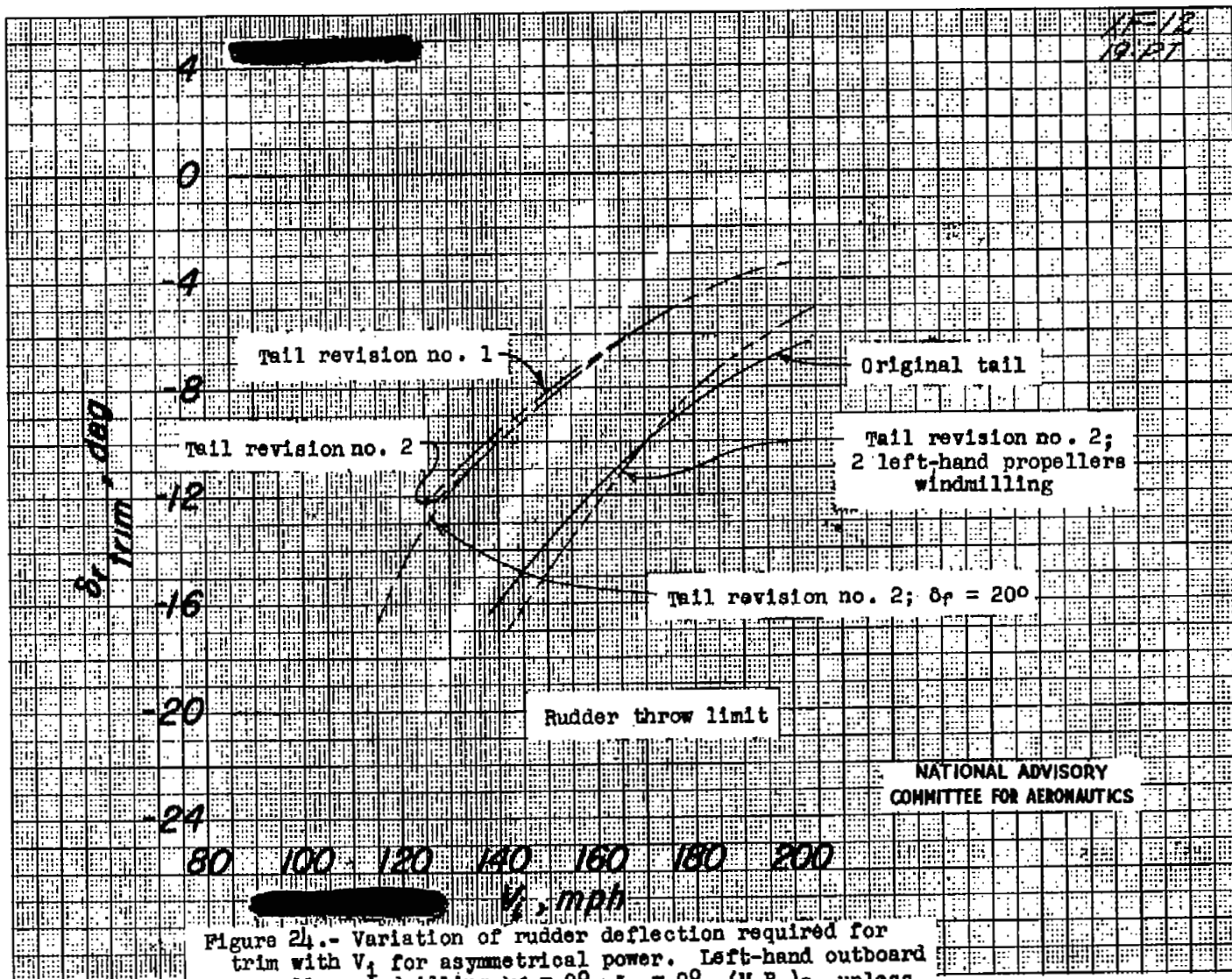
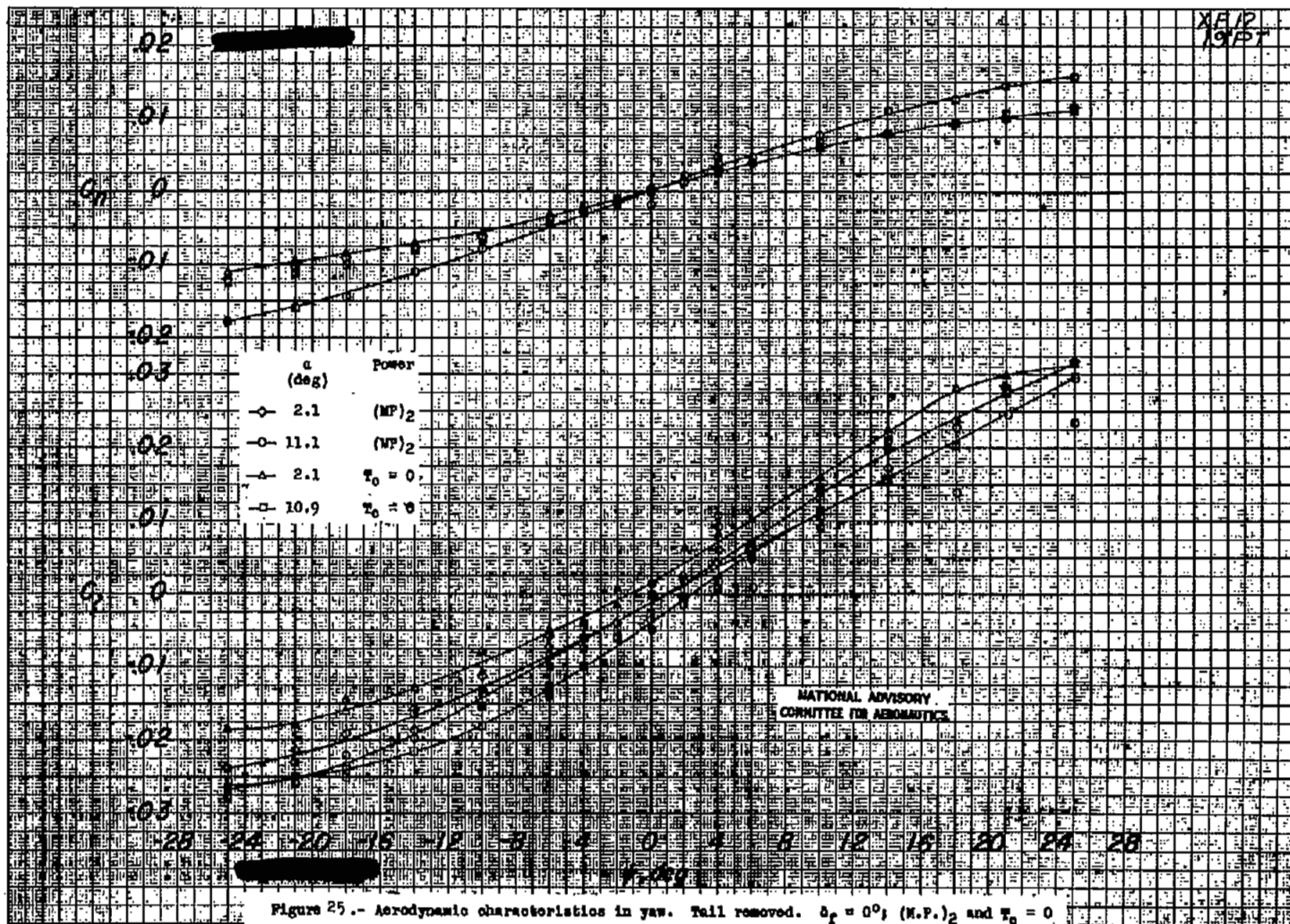


Figure 24.- Variation of rudder deflection required for trim with V_1 for asymmetrical power. Left-hand outboard propeller windmilling, $\psi = 0^{\circ}$, $\delta_p = 0^{\circ}$, (M.P.)₂, unless otherwise noted.



204725

NACA RM. No. L7B21

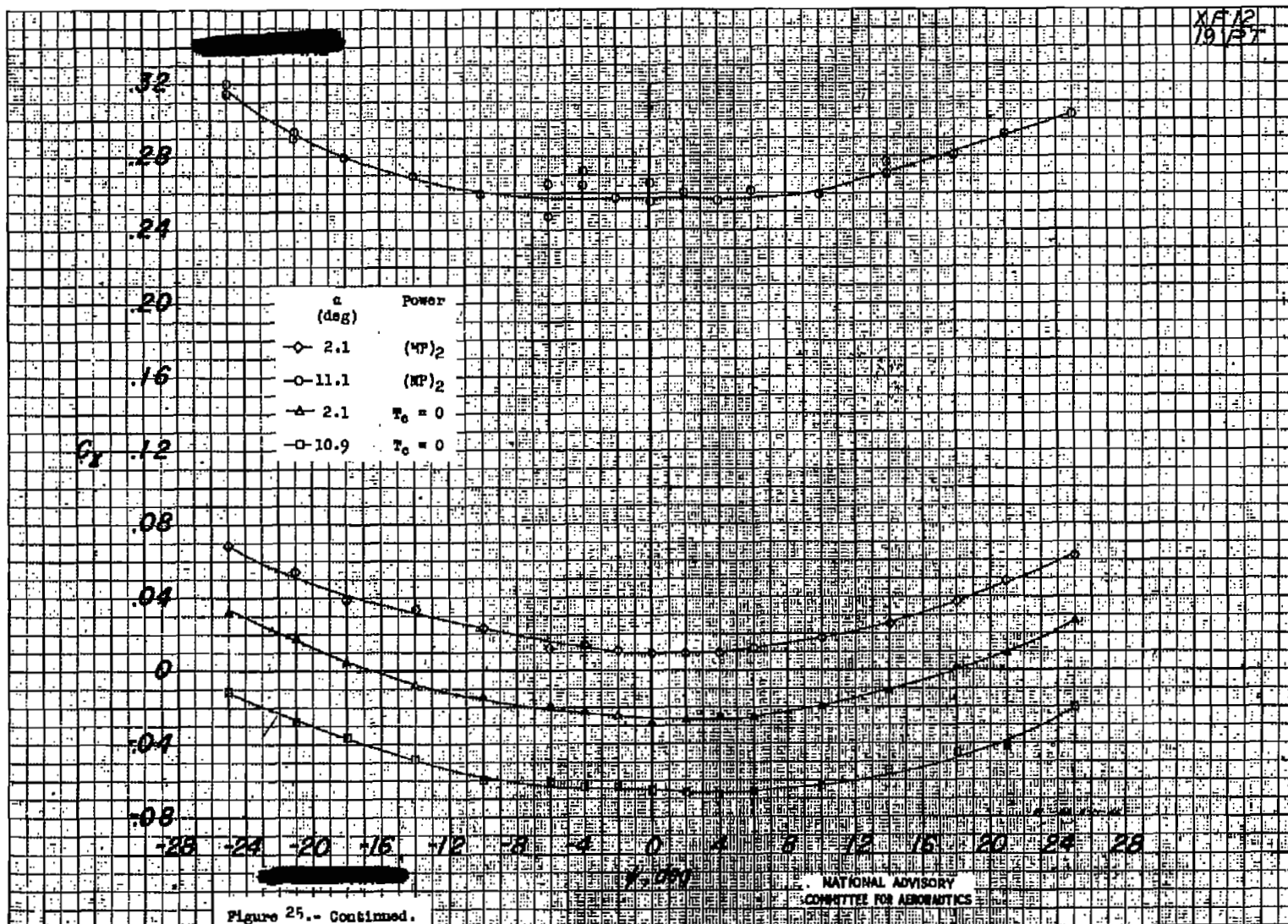


Fig. 25 cont.

20475

NACA RM No. L7B21

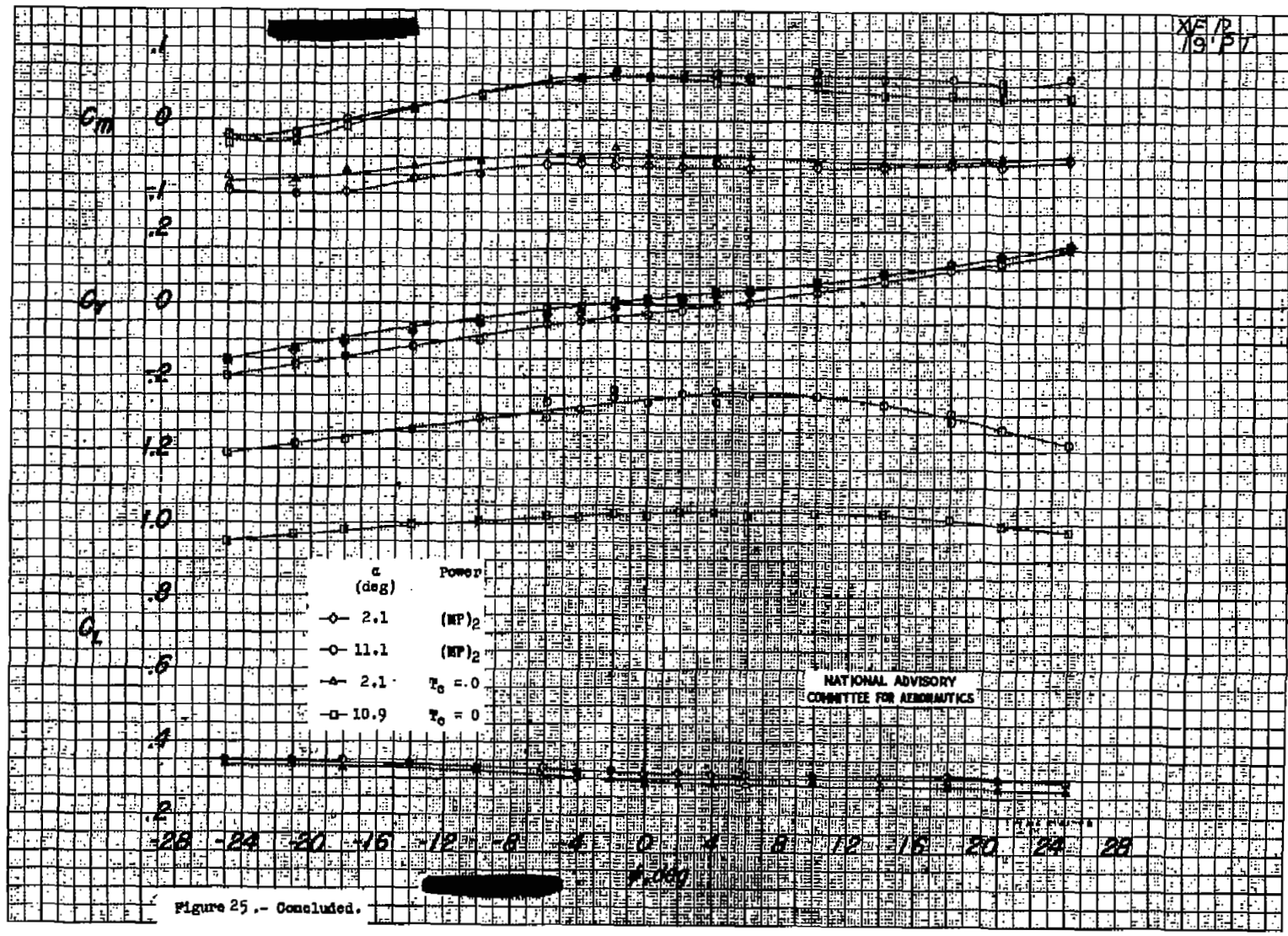
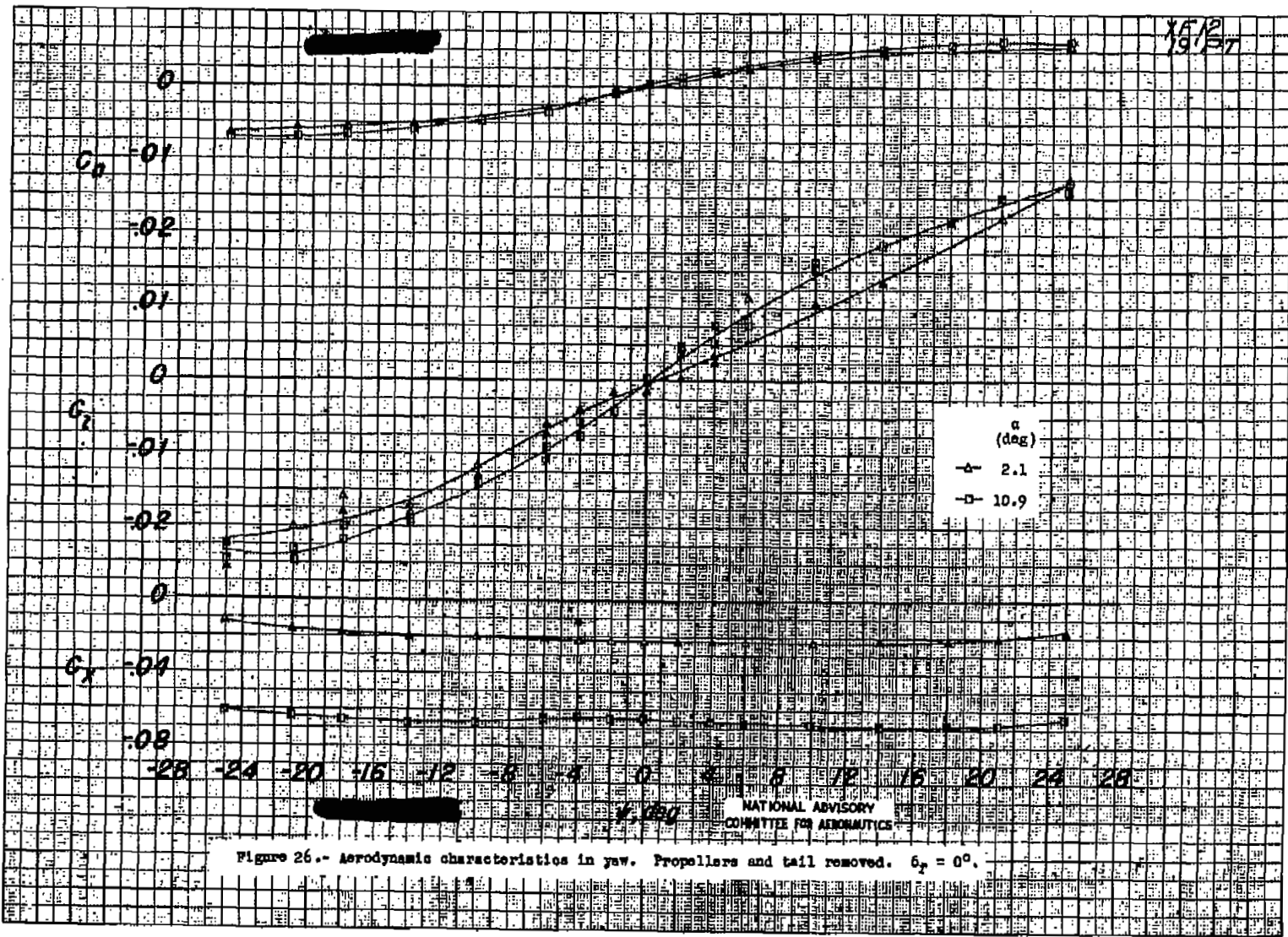


Figure 25.- Concluded.

Fig. 25 cont.

204705



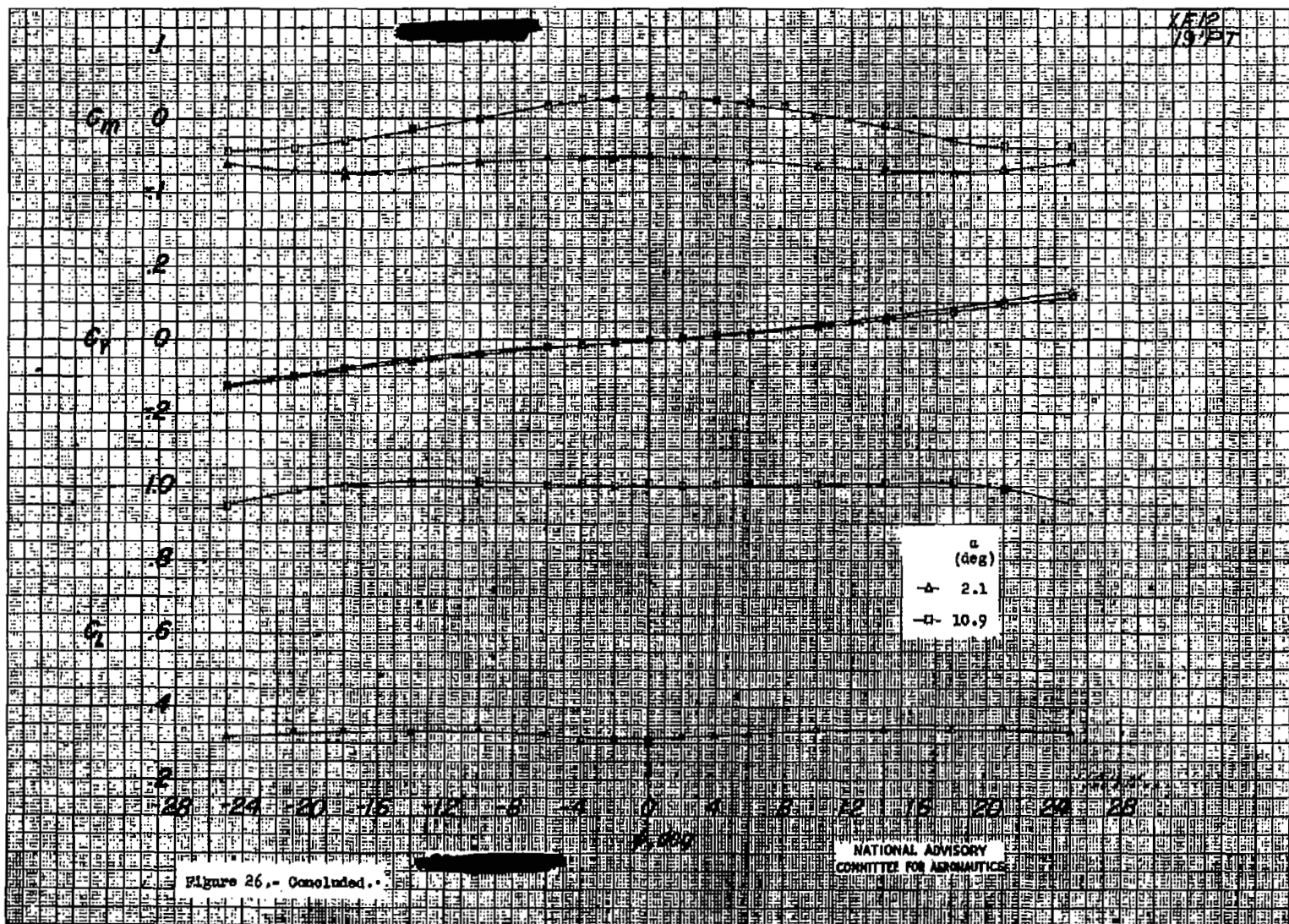


Fig. 26 conc.

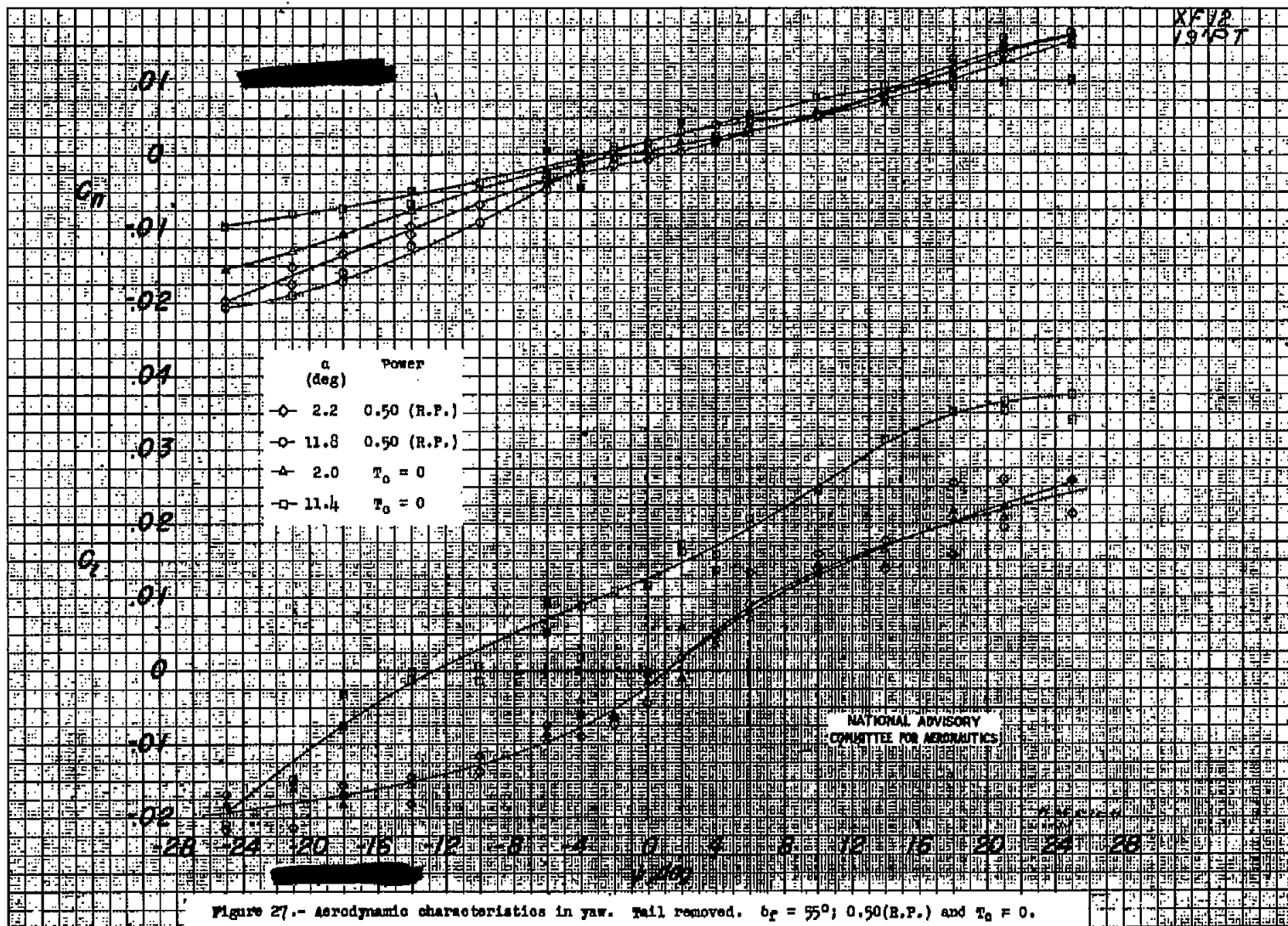


Figure 27.- Aerodynamic characteristics in yaw. Tail removed. $\delta_F = 95^\circ$; 0.50(R.P.) and $T_0 = 0$.

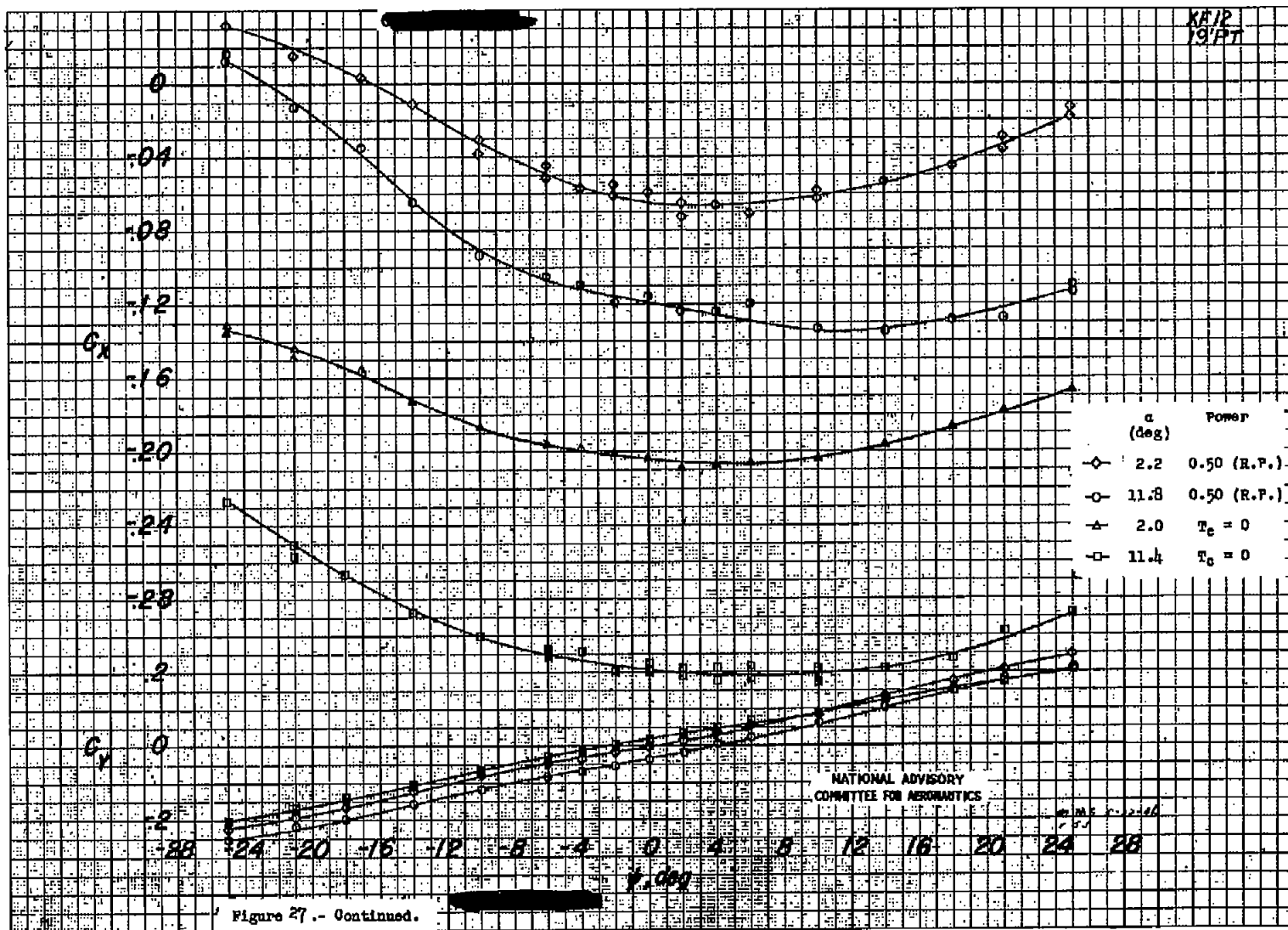
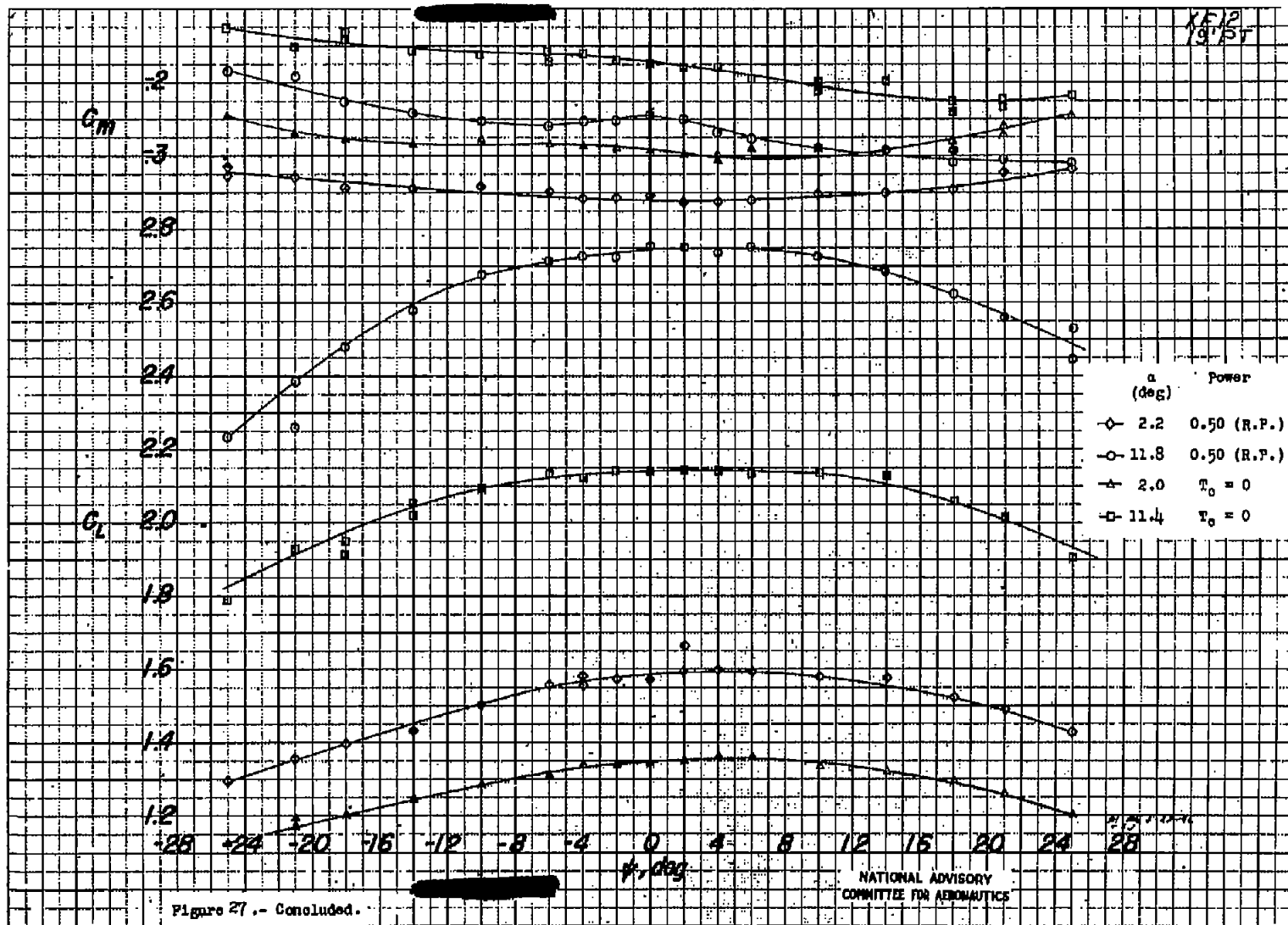


Figure 27.- Continued.



CONFIDENTIAL

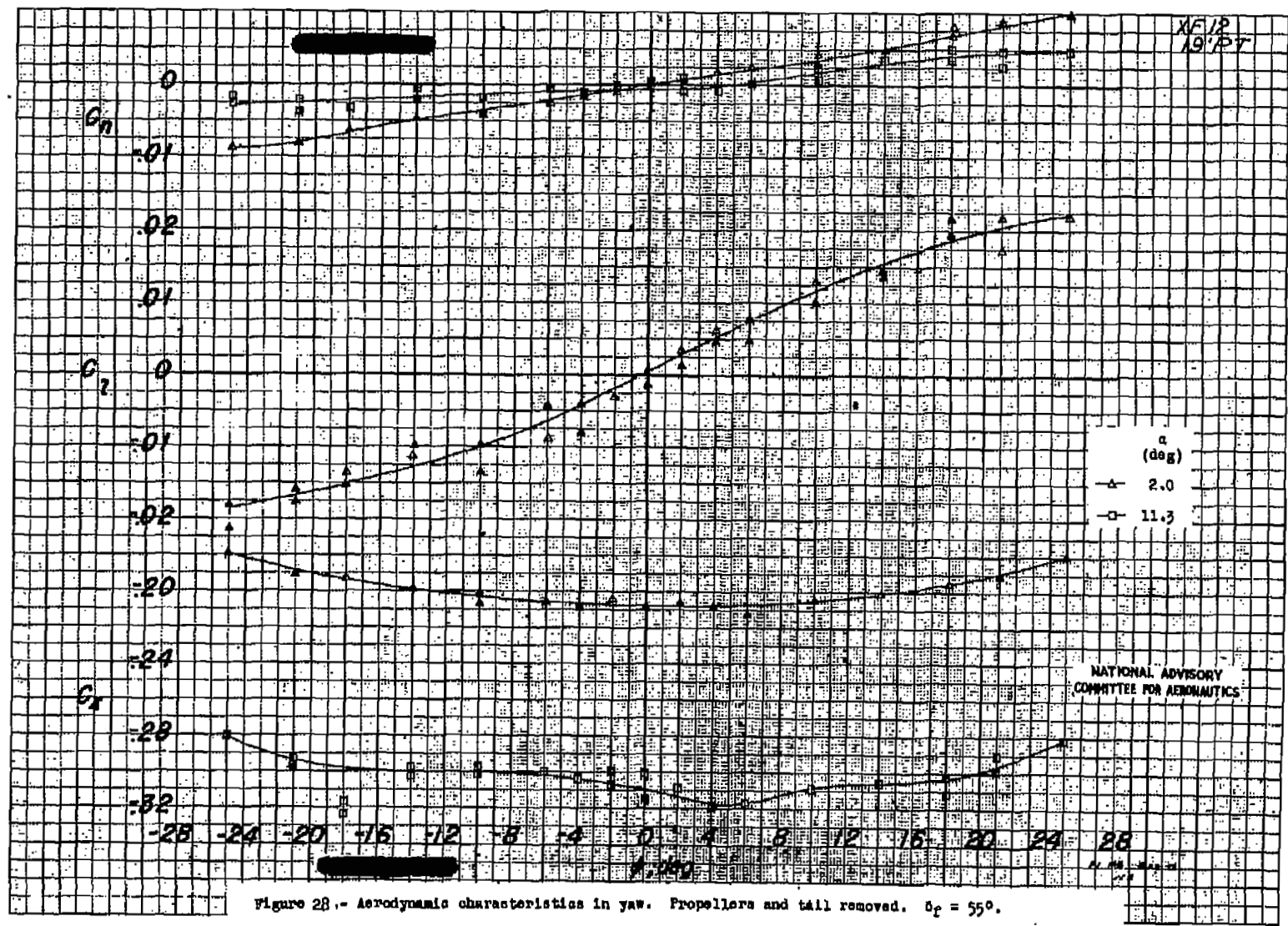
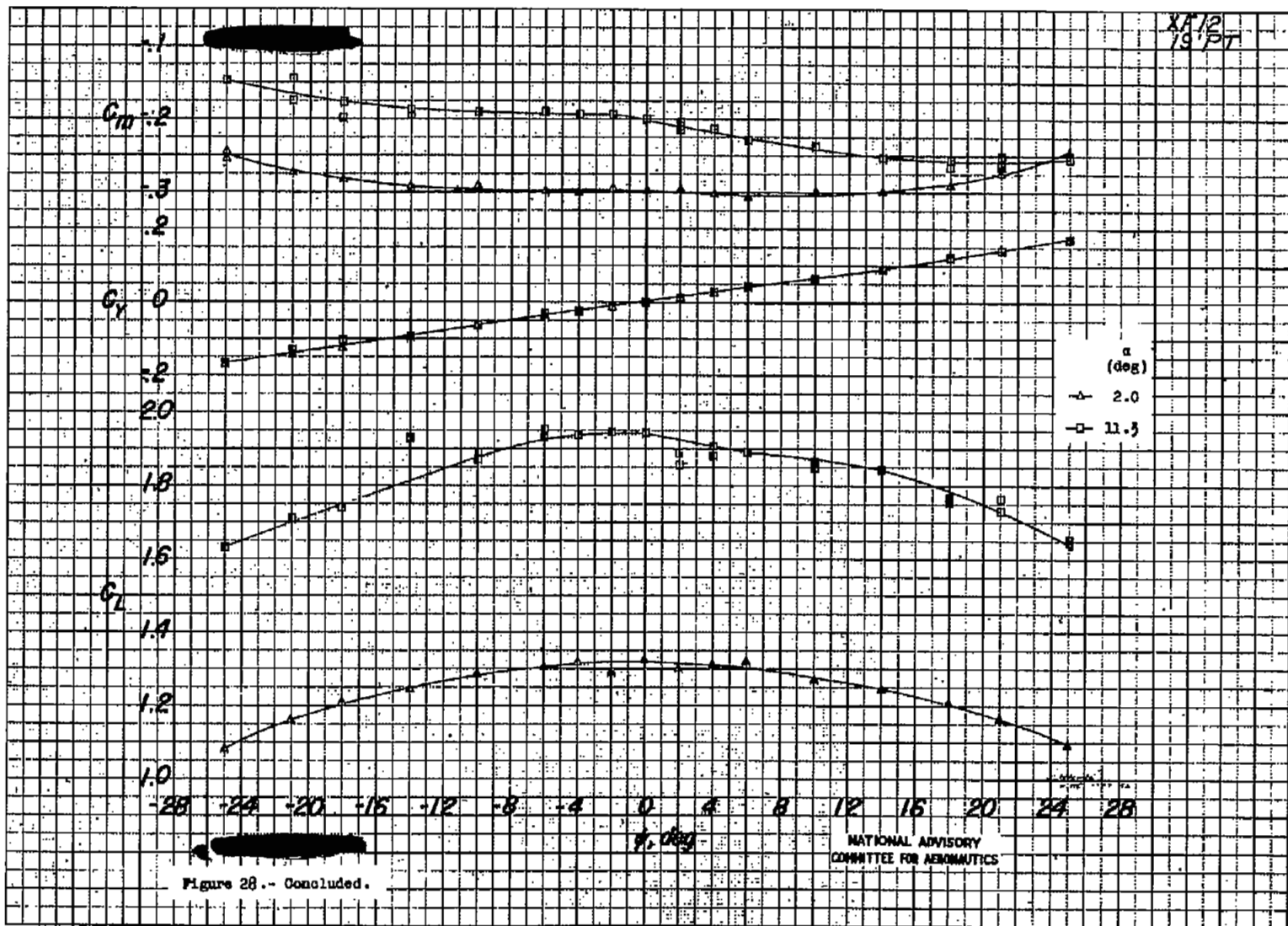
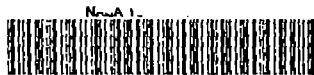


Figure 28.- Aerodynamic characteristics in yaw. Propellers and tail removed. $\beta_p = 55^\circ$.





3 1176 01437 5019